GROUNDWATER POTENTIAL ASSESSMENT OF KINTAMPO NORTH MUNICIPALITY OF GHANA, USING THE ELECTROMAGNETIC METHOD AND VERTICAL ELECTRICAL SOUNDING

BY

ANECHANA ROBERT, BSC (APPLIED PHYSICS)

A THESIS SUBMITTED TO THE DEPARTMENT OF PHYSICS,

KWAME NKRUMAH UNIVERSITY OF SCIENCE AND TECHNOLOGY

IN PARTIAL FULFILLMENT OF THE REQUIREMENTS FOR THE DEGREE

OF

MASTER OF PHILOSOPHY (GEOPHYSICS)

COLLEGE OF SCIENCE

DEPARTMENT OF PHYSICS

SUPERVISOR: MR REGINALD MENSAH NOYE

OCTOBER, 2013.

DECLARATION

I hereby declare that this submission is my own work towards the M.Phil. and that to the best of my knowledge, it contains no material previously published by another person nor material which has been accepted for the award of any other degree of the university, except where due acknowledgement has been made in the text.

…………………………………… …………………………………….. …………………

Student Name and ID Signature Date

Certified by:

………………………………… …………………………….... …………………..

Supervisor Name Signature Date

Certified by:

……………………………… ……………………………. ….………………

Head of Dept. Name Signature Date

ABSTRACT

Geophysical methods of exploration involving the electromagnetic profiling and the vertical electrical sounding were employed to prospect for groundwater in the Kintampo North Municipality. Electromagnetic profiling using Geonics EM 34-3 and Vertical electrical sounding using the Schlumberger electrode array configuration were deployed along traverses within the area. The EM data was collected at 20 m intervals along 20 profiles, ranging from 70 to 240 m, while the soundings were conducted at suitable locations of anomaly identified on the EM profiles. Points of sharp positive EM anomalies (crossovers) and necks were considered priority areas for resistivity sounding and groundwater development, since they often suggested lithological variations within the unconsolidated overburden, and/or water-filled fissures in the bedrock. The qualitative analysis of the electromagnetic data identified relatively high conductive regions indicating possible fracture zones or weathered layers along the traverses. The quantitative interpretation of the modelled sounding curves delineated between three and five subsurface layers at different communities within the Kintampo North Municipality. These layers were inferred to be the top soil, sandy-clay/clayey-sand, weathered/fractured layer, and the fresh bedrock. The weathered layers and the fractured basements constitute the aquifer units across the area. The modelled VES curves characterized the topsoil/weathered basement with resistivity range of 3.4×10^{-1} to about 3.9×10^{4} Ωm with an estimated depth to basement ranging from 5 m to 66 m. The possible fracture zones underlying the basement is represented by electrical resistivity range of 54.9 to 295 Ωm at depth range of 30 m – 60 m. The results of the study confirm that the integrated Electromagnetic and VES methods are very suitable for sitting boreholes in these communities within the complex Voltaian sedimentary formation. It is suggested that, Geophysical methods should hence, form an integral part of groundwater exploration programmes in solving problems associated with groundwater prospecting to locate potential aquifers for the supply of potable water to rural communities.

ACKNOWLEDGEMENTS

Thanks be to God almighty for the strength, health, courage and wisdom He has given me to write this Master of Philosophy (MPhil) thesis report.

I wish to express my heartfelt gratitude and appreciation to my supervisor, Mr. R. M. Noye and co-supervisor Professor Aboagye Menyeh for all their efforts and contributions they made to see to the completion of this work. Their patience, understanding, encouragement and pieces of advice were pivotal to the success of this work. I am equally grateful to all the geophysics lecturers at the Physics Department for their assistance, motivation and encouragement most especially Professor S. K. Danour whose efforts led to the CSIR-GWD releasing their data out of which this thesis work is a fruit.

I am also grateful to the management and staff of the Council for Scientific and Industrial Research- Groundwater Division (CSIR-GWD) for opening their doors when I knocked on them. They granted me permission to use their EM and VES data to interpret and publish this thesis besides the geophysical advice I received from them, most especially Mr Evans Manu and Mr Collins Okrah.

Finally, I thank my colleagues' Postgraduate students at the Physics Department, K.N.U.S.T for their diverse assistance in making this work a reality.

My family supported me throughout this study, especially during the frustrating periods when my research progressed rather slowly. Am most grateful to them.

TABLE OF CONTENT

LIST OF TABLES

TABLE **PAGE**

LIST OF FIGURES

FIGURE **PAGE**

LIST OF APPENDICES

CHAPTER ONE

1.1.0 INTRODUCTION

Globally, water is obtainable as either groundwater (GW) or surface water. Water extracted from the ground has three main uses: agriculture, industry, and domestic consumption. It is more advantageous as a source of potable water due to the fact that it is usually free from biological and chemical contaminants. It needs little or no purification before it can be used for domestic and industrial purposes. It is not easily affected by drought and odour and colouring is usually absent. Groundwater has constant temperature and chemical composition. Suspended solutes (turbidity) are usually absent. It has far greater storage as compared to surface water (Ademilua and Talabi, 2012).

Groundwater is the most widespread and highly used water resource. It is of inestimable value to the residents of dry regions, being the only reliable water resource they have. The yearly consumption of groundwater world-wide is estimated to be about 1000 km^3/yr, and the global groundwater recharge at 12,700 km^3/yr (http://en.wikipedia.org/wiki/Groundwater). Over half of the world's population depends on groundwater for drinking water supplies. In the UK, about 30% of the public water supplies are derived from groundwater. In the USA about 50%, Denmark 99% (Tebutt, 1992; Mato, 2002) and in Germany, 70% (Mato, 2002). 52% of rural inhabitants have access to potable water mainly from groundwater sources in Ghana (Ewusi, 2006; Gyau-Boakye and Dapaah-Siakwan, 1999).

Groundwater has been found to be sufficient both in quantity and quality for most rural communities. Mygatt (2006), estimated that about 2 billion people in urban and rural communities worldwide depend on groundwater for daily consumption. The importance of groundwater will grow considerably in the future, as it is a safe and qualitatively high drinking water resource. If it is used reasonably and sustainably, it can provide an important contribution in solving regional water crises on earth.

With the increasing population explosion, increasing industrialization and agricultural growth, the demands on potable water supply have increased beyond our perception (Ariyo and Adeyemi, 2009). In many developing countries, availability of potable water has become a critical and urgent problem and it is a matter of great concern to families and communities. About 80 % of all diseases in Ghana are caused by unsafe water and poor sanitation but more than nine million people don't have access to safe drinking water (*http*://www.*wateraid.org/ghana*). Water resources in Ghana play a central role in the promotion of living standards, enhancing economic growth, provision of food security and livelihood, and eventually alleviation of poverty. As in most parts of the world, Ghana too is experiencing population growth and associated demand on food production. Therefore increases in demand for water produce stress on available water resources.

1.1.1 BACKGROUND

The climatic condition of Ghana is such that, the rainfall pattern is not uniform. It is temporal and spatially distributed. There is a season of surplus water and one of water shortage in the streams and rivers. The annual rainfall decreases towards the north and south-east of the country. This means that many rivers and streams, particularly, in the north and south-east may not be perennial. During the wet season, unsafe sources of water get more contaminated by runoff water from polluted sites. In the dry season, even the contaminated water becomes scarce since most of the streams usually dry up. This compels especially women and children to walk over long distances to look for water for domestic chores and drinking.

Rainfall harvesting cannot also be done all year round due to the seasonal and erratic rainfall pattern. This is compounded by the fact that, the storage facilities required for harvesting rainfall for use by rural families throughout the year is economically beyond their reach. It is within our comprehension that the amount of surface water cannot cope with the ever increasing demands, and the alternative source of perennial water supply lies basically in the efficient utilization of groundwater and efficient management of aquifers, hand-dug wells and boreholes.

The tapping of groundwater resources, both for drinking water supply and for irrigation purposes, date back to ancient times. The development of water resources seems to have started first in India and Egypt. Open wells for irrigation and drinking water were in common use in India as early as in the Mahabharata period, about 5000 BC to 6000 BC. Exploitation of groundwater on modern lines can be said to have started at the turn of the century. The first tube well was sunk in 1935 in Uttar Pradesh. In China, wells were drilled at least 3,000 years ago with hand operated churn drills, to depths as deep as 100 m and lined with bamboo casings. Hand-dug wells have been sunk since times immemorial, sometimes to a considerable depth, and such wells continue to be made in several parts of the world. The technology for tapping groundwater at great depth is of recent date. In order to pursue the development of groundwater, it is essential to have a reliable estimate of groundwater potential (Singh, 1985). This is possible by a systematic exploration program using modern scientific tools. The use of geophysical methods provide valuable information with respect to distribution, thickness and depth of groundwater bearing formations.

Electromagnetic (EM) profiling and VES are the two complementary, widely used geophysical methods in the delineation of basement layers and location of fissured media and associated aquiferous zones such as fractures, faults and joints in sedimentary formations (Beeson and Jones, 1988; Hazel *et al*., 1988; Okrah *et al*., 2012; Olayinka *et al*., 2004). In many instances, reconnaissance EM surveys are used to locate aquiferous zones such as fractures, faults and joints (Palacky *et al.*, 1981; Bernard and Villa, 1991), which is then complemented by a subsequently detailed use of conventional resistivity sounding method. Hopefully, such combination can greatly assist in the successful location of productive boreholes in the sedimentary formation.

The vertical electrical sounding on the other hand provides information on the vertical variation in electrical resistivity with depth. It is commonly used to assess the reliability of the features delineated from EM survey.

The dispersed communities in the Kintampo North Municipality requires a number of boreholes to meet their desired water needs. Water resources development on any scale requires careful planning for appropriate delivery. However, previous studies (Beeson and Jones, 1988; Palacky *et al.*, 1981; Okrah *et al.*, 2012; Olayinka *et al.*, 2004) have shown that an approach through integrated EM profiling and depth sounding would enhance the reliability of data interpretation and the success rate of productive boreholes. This study is focused on assessing the groundwater prospect of the area, and more importantly, the delineation of areas suitable for drilling of boreholes by using an integrated EM and VES survey.

1.2.0 STATEMENT OF THE PROBLEM

Apart from the cities and urban centres which have pipe borne water in Ghana, most rural communities depend on surface and groundwater. Even in the cities and urban centres many communities depend on shallow hand dug wells which are mostly private owned. In a recent household survey in the Kintampo North Municipality, it was established that, 4.1% of the sample population use pipe-borne water system (*http://www. kintamponorth. ghanadistricts.gov.gh*). It must be noted that only one town in the Municipality, that is, Kintampo, enjoyed the output of Small Towns Water System/Ghana Water Company Limited (GWCL) services of providing pipe borne water weekly. The community water and sanitation project (CWSP) report (2012) in the Municipality indicates that about 14 communities use water from boreholes. However, it must be said that most of these boreholes dry up in the dry season compelling most communities to revert to the old system of drinking from ponds and cut out streams. The result has been a re-occurrence of water borne diseases year after year even when improvement has previously been made. Constant breakdown of boreholes in the Kintampo North Municipality as a result of excessive consumption pressure on the few boreholes by communities also tends to lend support for more boreholes to be drilled.

The geology of the Voltaian is very complex and therefore striking groundwater in the Basin has been a difficult task for past researchers as reported by the Ghana Rural Water Project of the World Vision International (WVI). The use of multiple methods to explore for groundwater triangulates data and overcomes the vulnerability to errors linked to a single method (Patton, 1990). It is therefore hoped that with the integrated geophysical survey, good quality and reliable data will be obtained. Hence, this research would go a long way to minimize the water shortage problem of most communities in the Kintampo North Municipality.

1.3.0 JUSTIFICATION OF THE STUDY

Drilling of unproductive boreholes over the years has been a matter of concern to the inhabitants of rural communities and most importantly to donor agencies and water managers in the country.

The need for the exploration and exploitation of the weathered and fractured aquifers in the study area is necessary to identify potential sources for groundwater and this could only be achieved by a combination of detailed geological, hydrogeological and integrated geophysical studies.

1.3.1 PURPOSE AND OBJECTIVES OF THE STUDY

The objective of this study was to carry out integrated geophysical investigations that are based on the Geonics EM 34-3 conductivity meter and the ABEM Terrameter SAS 1000C resistivity equipment to:

- Determine overburden thickness / depth to bedrock estimation
- Select subsurface aquifer zones for borehole drilling
- To determine vertical variation in electrical resistivity with depth.
- locate geological formations that could be related to groundwater bodies

in thirteen (13) communities in the Kintampo North Municipality of the Brong Ahafo Region of Ghana.

1.4.0 RESEARCH HYPOTHESIS

The research hypothesis, adopted in this work is that, the Voltaian is heterogeneous and the aquifers within it are localized. Consequently, the need for delineation and identification of aquifers in the study area is very important.

1.5.0 SIGNIFICANCE OF THE STUDY

Over much of Africa, groundwater is the only realistic water supply option for meeting dispersed rural water demand. Alternative water resources can be unreliable and difficult or expensive to develop: surface water is prone to contamination, often seasonal, and needs to be piped to the point of need; rainwater harvesting is expensive and requires good rainfall throughout the year (MacDonald, 1997). These characteristics of groundwater makes it well suited to the more demand responsive and participatory approaches of rural water and sanitation programmes:

- Groundwater resources are often resistant to drought.
- Groundwater can generally be found close to the point of demand.
- Groundwater is generally of excellent natural quality and requires no prior treatment.
- Groundwater can be developed incrementally, and often accessed cheaply.
- Technology is often amenable to community operation and management.
- Groundwater is naturally protected from contamination.

Considering the numerous advantages of groundwater prospecting stated above, it is therefore not surprising that the percentage of the rural communities, which depend on boreholes and wells have increased substantially since 1984. Ghana Government, Council for Scientific and Industrial Research (CSIR), the Community Water and Sanitation Agency (CWSA) and other Non-Governmental Organizations (NGOs) such as World Vision International (WVI) Ghana have embarked on providing more boreholes to communities.

1.6.0 SCOPE OF THE WORK

This project involves an integrated geophysical survey using the electromagnetic method for investigating ground conductivity and vertical electrical sounding to measure apparent resistivity with change in vertical variation to delineate groundwater potential zones within the Kintampo North Municipality. The project work was carried out as part of the Water Research Institute (WRI) of the Council for Scientific and Industrial Research's Groundwater Division (CSIR-GWD) groundwater survey project in the Brong-Ahafo Region. The project work is therefore made up of the geophysical field survey work in the communities in the study area, analysis, modeling, quantitative and qualitative interpretation of the results.

1.7.0 METHODOLOGY

A desk study was the first step in this research. The next was a Reconnaissance Survey of beneficiary communities and its immediate neighbourhood to update baseline information, location of target areas for geophysical surveys, hydrogeological survey of the area and terrain assessment. The last step was Processing, Analysis and Interpretation of Data. These encompasses field measurements and interpretation of the results for inference on the potential sites for drilling boreholes. It involves a combination of geological, hydrogeological, geophysical, and socio-cultural experience, right judgment and other considerations to select the most suitable site for drilling. Community participation was vital to the sustainability of boreholes as such, they always become the integral part of the processes leading to the final selection of sites for drilling.

CHAPTER TWO

LITERATURE REVIEW

2.1.0 INTRODUCTION

Ghana has ample surface water resources, however, these resources are unable to satisfy the water demand for socio-economic development everywhere in the country (Kortatsi, 1994). Hence there is increased groundwater exploration activities in the country.

The science of Geophysics applies the principles of physics to study the earth. The basic aim of a geophysical investigation is to study the subsurface geological formation by measuring physical field(s) on or beneath the surface, in the borehole or in the air. The available physical fields used for such investigations are electrical, seismic wave field, gravity, magnetic, etc. Some of these fields are generated by an active experiment such as seismic, electrical and electromagnetic whereas other fields are passive which do not require any man made source. Characteristics of these physical fields are governed by the properties of the medium in which they propagate, as well as their source. It is the medium property which is determined by geophysical techniques and this is subsequently interpreted in terms of subsurface geological formation. The highly varying of all the physical properties of geological formation is the electrical resistivity/conductivity. Accordingly, electrical resistivity/conductivity methods have extensively been used in solving various problems related to the geohydrological investigations (Keller and Frischknecht, 1966). Integrated electromagnetic and electrical resistivity survey is the most effective and economic technique for solving various problems related to groundwater investigation and in estimating the hydrogeological parameters.

Groundwater is characterized by some physical parameters that are determined by geophysical methods like electrical resistivity, magnetic and gravity. These parameters include: permeability, porosity, transmisivity and conductivity. This work however involve the application of electromagnetic and electrical resistivity to investigate the groundwater potential at selected communities in the Kintampo North Municipality. Geophysical survey involving Electrical resistivity and Electromagnetic methods constitute the most reliable means outside direct mechanical drilling through which sedimentary structures such as fractures, joints/faults or weathered zone that are of hydrogeological significance can be mapped (Vanderberghe, 1982).

2.2.0 The Electromagnetic Method

Among the widely used geophysical methods, EM methods have been identified as good for detecting and delineating fracture zones (Chegbeleh *et al*., 2009). The EM systems as stated in (McNeil and Snelgrove, 1986) were originally developed for mineral exploration and later discovered to be very capable of detecting and measuring the small conductivity changes caused by the presence and quality of groundwater. They have also been used to detect geological structures favourable for groundwater such as faults and fracture zones.

The basic field equipment used for the EM survey, consist of a battery, a transmitter coil about 800 mm in diameter, a distance measuring device, a receiver coil and a volt meter connected to the receiver coil. The distance between transmitter and receiver coils is measured electronically and set at 10 m, 20 m and 40 m spacing. The coils are placed at a known distance apart and coupled, either both horizontally or vertically on the ground. The transmitter is turn on, the distance between the transmitter and the receiver is adjusted and the apparent terrain conductivity is read directly off the receiver. When both coils are placed horizontally on the ground, the transmitter generates an electrical field with a vertical dipole, so this is called the vertical dipole mode. Similarly when the coils are vertical the equipment is in the horizontal dipole mode. The vertical dipole mode has a greater penetration than the horizontal dipole mode. With a 40 m coil spacing and the coil in vertical dipole mode, the equipment can penetrate to a maximum depth of 60 m.

2.2.1 Brief Historical Background of the Electromagnetic Method

The magnetic and gravity methods are usually described as passive methods in that the source of the field is generated by the earth itself and only measurement of it and its perturbations are required. The electrical and electromagnetic methods to be discussed next are usually considered as active methods because a controlled source is used to create electric or magnetic fields which interact with the earth and the response is measured (Sharma, 1999). With the notable exception of techniques that use electromagnetic fields caused by natural sources, most of the methods described next use electrodes to inject current into the ground, or loops of alternating current to create alternating magnetic fields which in turn create currents in the ground through Faraday's law of induction. For all the electric and EM methods the objective and underlying principles are the same. The goal is to map the distribution of electrical conductivity and the means is to measure the fields created when current is made to flow in the ground (Reynolds, 1997). The electrical resistivity method is formally the low frequency limit of the general electromagnetic method in which the time rate of change of any magnetic fields is so small that Faraday induction can be ignored.

2.2.2 General Principle of the Electromagnetic Method

Electromagnetic (EM) surveying methods make use of the response of the ground to the propagation of electromagnetic fields, which are composed of an alternating electric intensity and magnetizing force (Kearey *et al.*, 2002). Primary electromagnetic fields may be generated by passing alternating current through a small coil made up of many turns of wire or through a large loop of wire. The response of the ground is the generation of secondary electromagnetic fields and the resultant fields may be detected by the alternating currents that they induce to flow in a receiver coil by the process of electromagnetic induction. The primary electromagnetic field travels from the transmitter coil to the receiver coil via paths both above and below the surface (Fig. 2.1). Where the subsurface is homogeneous, there is no difference between the fields propagated above the surface and through the ground other than a slight reduction in amplitude of the latter with respect to the former. However, in the presence of a conducting body the magnetic component of the electromagnetic field penetrating the ground induces alternating currents, or eddy currents, to flow in the conductor

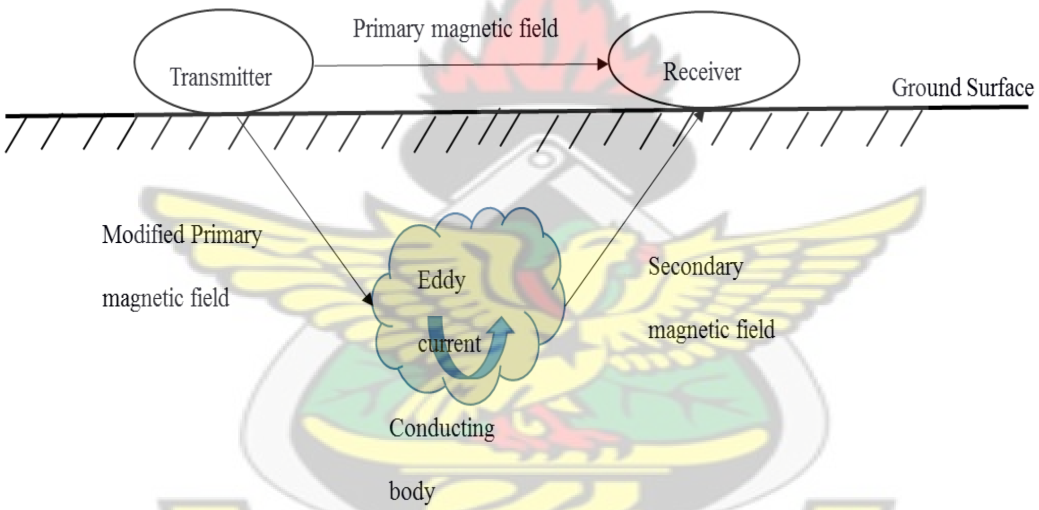

Fig. 2.1 General Principle of the Electromagnetic Method (modified after Kearey and Brooks, 1987).

The eddy currents generate their own secondary electromagnetic field which travels to the receiver. The receiver then responds to the resultant of the arriving primary and secondary fields so that the response differs in both phase and amplitude from the response to the primary field alone. These differences between the transmitted and received electromagnetic fields reveal the presence of the conductor and provide information on its geometry and electrical properties (Kearey *et al.*, 2002).

2.2.3 Theory of the Electromagnetic Method

The propagation and attenuation of electromagnetic waves can be illustrated using Maxwell's equations in a form which relates these four electric and magnetic field vectors: ***E, H, B,*** and ***D***. such that,

$$\nabla \times E = -\frac{\partial B}{\partial T} \quad (1)$$

$$\nabla \times H = J + \frac{\partial D}{\partial t} \quad (2)$$

$$\nabla . B = 0 \quad (3)$$

$$\nabla . D = Q \quad (4)$$

Where E is the electric field intensity (Vm^{-1})

B is the magnetic flux density (Wbm^{-2} or Tesla)

H **i**s the magnetic field density (Am^{-1})

J is the current density (Am^{-2})

D is the electric displacement (Cm^{-2})

Q is the electric charge density (Cm^{-3})

From the above mathematical statements,

Equation (1) is simply Faraday's law of electromagnetic induction; which states that electric field exists in a region of a time-varying magnetic field, such that the induced e.m.f is proportional to the negative rate of change of magnetic flux.

Equation (2) contains the statement of Ampere's law: every current flow produces a magnetic field around itself, which is proportional to the total current (conduction plus displacement current). Equation (3) simply states that isolated magnetic poles (magnetic single poles) do not exist. Equation (4) is the mathematical statement of Coulomb's law: the lines of electric field start from and end on electric charges.

A time-varying magnetic field arising from alternating current in the transmitter coil, $\boldsymbol{T_x}$ induces a very small currents in the earth (assumed uniform). These induced currents generate a secondary magnetic field, $\boldsymbol{H_s}$ which is sensed, together with the primary field, $\boldsymbol{H_p}$ by the receiver coil, $\boldsymbol{R_x}$ located at a short distance, S from the transmitter coil as in Fig. 2.2 (McNeil, 1980).

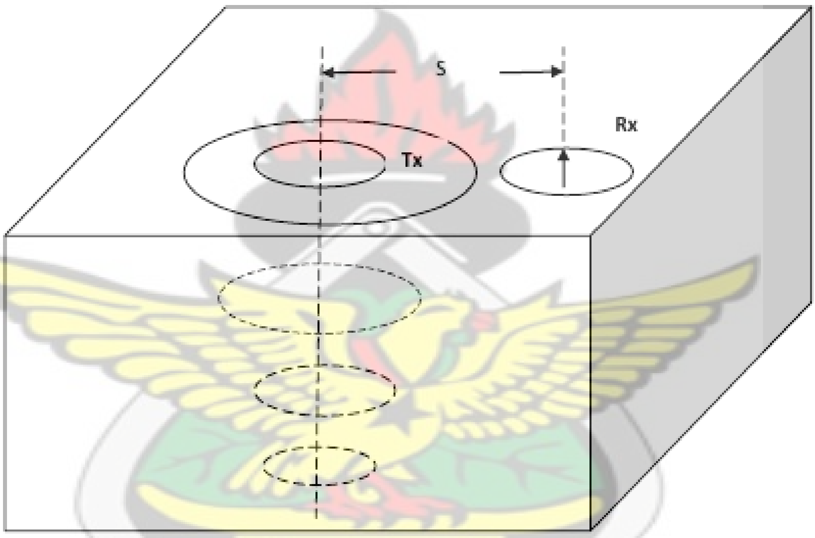

Fig. 2.2 Induced current flow in homogenous half space (modified after McNeil, 1980)

In general the secondary magnetic field, $\boldsymbol{H_s}$, is a complicated function of the intercoil spacing **s**, the operating frequency **f**, and the ground conductivity **σ**. However under certain constraints, the secondary magnetic field $\boldsymbol{H_s}$ is a very simple function of these variables. The constraints (condition of low induction numbers) are incorporated in the design of the GEONICS EM 34-3 equipment so that the secondary magnetic field is given by

$$\frac{H_S}{H_P} = \frac{i\omega\mu_o\sigma s^2}{4}$$

(5)

Where $\boldsymbol{H_s}$ = Secondary magnetic field at the receiver coil,

$\boldsymbol{H_p}$ = Primary magnetic field at the receiver coil,

$i = \sqrt{-1}$

$\omega = 2\pi f$

f = frequency (Hz)

μ_o = permeability of free space,

σ = ground conductivity (mmhom^{-1})

s = intercoil spacing (m)

The ratio of the secondary to the primary magnetic field is now linearly proportional to the terrain conductivity, σ. This is a fact, which makes it possible to construct linear terrain conductivity meter to give a direct reading by simply measuring the ratio. Given H_S/H_P, the apparent conductivity, σ_a, indicated by the instrument is defined as

$$\sigma_a = \left(\frac{4}{\omega\mu_o s^2}\right) x \left(\frac{H_S}{H_P}\right) \tag{6}$$

Where σ_a is in m.mho (Siemen) per meter or milliohm per meter.

Substituting $\omega = 2\pi f$ into (6)

We obtain $$\sigma_a = \left(\frac{4}{2\pi f\mu_o s^2}\right) x \left(\frac{H_S}{H_P}\right)$$

So that, $$\sigma_a = \left(\frac{2}{\pi f\mu_o s^2}\right) x \left(\frac{H_S}{H_P}\right) \tag{7}$$

This gives the apparent conductivity, σ_a in terms of the frequency, f and intercoil spacing, s.

$$\text{For} \quad k = \left(\frac{4}{2\pi f \mu_o s^2} \right)$$

$$\text{Leads to} \qquad \sigma_a = k \, x \left(\frac{H_S}{H_P} \right)$$

$$\text{Where} \quad k = \left(\frac{4}{2\pi f \mu_o s^2} \right) = \text{constant}$$

2.2.4 Physical Quantities and Field Equations

In homogenous isotropic media the physical quantities relating the electric and magnetic field vectors are: $D = \varepsilon E$ (8)

$$B = \mu H \tag{9}$$

$$J = \sigma E \tag{10}$$

Where ε is the dielectric permittivity (Fm^{-1}), **μ** is the magnetic permeability (H/m), and **σ** is the electric conductivity of the medium (mmhom^{-1}). By using these relationships we can reduce or simplify Maxwell's Equations in terms of only two vectors, ***E*** and ***H***. Furthermore, by assuming for ***E*** and ***H*** a time dependence of the form

$$E(t) = E_o e^{i\omega t} \tag{11}$$

When equations (8) and (9) takes the following form,

$$\nabla^2 E = i\omega\mu\sigma E - \varepsilon\mu\omega^2 E \tag{12}$$

$$\nabla^2 H = i\omega\mu\sigma H - \varepsilon\mu\omega^2 H \tag{13}$$

Where $\omega = 2\pi f$ is the angular frequency of the field.

These are basic equations for propagation of electric and magnetic field vectors in an isotropic homogenous medium with physical properties ε, μ, and σ. In air and poorly conducting rocks $\sigma = 0$; $\varepsilon = \varepsilon_o = 8.85 \times 10^{-12}\,\mathrm{Fm}^{-1}$ and $\mu = \mu_o = 4\pi \times 10^{-7}\,\mathrm{Hm}^{-1}$.

With these small values, both the real and imaginary parts become so small that the right-hand side of the equations (12) and (13) are practically zero. Therefore, for non-conducting media or rocks the field equations become

$$\nabla^2 E = 0, \text{ and } \nabla^2 H = 0 \tag{14}$$

However, in media of moderate to high conductivity such as saline water, massive sulphide and graphite we have $\sigma \approx 1 - 10^{-3}$ $\mathrm{mhom}^{-1}, \varepsilon \approx 10\varepsilon_o$ and $\mu = \mu_o$. With these values the first terms on the right-hand side of equations (12) and (13) become quite significant, but the second terms are still negligible. Therefore, in media or rocks of appreciable or finite conductivity, the equations are simplified to

$$\nabla^2 E = i\omega\mu\sigma E \tag{15}$$

$$\nabla^2 H = i\omega\mu\sigma H \tag{16}$$

The relative magnitude of the term $\omega\mu\sigma$ is of great physical significance, both with regard to the attenuation of electromagnetic fields and the generation of induced fields (Sharma, 1986).

2.2.5 Electromagnetic Field Attenuation

According to Sheriff (1991), attenuation is the reduction in amplitude or energy caused by the physical characteristics of the transmitting media or system, including geometric effects such as the decrease in amplitude of a wave with increasing distance from the source. As stated by Telford *et al.*, (1994), the electromagnetic wave is attenuated when travelling through some media but not in free space.

This attenuation is due to the interaction of the electromagnetic waves with matter as the waves are propagated through it. There is therefore, a decrease in amplitude or energy of the waves.

The amplitude of a plane wave is reduced by the factor $e^{-\alpha z}$ in travelling a distance of Z m, where the attenuation factor is α (Sheriff, 1991). The attenuation factor (α) is given by

$$\alpha = \sqrt{\left(\frac{\omega\mu\sigma}{2}\right)} \qquad (17)$$

The physical meaning of the attenuation factor as stated by (Telford *et al.,* 1994) is that when α is small, the magnetic field will propagate through the medium without much attenuation and in the process fail to induce any appreciable current flow in it. As a result, very little secondary magnetic field will be generated. But when α is large, the large surface creates a large secondary magnetic field, out of phase with the original, which partially or completely cancels the primary field. Since $\omega = 2\pi f$, α is frequency dependent (as well as conductivity, σ). Thus the rate of attenuation depends on the frequency and the electrical properties of the rock material through which the electromagnetic wave travels. Therefore, the higher the frequency, the greater the rate of attenuation (Dobrin and Savit, 1988).

2.2.6 Depth of Penetration of Electromagnetic Fields

The skin depth, Z_s is the depth at which the amplitude of the field A_z, is decreased by the factor $\frac{1}{e}$ or 37% relative to its initial or surface amplitude A_o, ($A_z = A_o e^{-1}$). The skin depth of electromagnetic field depends on its frequency and the electrical conductivity of the medium through which it is propagating (Kearey *et al.*, 2002). But the attenuation factor, α

also depends on frequency and electrical conductivity. The depth of penetration, Z_s will in turn depend on the attenuation factor, α. The depth of penetration is given by

$$Z_s = \frac{1}{\alpha} \quad \text{and} \quad Z_s = \frac{1}{\sqrt{\left(\frac{\omega\mu\sigma}{2}\right)}}$$

Since $\omega = 2\pi f$ and $\mu = \mu_o = 4\pi \times 10^{-1} Hm^{-1}$

$$Z_s = \frac{503.8}{\sqrt{\sigma f}} = 503.8(\sigma f)^{-1/2} \tag{18}$$

Where Z_s is in metres (m), σ in Siemen per metre (Sm^{-1}) and f in Hertz (Hz).

The skin depth increases as both the frequency of the electromagnetic field and the conductivity of the ground decreases. Therefore, the frequency dependence of the depth of penetration places constraints on the electromagnetic method. This is because very low frequencies are difficult to generate and measure (Kearey and Brooks, 1987). Additionally, electromagnetic methods are limited by depth of the induced current penetration, hence the electromagnetic methods are unsuitable for oil exploration because of the depth penetration limitation (Robinson and Coruh, 1988).

2.2.7 Electrical Conductivity in Rocks

The electrical conductivity in rocks is electrolytic (ionic), electronic (metallic) and dielectric (insulators). The electrical conductivity (σ) of a substance is a measure of how easy or how difficult an electrical current can be made to flow through it. Except for metallic minerals, graphite's and clay, most soil materials are poor conductors. Hence any significant current flow in these soils is mainly due to the water they may contain and its ionic content. It is expressed mathematically as (McNeil *et al.*, 1995):

$$\sigma = \frac{GL}{A}, \quad \text{mhos/m.} \tag{19}$$

Where $G = \frac{I}{V}$, mhos, A = area, V = voltage, I = current, L = distance between electrodes and

G = conductance.

Most soil and rock minerals are electrical insulators with very high resistivities. However, on some rare occasions, conductive minerals such as magnetite, speculum's hematite, carbon, graphite, pyrite and pyrrhotite occur in sufficient quantities in rocks to greatly increase their overall conductivity. This note assumes that minerals are absent (McNeil, 1980). So that the effective resistivity of a rock can then be expressed empirically in terms of the resistivity and volume of the pore water present, as in Archie's law.

$$\rho_e = a\Phi^{-m}S^{-n}\rho_w \tag{20}$$

where ρ_e is the effective resistivity of the rock, Φ is the fractional pore volume (porosity), S is the fraction of the pores containing water, ρ_w is the resistivity of water in pores, n = 2, and a and m are empirical constants: $0.5 \le a \le 2.5, 1.3 \le m \le 2.5$. But ρ_w can vary considerably according to the quantities and conductivities of dissolved salts as chlorides, sulphates, and other minerals present. Electrical conductivity is, therefore, determined (McNeil, 1980) for both rocks and soils by

- Porosity: shape and size of pores, number, size and shape of interconnecting passages
- The extent to which pores are filled by water that is, the moisture content
- The concentration of dissolved electrolytes in the contained moisture
- Temperature and phase state of the pore water and
- Amount and composition of colloids (McNeil, 1980)

2.2.8 The Electromagnetic Method in Groundwater Prospecting

In areas where groundwater occurrences are structurally controlled as in the Voltaian, it is suitable to use a method that is sensitive to fractures. EM methods have been identified to be good for detecting and delineating fracture zones. They have also been used to detect geological structures favourable for groundwater such as faults and fracture zones with successful results (Chegbeleh *et al.*, 2009; Okrah *et al.*, 2012). In areas with shallow depth to the bedrock, fracture zones which are often vertical or slightly dipping conducting sheets, are most often the target in water prospecting (Singhal and Gupta, 1999).

2.2.9 Principle of the Resistivity Method

The principle is that resistivity varies depending on the material encountered. And that the distribution of electrical potential in the ground around a current-carrying electrode depends on the electrical resistivities and distribution of the surrounding soils and rocks.

The purpose of electrical surveys is to determine the subsurface resistivity distribution by making measurements on the ground surface. From these measurements, the true resistivity of the subsurface can be estimated. The ground resistivity is related to various geological parameters such as the mineral and fluid content, porosity and degree of water saturation in the rock. Electrical resistivity surveys have been used for many decades in hydrogeological, mining and geotechnical investigations. More recently, it has been used for environmental surveys.

The resistivity measurements are normally made by injecting current into the ground through two current electrodes (C_1 and C_2) as in Fig. 2.3, and measuring the resulting voltage difference at two potential electrodes (P1 and P2).

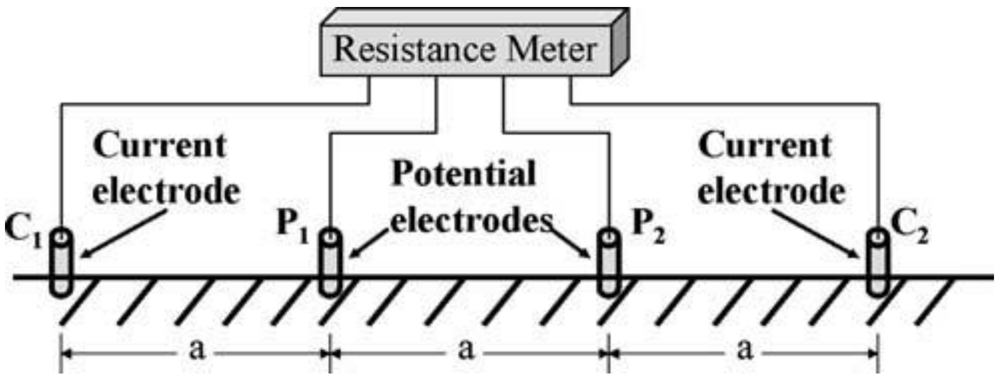

Fig. 2.3 Conventional four electrode array to measure the subsurface resistivity (Modified after Rhoades and Halvorson, 1977).

From the current (I) and voltage (V) values, an apparent resistivity (ρ_a) value is calculated.

$$\rho_a = \frac{kV}{I} \tag{21}$$

Where k is the geometric factor which depends on the arrangement of the four electrodes as shown in Fig. 2.4.

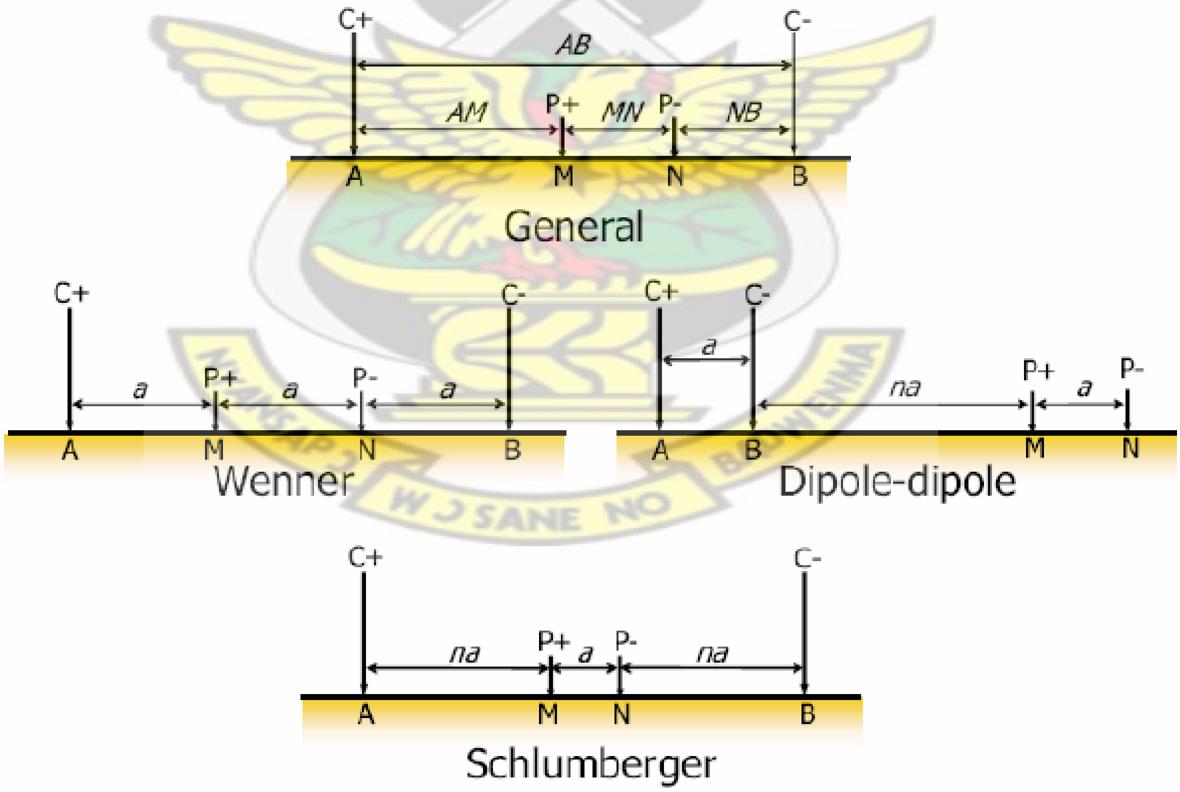

Fig. 2.4 Common arrays used in resistivity surveys (Modified after Berkeley, 2002).

Resistivity meters normally give a resistance value, R = V/I, so in practice the apparent resistivity value is calculated by, $\rho_a = kR$, where k is the geo-electric factor.

The calculated resistivity value is not the true resistivity of the subsurface but an "apparent" value, which is the resistivity of a homogeneous ground which will give the same resistance for the same electrode arrangement. The relationship between the "apparent" resistivity and the "true" resistivity is a complex relationship. To determine the true subsurface resistivity, an inversion of the measured apparent resistivity values using a computer program RES1D was carried out.

2.2.10 Theory of the Electrical Resistivity Method

For a geometrically ideal situation with a current through a homogenous media in a well-defined uniform cross section between two potential electrodes, using the ohms law, the resistance R is given by $R = \frac{V}{I}$.

Where R is the resistance, V is the voltage and I is the current.

The resistance is also proportional to the cross sectional area and the distance between the electrodes and the relationship is given by $R = \frac{\rho L}{A}$.

Combining the two equations, $\frac{V}{I} = \frac{\rho L}{A}$. Where A is the cross sectional area, V is the voltage, I is the current and L is the distance between the electrodes.

The constant of proportionality ρ is the apparent resistivity and data from resistivity surveys are represented by apparent resistivity which takes into account, the arrangement and spacing of electrodes. From the relationship above the potential at any point is given by

$$V = \frac{\rho I}{2\pi r}.$$

Where V is the potential in volts, ρ is the resistivity of the medium and r is the distance from the electrode. For an electrode pair with current I at electrode C_1, and -I at electrode C_2 as shown in Fig. 2.5 below,

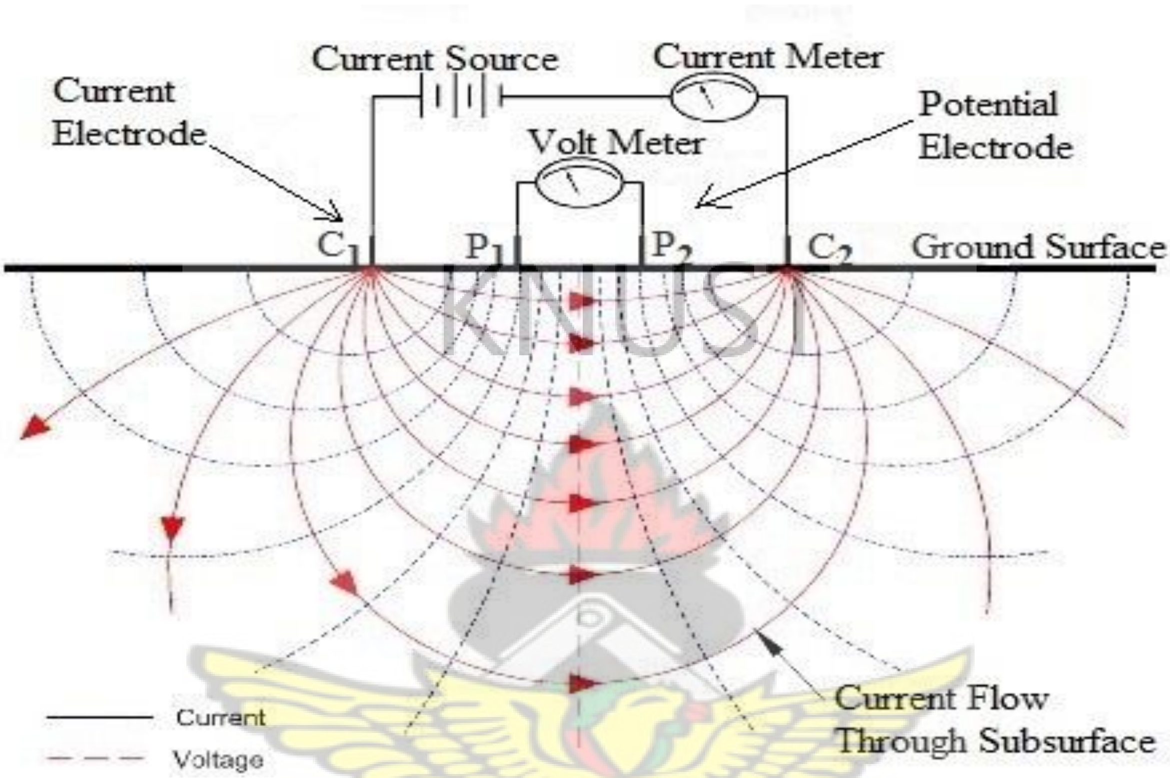

Fig. 2.5 Current flow pattern in a resistivity survey (http://en.openei.org/wiki/Direct-Current_Resistivity_Survey)

The resistivity of the ground is calculated from the potential difference between P_1 and P_2. The potential V_{P1} at the internal electrode P_1 is given by the algebraic sum of the potential contributions V_{C1} and V_{C2} from the current source at C_1 and the sink at C_2.

$$V_{P1} = V_{C1} + V_{C2}$$

The potentials at electrode P1 and P2 are

$$V_{P1} = \frac{\rho I}{2\pi}\left(\frac{1}{C_1P_1} - \frac{1}{C_2P_1}\right) \text{ and}$$

$$V_{P2} = \frac{\rho I}{2\pi}\left(\frac{1}{C_1P_2} - \frac{1}{C_2P_2}\right)$$

The two pairs of electrodes P_1 and P_2 (Fig. 2.5) carry no current but are used to measure the potential difference between the points P1 and P2. The change in potential ΔV may be measured as:

$$\Delta V = V_{P1} - V_{P2} = \frac{\rho I}{2\pi}\left(\frac{1}{C_1P_1} - \frac{1}{C_2P_1} - \frac{1}{C_1P_2} + \frac{1}{C_2P_2}\right)$$

$$\rho = \frac{\Delta V 2\pi}{I\left(\frac{1}{C_1P_1} - \frac{1}{C_2P_1} - \frac{1}{C_1P_2} + \frac{1}{C_2P_2}\right)}$$

Where $k = \quad 2\pi\left(\frac{1}{C_1P_1} - \frac{1}{C_2P_1} - \frac{1}{C_1P_2} + \frac{1}{C_2P_2}\right)^{-1}$

is the geometric factor, and is only a function of the geometry of the electrode arrangement. Resistivity can be found from measuring values of V, I and k. So the apparent resistivity (ρ_a) equation becomes,

$$\rho_a = \frac{\Delta V 2\pi}{I}\left(\frac{1}{\frac{1}{C_1P_1} - \frac{1}{C_1P_2} - \frac{1}{C_2P_1} + \frac{1}{C_2P_2}}\right).$$

In a Schlumberger array where **'a'** is the space between the potential electrodes (Fig. 2.6), the geometric factor is as indicated in Table 2.0.

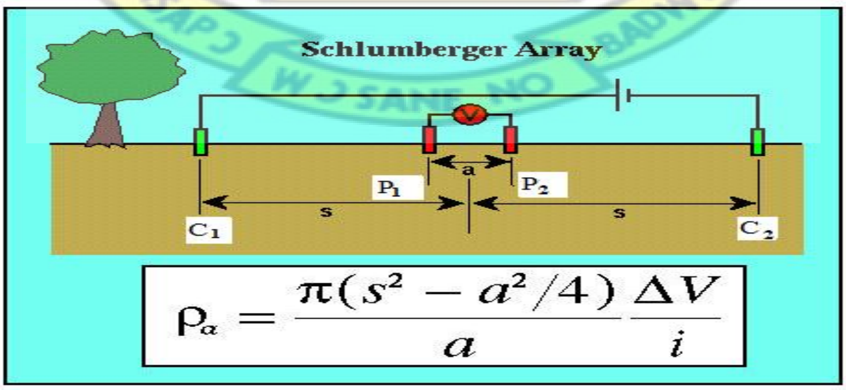

Fig. 2.6 Schlumberger Array (Modified after Berkeley, 2002).

Since geological materials are very rarely homogenous, the value obtained from the equation above is called the apparent resistivity (ρ_a). To estimate the real resistivity in the ground, an inversion of the measured apparent resistivity values is made (Parasnis, 1986).

Table 2.0: Geometric factor (k) for some common configurations (Vogelsang, 1994).

Array	**Geometric factor k**
Wenner	$2\pi a$
Schlumberger	$\frac{\pi}{a}\left[\left(\frac{2s}{2}\right)^2 - \left(\frac{a}{2}\right)^2\right]$
Dipole-dipole	$\pi n(n+1)(n+2)a$

Where: a = potential electrode spacing (P_1P_2)

S = half current electrode spacing (C_1C_2 / 2)

n = 1, 2, 3 …etc

2.2.11 The Resistivity Method in Groundwater Prospecting

Electrical resistivity techniques have been used in many geological formations for characterizing the subsurface for many years (Roman, 1951; and Heather *et al*., 1999). In the earlier applications, the technique was considered to be very labour intensive. The development of the multi-electrode surveys has been able to reduce this aspect of the survey (Heather *et al*., 1999).

Groundwater, through the various dissolved salts it contains, is ionically conductive and enables electric currents to flow into the ground. By measuring the ground and subsurface resistivity therefore gives the possibility to identify conditions necessary for the presence or otherwise of water. Resistivities of rocks generally depend on the water content (porosity), the resistivity of the water, the clay content and the content of metallic minerals (Bernard, 2003). The following considerations help in the determination of the resistivity of rocks.

- A hard rock without pores or fractures is very resistive to the flow of electric current. This is generally observed in hard fresh Precambrian rocks.
- Dry sand without water is very resistive.
- Porous or fractured rock bearing free water has resistivity, which depends on the resistivity of the water and on the porosity of the rock.
- Impermeable clay layer, which is wet, has low resistivity but may not contain enough yields for successful groundwater exploitation.
- Mineral ore bodies (iron, sulphides) have very low resistivity due to their electronic conduction; usually lower or much lower than 1Ωm^{-1} (Bernard, 2003).

To identify the conditions necessary for the presence of groundwater from resistivity measurements, the absolute value of the ground resistivity must be considered. Usual target for aquifer resistivity can be between 50 Ωm to 2000 Ωm. (Bernard, 2003).

- In hard rock environment, which is considered very resistant to the flow of electric current, a low resistivity anomaly will be the target for groundwater.
- In a clayey or salty environment that is normally considered conductive, a comparatively high conductivity anomaly will most probably correspond to fresh water and thus will be the target in the case for groundwater exploration for domestic use.

Resistivity values of earth materials cover a wide range. The variety of resistivity has been the essential reason why the technique can be used for different applications (Loke, 2001).

In resistivity measurements, highest resistivities are associated with igneous rocks. Sedimentary rocks tend to be most conductive due to their high fluid content. Metamorphic rocks have intermediate resistivities (see Table 2.1). Granites and quartzite have high resistivity ranges; sandstone and shale have intermediate resistivity ranges (Bernard, 2003). The resistivity therefore in a particular geological environment has an influence on the aquifer resistivity.

Table 2.1: Resistivity values of some common rocks, minerals and chemicals (Loke, 1999).

Material	Resistivity (ohm.m)	Conductivity (Siemen/m)
Igneous & metamorphic rocks	$5x10^{3}$ - 10^{6}	10^{-6} – $2x10^{-4}$
Granite	10^{3} – 10^{6}	10^{-6} – 10^{-3}
Basalt	$6x10^{2}$ – $4x10^{7}$	$2.5x10^{-8}$ – 10^{-3}
Slate	10^{2} – $2.5x10^{8}$	$4x10^{-9}$ – 10^{-2}
Marble	10^{2} – $2x10^{8}$	$5x10^{-9}$ – 10^{-2}
quartzite		
Sedimentary rocks		
Sandstone	8– $4x10^{3}$	$2.5x10^{-4}$ – 0.125
Shale	20 – $2x10^{3}$	$5x10^{-4}$ – 0.05
Limestone	50 – $4x10^{2}$	$2.5x10^{-3}$ – 0.02
Soils and water		
Clay	1 – 100	0.01 – 1
Alluvium	10 – 800	$1.25x10^{-3}$ – 0.1
Groundwater (fresh)	10 – 100	0.01 – 0.1
Sea water	0.2	5
Chemicals		
Iron	$9.074x10^{-8}$	$1.102x10^{7}$
0.01 M Potassium chloride	0.708	1.413
0.01 M Sodium chloride	0.843	1.185
0.01 M Acetic acid	6.13	0.163
Xylene	$6.998x10^{16}$	$1.429x10^{-17}$

2.2.12 Geophysical Methods used in Groundwater Prospecting

There are several different geophysical methods that can be used during groundwater exploration. For estimating physical vertical changes in the ground, e.g. how the weathering zone thickens and where the groundwater table is located, the electrical methods (resistivity and electromagnetic methods) are the most appropriate. If the goal is to find vertical structures like, fracture zones, Electromagnetic methods, Remote Sensing, Resistivity methods may be suitable (Singhal and Gupta, 1999). Electromagnetic and resistivity methods have been widely used in groundwater prospecting due to the close good correlation and relationship between electrical conductivity and hydrological parameter (Goldmann and Neubauer, 2004). Therefore, an integrated use of electromagnetic (EM 34-3) and direct-current (DC) resistivity techniques have the potential to be successful (Bernard and Valla, 1991). The electromagnetic terrain conductivity method (EM 34-3) has also been used as a fast reconnaissance tool to identify areas of possible linear features such as joints and fracture zones (McNeil, 1990) before resistivity soundings. Application of Schlumberger resistivity sounding is well known for determining resistivity variation with depth to the aquifer (Okrah *et al*., 2012).

2.3.0 The Underground Water

Underground water includes all water that occurs below the earth's surface, occupying interstices or voids of pervious rocks and soil; like surface water, it is derived principally from precipitation that falls upon the earth's surface and percolates downward under gravity (*http://www.tshaonline.org/handbood/online/articles/gru01*). Underground water in the zone of saturation may occur in either water table (unconfined) aquifers or artesian (confined) aquifers. Confined water is generally under pressure greater than atmospheric pressure, and wells penetrating a confined aquifer will permit water to rise above the confining strata. If sufficient pressure exists, flowing wells may result. In the case of water table aquifers, water is derived from local precipitation; but in the case of artesian wells, water may enter the permeable strata ten or even hundreds of miles from the point where it is intercepted by wells.

While the definition of groundwater as the water contained beneath the surface in rocks and soil is conceptually simple and convenient, in practice the picture is more complex, and confusion can arise. The water beneath the ground surface includes that contained in the soil, that in the intermediate unsaturated zone below the soil, that comprising the capillary fringe and that below the water table.

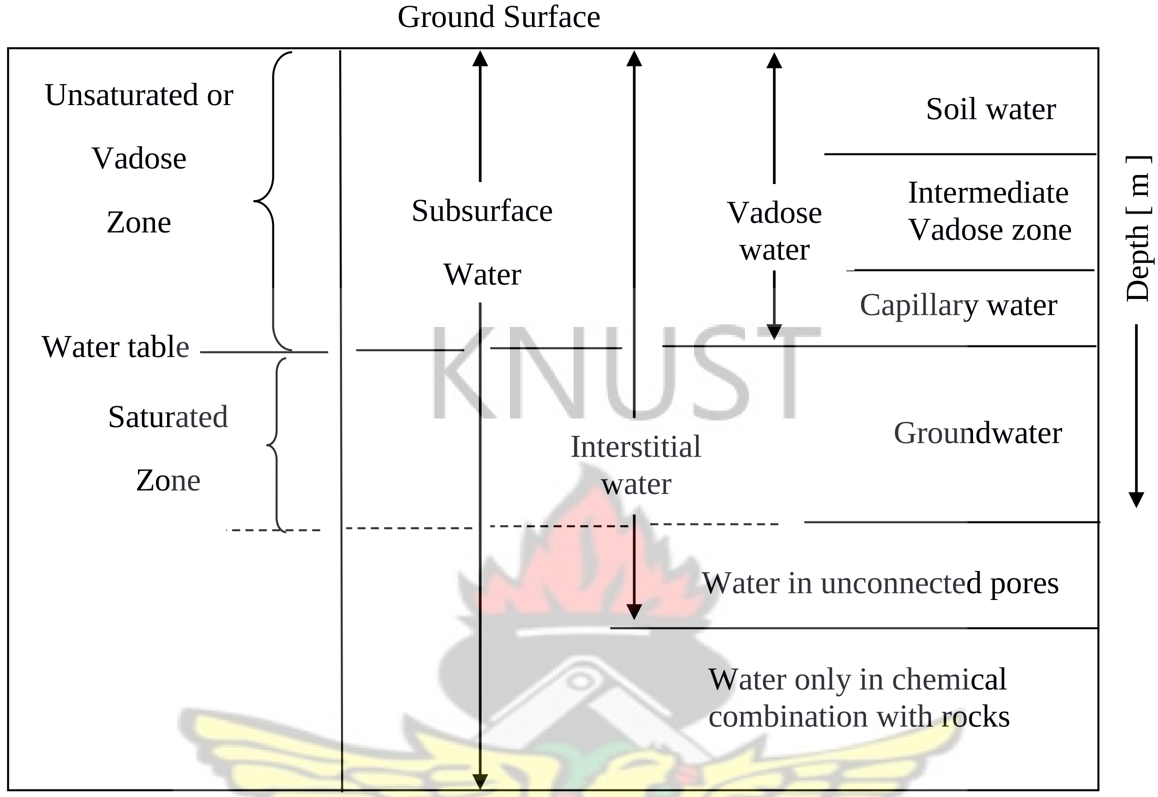

Fig. 2.7 Classification of sub-surface water (Modified after Driscoll, 1986).

The soil is commonly understood to comprise the broken down and weathered rock and decaying plant debris at the ground surface. The region between the soil and the water table is commonly referred to as the unsaturated zone or sometimes the vadose zone (Driscoll, 1986).

Strictly speaking, therefore, groundwater refers only to water in the saturated zone beneath the water table, and the total water column beneath the Earth's surface is usually called subsurface water (Fig. 2.7). In practice, of course, the saturated and unsaturated zones are connected, and the position of the water table fluctuates seasonally and with the effects of groundwater abstraction.

2.3.1 Introduction to Groundwater

Groundwater is a mysterious nature's hidden treasure. Its exploitation has continued to remain an important issue due to its unalloyed needs. Though there are other sources of water; streams, rivers ponds, etc., none is as hygienic as groundwater because groundwater has an excellent natural microbiological quality and generally adequate chemical quality for most uses (MacDonald *et al*., 1997). To unravel the mystery of groundwater, a detailed geological and hydro-geological understanding of the aquifer types and their spatial location are paramount in order to characterize the hydric zones in an area.

2.3.2 Groundwater Occurrence and Accumulation

Groundwater occurs in many different geological formations. Nearly all rocks in the upper part of the Earth's crust, whatever their type, origin or age, possess openings called pores or voids. It is in these openings that groundwater occupies. Aquifers are geologic formations that are capable of yielding economic quantities of water to wells and boreholes. The volume of water that can be contained in the rock depends on the proportion of these openings or pores in a given volume of rock, and this is termed the porosity of the rock. The porosity of a geological material is the ratio of the volume of the voids to the total volume, expressed as a decimal fraction or percentage. Increasing pore space results in higher porosity and greater potential to store water. Typical porosity ranges are shown in Table 2.2 for common geological materials.

Table 2.2. Porosity and specific yield of geological materials (Freeze and Cherry, 1979).

Material	Porosity	Specific yield
Unconsolidated sediments		
Gravel	0.25 – 0.35	0.16 – 0.23
Coarse sand	0.30 – 0.45	0.1 – 0.22
Fine sand	0.26 – 0.5	0.1 – 0.25
Silt	0.35 – 0.5	0.05 – 0.1
Clay	0.45 – 0.55	0.01 – 0.03
Sand and gravel	0.2 – 0.3	0.1 – 0.2
Glacial till	0.2 – 0.3	0.05 – 0.15
Consolidated sediments		
Sandstone	0.05 – 0.3	0.03 – 0.15
Siltstone	0.2 – 0.4	0.05 – 0.1
Limestone and dolomite	0.01 – 0.25	0.005 – 0.1
Karstic limestone	0.05 – 0.35	0.02 – 0.15
Shale	0.01 – 0.1	0.005 – 0.05
Igneous and metamorphic rocks		
Vesicular basalt	0.1 – 0.4	0.05 – 0.15
Fractured basalt	0.05 – 0.3	0.02 – 0.1
Tuff	0.1 – 0.55	0.05 – 0.2
Fresh granite and gneiss	0.0001 – 0.03	<0.001
Weathered granite and gneiss	0.05 – 0.25	0.005 – 0.05

Not all of the water contained in fully saturated pore spaces can be abstracted by wells and boreholes and used. Under the influence of gravity when, for example, the water level falls, some of the water drains from the pores but some remains, held by surface tension and molecular effects. The ratio of the water that drains by gravity from an initially saturated rock mass to its own total volume is defined as the specific yield of the material, and typical values are also shown in Table 2.2.

Another important way of distinguishing aquifers and the way in which groundwater occurs, when considering both its development and protection, is shown in Fig. 2.8. In Fig. 2.8, an unconfined aquifer is one in which the upper limit of the zone in which all the pore spaces are fully saturated, i.e. the water table, is at atmospheric pressure. At any depth below the water table the water pressure is greater than atmospheric, and at any point above, the water pressure is less than atmospheric. In contrast, at greater depths, the effective thickness of an aquifer often extends between two impermeable layers (Fig. 2.8).

If the overlying layer has low permeability and restricts the movement of water, then it is known as an aquitard and causes the aquifer beneath to be partially or semi confined. If the overlying layer has such low permeability that it prevents water movement through it, then the aquifer is fully confined. In these situations, at any point in the confined aquifer, the water pressure is greater than atmospheric, because of the elevation of the outcrop receiving recharge. If a borehole is drilled through the confining layer into the aquifer, water rises up the borehole to a level that balances the pressure in the aquifer. An imaginary surface joining the water level in boreholes in a confined aquifer is called the potentiometric surface, which can be above or below the groundwater surface in the overlying unconfined aquifer (Fig. 2.8). If the pressure in a confined aquifer is such that the potentiometric surface is above ground level, then a drilled borehole will overflow (Fig. 2.8). For a phreatic aquifer, which is the unconfined aquifer to be formed below the surface, the potentiometric surface and groundwater surface correspond, and this is called the water table, Fig. 2.8.

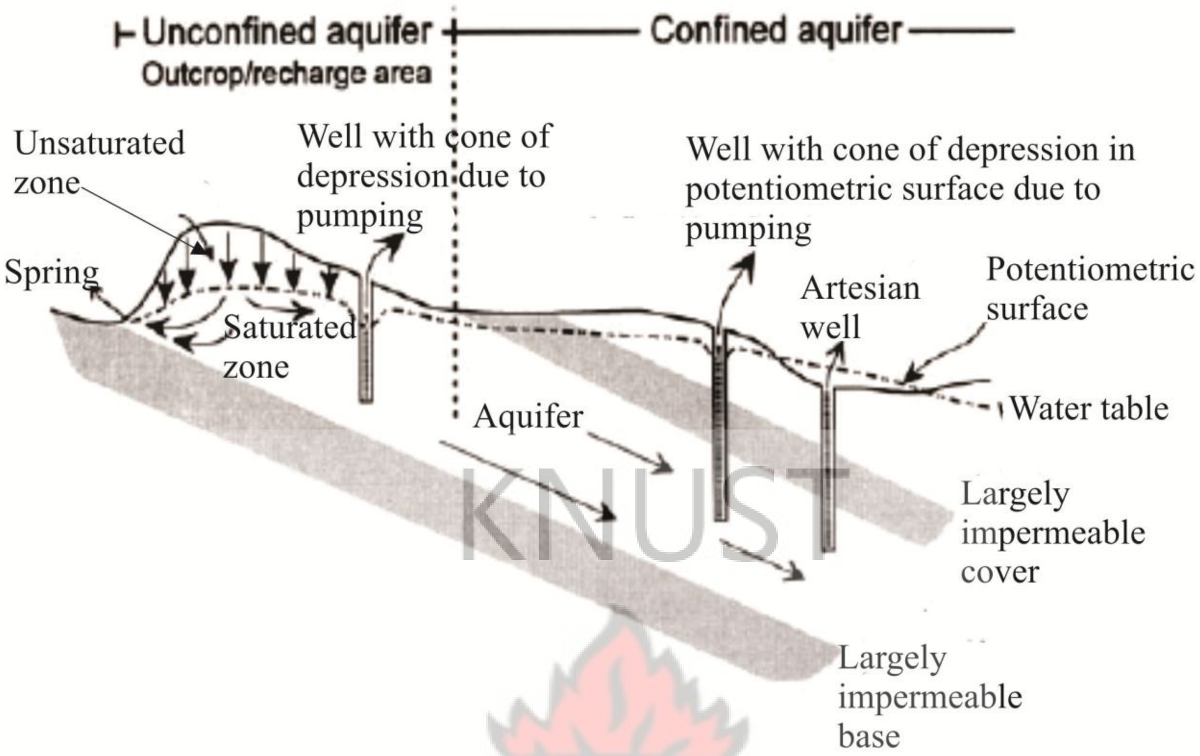

Fig. 2.8 Schematic cross-section illustrating confined and unconfined aquifers (Modified after Chilton and Seiler, 2006).

From the groundwater development point of view, unconfined aquifers are often favoured because their storage properties make them more efficient for exploitation than confined aquifers, and they are likely to be shallower and therefore cheaper to drill into and pump out water.

2.3.2.1 The Sources and Origin of Groundwater

It originates as rainfall or snow, and then moves through the soil into the groundwater system, where it eventually makes its way back to surface streams, lakes, or oceans. Groundwater makes up about 1% of the water on Earth (most water is in oceans). But, groundwater makes up about 35 times the amount of water in lakes and streams . Groundwater occurs everywhere beneath the Earth's surface, but is usually restricted to depths less than about 750 m. The volume of groundwater is equivalent to a 55 m thick layer spread out over the entire surface of the Earth.

(www.tulane.edu/...). When rains fall on the surface of the earth, the water seeps down through the soil and into a zone called the zone of aeration or unsaturated zone where most of the pore spaces are filled with air. The water continues to seep deeper and deeper till it eventually enters a zone where all pore spaces and fractures are filled with water. This zone is called the saturated zone. The surface below which all openings in the rock are filled with water (the top of the saturated zone) is called the water table as shown in Fig. 2.9.

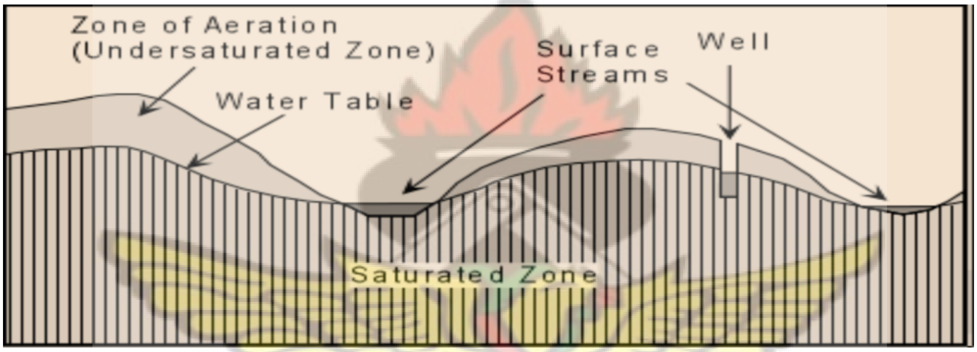

Fig 2.9 The Water Table during Rainfall (modified after Santosh, 1996).

This water table occurs everywhere beneath the earth's surface. In desert regions it is always very low beneath the surface. But in more humid regions it reaches the surface at streams and lakes, and generally tends to follow surface topography. The depth to water table may however change, as the amount of water flowing into and out of the saturated zone changes. During dry seasons, the depth to the water table increases. During wet seasons, the depth to the water table decreases as shown in Fig. 2.10.

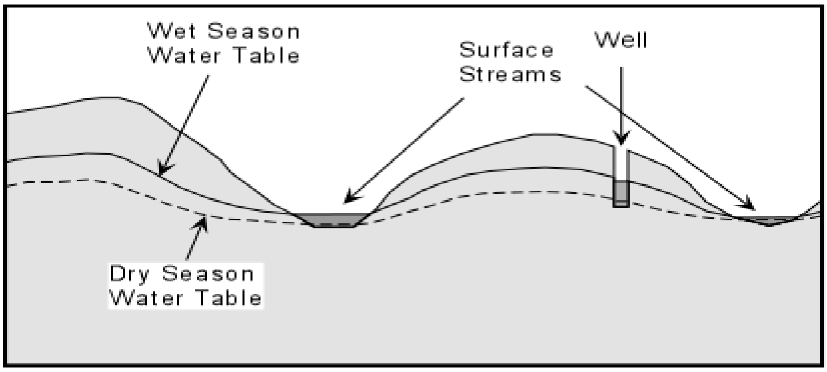

Fig. 2.10 The Water Table in the Desert (Santosh, 1996).

The distribution of water on the land is dependent upon the complex interaction between atmosphere and oceans refers to as the climate. The hydrologic cycle is a linkage involving evaporation, condensation, run-off, infiltration, percolation, and transpiration as shown in Fig. 2.11 below.

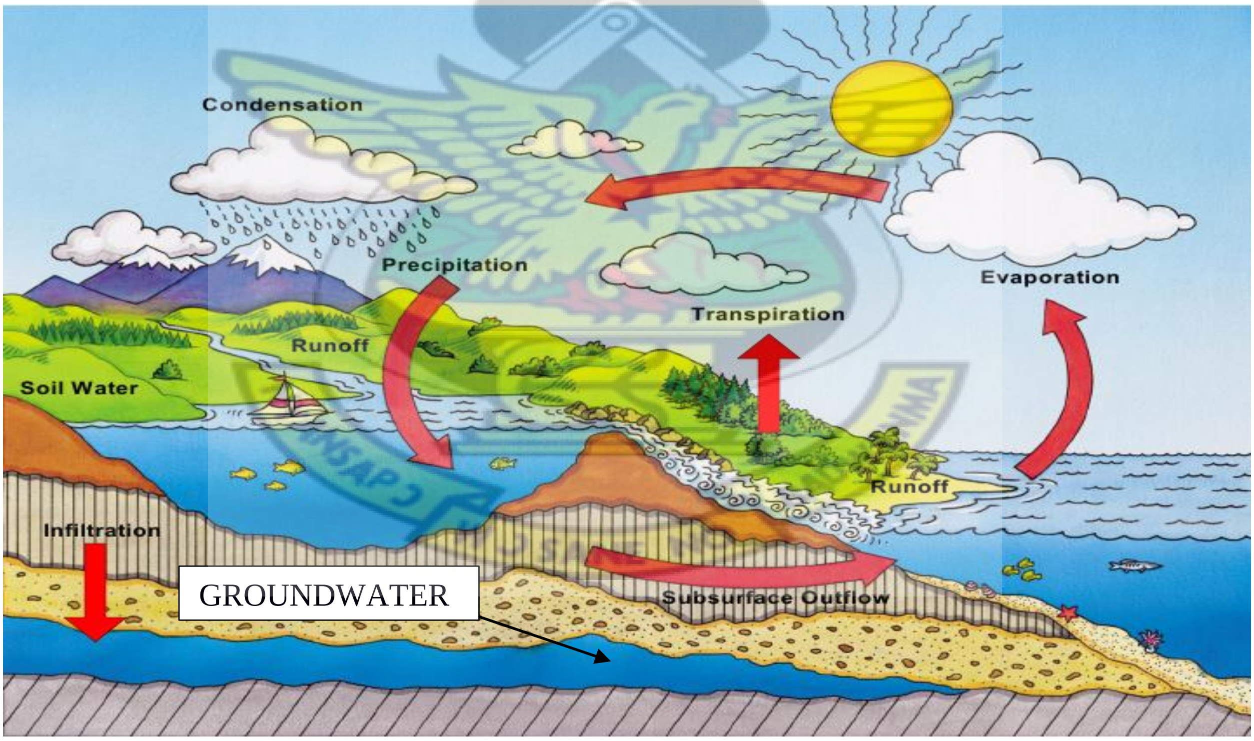

Fig 2.11 The Hydrologic Cycle (modified after Santosh, 1996).

These processes cause water to change state (vapour, liquid, solid) as it moves between different elements of the earth system (Santosh, 1996).

A slim fraction of water falling as precipitation infiltrates below the surface through bedrock or soils to form groundwater. Some of the soil moisture is lost to evaporation or taken up by vegetation and the remainder recharges the groundwater system. Groundwater flow is termed percolation and occurs at rates from meters per day to millimeters per year. Consequently the residence time for groundwater (the length of time water remains in a given location) may be measured in intervals of weeks or thousands of years. Even the slowest flow rates will eventually return the groundwater to the ocean, completing the hydrologic cycle (Santosh, 1996). Therefore, the mode of occurrence of groundwater depends largely on the type of formation, and hence on the geology of the area. Groundwater occurs in many types of geological structures and those known as aquifers are of most importance. An ***aquifer*** is a large body of permeable material where groundwater is present in the saturated zone. Good aquifers are those with high permeability such as poorly cemented sands, gravels, and sandstones or highly fractured rock ***(www.tulane.edu/...)***.

2.3.2.2 Rock Properties Affecting Groundwater

Groundwater is characterized by a certain number of parameters, which geophysical methods are trying to determine from surface measurements, mostly indirectly, but sometimes directly. The most usual parameters are the porosity, the permeability, the transmissivity and the conductivity (Bernard, 2003) and (*www. iris-instruments.com*).

The porosity is the ratio between the volumes of the pores and that of the rock. When dealing with

saturated layers (under the water level, that is to say under the vadose zone where the pores are filled with air and with water), the water content is equal to the porosity.

$$\text{Porosity} = (\text{volume of pores}) / (\text{volume of the rock})$$

The volume of water that can be contained in the rock depends on the proportion of these openings or pores in a given volume of rock, and this is termed the porosity of the rock. Increasing pore space results in higher porosity and greater potential to store water. For the exploitation of water, it is important to determine the porosity of free water (water which can move), and hydrogeologists speak of the effective porosity which is the ratio of the volume of the pores which are interconnected to the volume of the rock (Bernard, 2003). As an order of magnitude, the effective porosity can be for instance 80% of the free water porosity. The porosity of a fissured rock can be a few percents, that of a gravel or a sand of the order of 30 %.

The permeability (actually the hydraulic conductivity) is the ability of a material to let a water current flow through it when hydraulic pressure is applied, can be defined on a sample of rock by the Darcy law:

$$\text{Permeability} = (\text{Yield} / \text{Section}) / \text{Pressure gradient}$$

The yield being expressed in m^3/s, the sample section in m^2, and the pressure gradient (difference of water pressure / sample length) in m/m, the unit of permeability is m/s. If the porosity is almost zero the permeability is necessarily also very weak. But the porosity can be high, such as in the case of a clay layer, and the permeability very weak. The porosity and the permeability are two parameters which are not independent from each other: the permeability already includes the information of the porosity for determining the volume of water which can be extracted from the ground. The permeability is linked not only to the volume of the available water, but also to the size of the pores: for a given value of the porosity, large size pores lead to a higher permeability than small size pores, as the water flows more easily in the first case than in the second one. The permeability of a clay layer can be as low as 10^{-10} m/s, of a weakly permeable layer 10^{-6} m/s, of a highly permeable layer 10^{-2} m/s (Bernard, 2003).

The transmissivity of an aquifer layer is the product of the permeability and its thickness:

$$\text{Transmissivity} = \text{Permeability} \times \text{Thickness}$$

The transmissivity is expressed in m^2/s. The interest of this parameter is that it is proportional to the production yield obtained by pumping:

$$\text{Production yield} = \text{parameter} \times \text{Transmissivity} \times \text{Drawdown}$$

The drawdown is the difference of level of the water in the pumping well and far away from it. The ratio yield / drawdown is called the specific capacity of the well. In the field, the transmissivity of a formation is usually determined by hydrogeologists by a pumping test.

Table 2.3 Representative values of porosity (modified after Morris and Johnson, 1967)

Material	**Porosity (%)**	**Material**	**Porosity (%)**
Gravel, coarse	28[5]	Loess	49
Gravel, medium	32[2]	Peat	92
Gravel, fine	34[4]	Schist	38
Sand, coarse	39	Siltstone	35
Sand, medium	39	Claystone	43
Sand, fine	43	Shale	6
Silt	46	Till, predominantly silt	34
Clay	42	Till, predominantly sand	31
Sandstone, fine grained	33	Tuff	41
Sandstone medium grain	37	Basalt	17
Limestone	30	Gabbro, weathered	43
Dolomite	26	Granite, weathered	45
Dune sand	45		

2.3.2.3 Geological Conditions Suitable for Groundwater Accumulation

Groundwater occurs in geological formations in the subsurface under hydrostatic pressure in the pores and cracks of rocks. The reason is that nearly all rocks in the uppermost part of the Earth’s crust, of whatever type, origin or age, possess openings called pores or voids (Fig 2.12a, b). In weathered sedimentary rocks such as the Voltaian system, groundwater occurs in the pores between grains and as well as in fractures within the rocks (Menyeh *et al.*, 2005).

Common permeable geological material includes sandstone, limestone, and marble and fault breccia. In the more consolidated rocks, such as lavas, gneisses and granites (Fig. 2.12c, d), the only void spaces may be fractures resulting from cooling or stresses due to movement of the earth's crust in the form of folding and faulting. These fractures may be completely closed or have very small and not very extensive or interconnected openings of relatively narrow aperture.

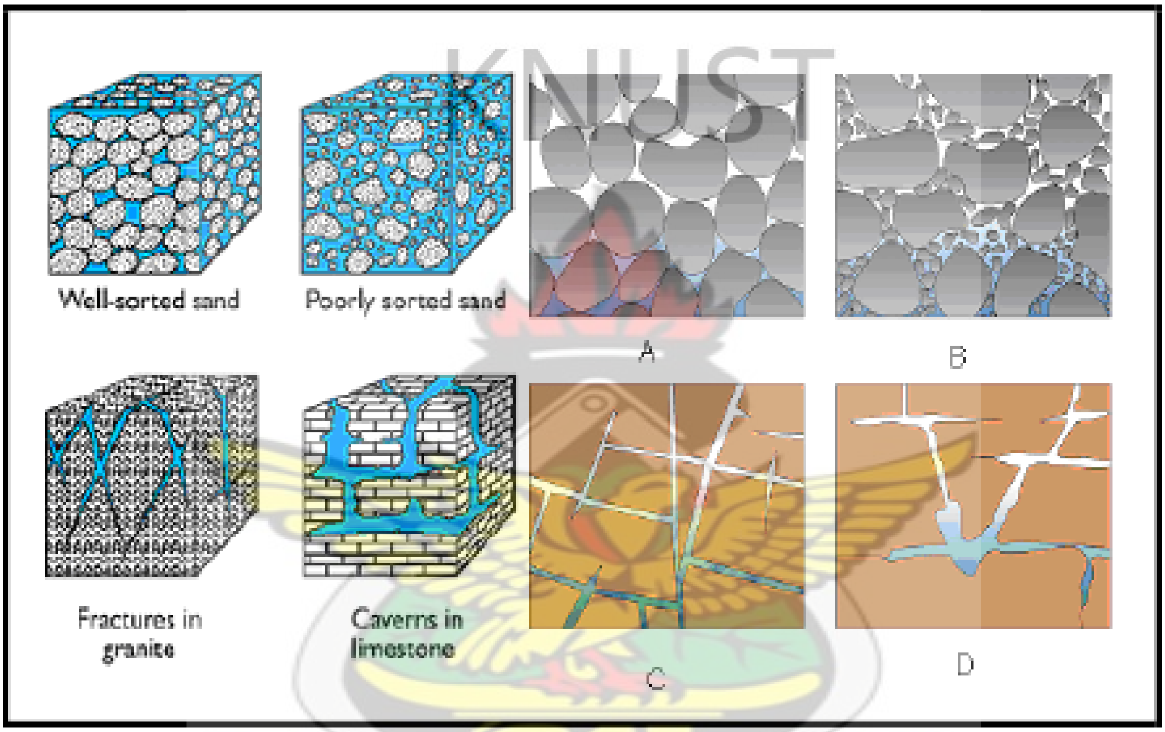

Fig. 2.12. Relation between Texture and Porosity (*www.hwe.org.ps/Education*)

The volume of water that can be contained in the rock depends on the proportion of these openings or pores in a given volume of rock, and this is termed the porosity of the rock. Increasing pore space results in higher porosity and greater potential to store water.

2.3.2.4 Groundwater Quality

The quality of groundwater is generally good for multipurpose use except for the presence of low pH waters, high level of iron, manganese and fluoride in certain localities as well as high mineralization in some coastal aquifers particularly in the Accra Plains (Amuzu, 1978). Low pH waters are found mainly in the forest zones of southern Ghana. About 30% of all boreholes in Ghana have iron problems (Ayibotele, 1985). High iron concentrations in the range 1-64 mg/L have been observed in boreholes in all geological formations. Iron originates partly from the attack of low pH waters on corrosive pump parts and partly from the aquifers. The percentage of Iron derived from the aquifers is however unknown (Asare and Boateng, 1992). High fluoride values in the range 1.5-5.0 mg/L on the other hand are found in boreholes located in the granitic formation of the upper east and west regions (Pelig-Ba, 1989). The waters in many hand dug wells in Voltaian basin look turbid and polluted as they contain high levels of nitrate in the range of (30-60) mg/L and abundant coliform (WRRI, 1992). This is probably due to improper construction and inadequate protection of the wells sites from surface runoff and animal droppings.

Groundwater salinity has also been a major challenge especially in the south-eastern and north-western parts of Ghana. Salinity in certain groundwater occurrences is also found especially in some coastal aquifers. Most people in Kintampo do not use the treated water (Water from the boreholes) for their domestic activities, especially drinking, because they claim the water does not taste good (Appiah and Momade, 2012; and Unihydro Limited, 2002) stated that, Kintampo has groundwater sources with elevated iron concentrations slightly higher than the (WHO, 2006) guideline of 0.3 mg/L, but less than 1 mg/L.

2.4.0 Geology of the Voltaian Sedimentary Basin

2.4.1 Introduction

Researchers such as (Cooper, 1926; Junner and Hirst, 1946; Bozhko, 1969; Anan-Yorke and Cudjoe, 1971; Affaton *et al*., 1980) have all reported that the Voltaian Basin is one of three major sedimentary basins within the West African Craton and has been the subject of considerable academic and economic interest since the 1920s.

2.4.2 Geology of the Voltaian Sedimentary System

The Voltaian System occupies about 40% of the entire land area of Ghana and it is thought to be about 3000 – 4000 m thick. It covers most of the northern part of Ghana. In most of these places surface water flows are ephemeral, occurring only during the wet season. The System consists of inter-bedded rocks including mudstones, sandstones, arkose, conglomerate, shale, and some limestone (Fig. 2.13). The rocks are flat lying or gently dipping except near the eastern margin of the basin adjacent to the contact with the Precambrian rocks where the lower members of the System are gentle- folded (Kesse, 1985).

The Voltaian rocks are generally consolidated and are not inherently permeable. Possible exceptions, however, do exist in areas where the jointed sandstones, arkoses and quartzite upon weathering have produced permeable surficial materials. Again, the rocks have undergone some degree of tectonic activity and most aquifers are made up of fractures. However, there exist unconsolidated systems dotted in many parts of the basin where good aquifers have been located.

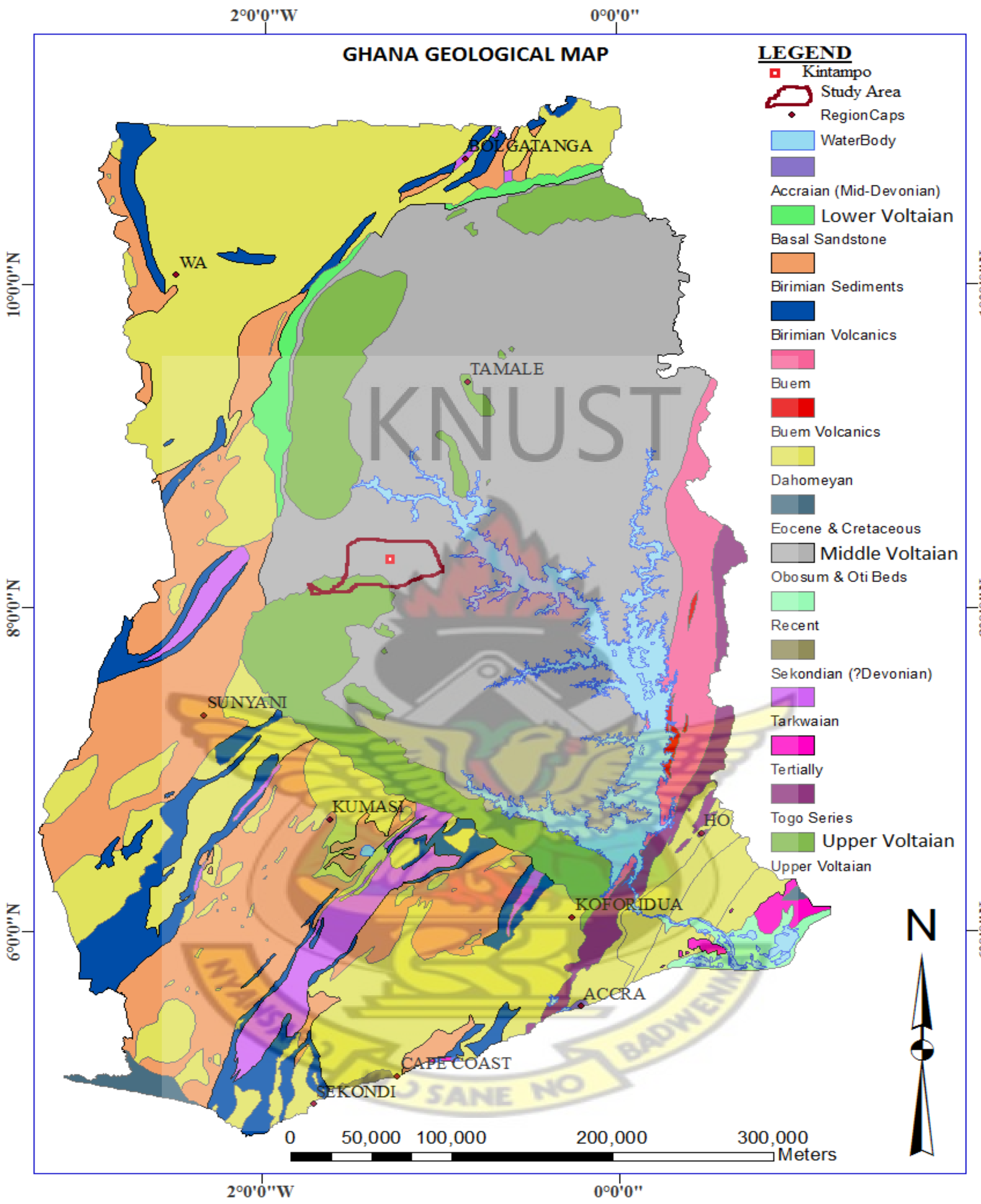

Fig. 2.13 Geological map of Ghana (modified after Kesse, 1985).

2.4.3 Hydrogeology of the Voltaian Sedimentary Formation

Generally, the Voltaian has very poor groundwater potential although some water supplies come from fractures in the argillaceous or loose zones in the arenaceous members (Chegbeleh *et al.*, 2009). Regional hydrogeological studies have shown that fractures or joints in the area are erratic and even absent in some places. In isolated cases, the fractures are non-productive. The area exhibits three classes of hydrogeological units, related to the regional geological settings: (i) Very high groundwater potential areas - the lower Voltaian areas, showing very good prospects for boreholes; (ii) Medium groundwater potential areas - the middle Voltaian area, showing moderate prospects for groundwater potential; and (iii) Very low groundwater potential areas – the upper Voltaian area, showing very low prospects for groundwater potential (Fig. 2.14).

This suggests that groundwater potential in the area is diverse and requires thorough investigation techniques for high success. Most of the aquifers located in the formation are semi-confined to confined. Many hydrogeologists such as (Gills, 1969; Frempong and Kortatsi, 1994; MacDonald *et al*., 1997; Dapaah-Siakwan and Gyau-Boakye, 2000; Acheampong and Hess, 2000; Agyekum and Dapaah-Siakwan, 2007) have reported about the generally poor yielding potential of the Voltaian rocks, though varying widely from 0.3 to72 m^3/hr (5 – 1,200 lpm) with the higher yields recorded in areas underlain by quartzitic sandstone rocks. Lower potentials on the other hand have been recorded in the clay rich Obosum shale and mudstone environment as also described by (Darko and Krasny, 2007; and Darko, 2001) further described the hydraulic characteristics of the Voltaian sedimentary environment as heterogeneous with intermediate to low transmisivity values that range widely between 0.3 and 267 m^2/day.

Available records show that for most of the areas, maximum borehole depth is about 90 m with an average depth of 48.1 m (Chegbeleh *et al.*, 2009). However, there is a report of few boreholes exceeding 100 m, even up to about 150 m deep in the far eastern part of the System (Cobbing and Davies, 2004). In some portions of the southern part of the Voltaian basin, the weathered or loose zones range from 4 to 20 m thick where many villagers rely on for hand dug borehole development (Akudago *et al.*, 2009; GMBH, 1984; Acheampong *et al.*, 2005). Borehole yields range from 5 to 1200 l/min, static water levels from 1 to 20 m and water table fluctuation averaging about 4 m (Acheampong and Hess, 1998; Buckley, 1986). The estimated transmissivities range from 0.3 to 270 m^2/day (Darko, 2001).

Groundwater recharge varies from location to location, depending on the infiltration capacity of the surface and the permeability of adjacent geologic material shielding the aquifer. Available literature indicates that groundwater recharge in the Voltaian ranges from 3.7-5% of annual rainfall (Martin and Van de Giesen, 2005; and Apambire, 2000). Groundwater abstraction is estimated to be less than 5% of the annual groundwater recharge (Martin and Van de Giesen, 2005; Lutz *et al*., 2007).

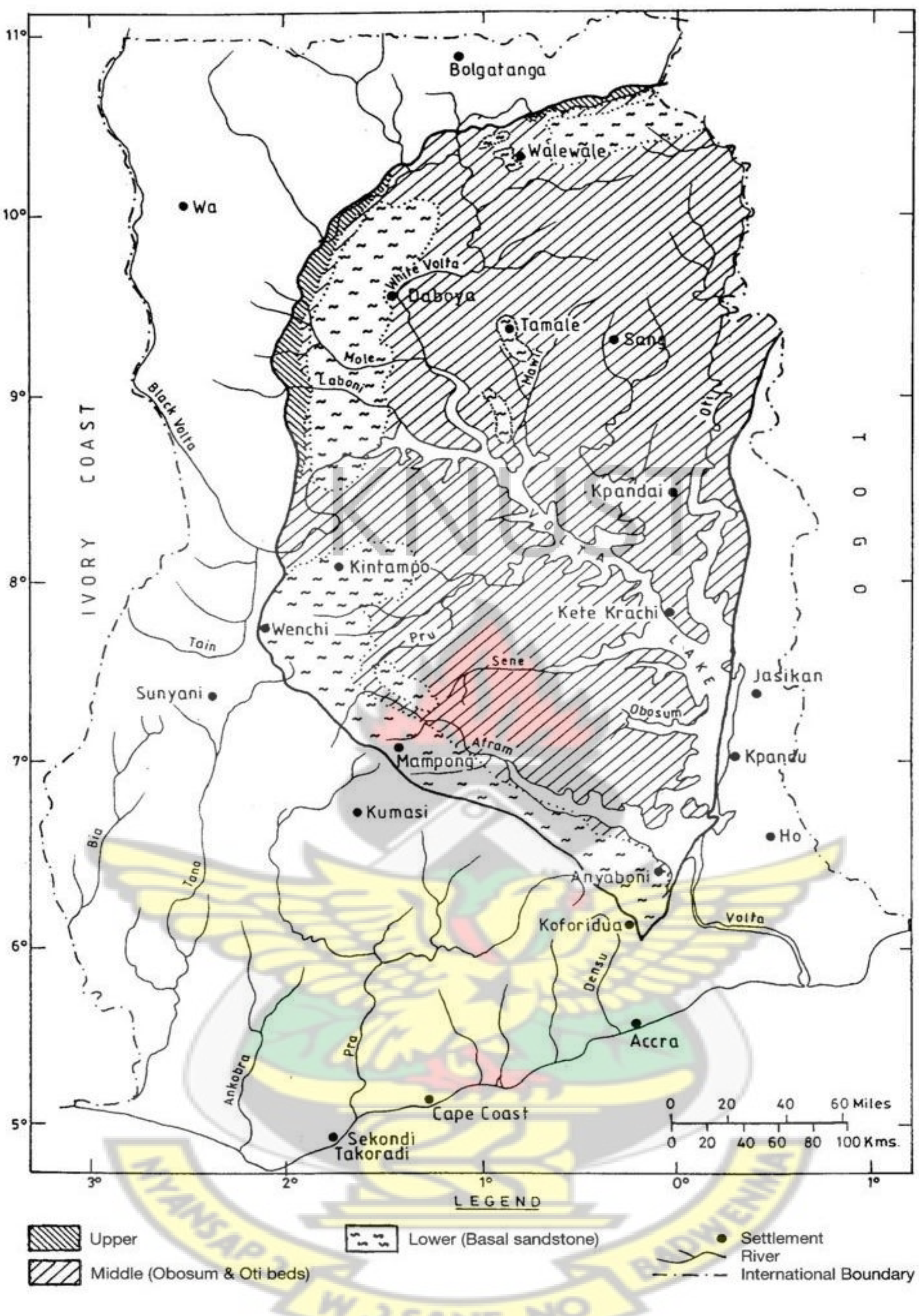

Fig. 2.14 Hydrogeological sub-provinces of the Voltaian System (modified after Ghana Geological Survey, 1965)

2.4.4 Aquifers in the Voltaian Sedimentary Formation

The rocks that underlie 99% of Ghana (the basement complex and the Voltaian formation) are essentially impermeable and have little or no primary porosity. Therefore groundwater occurrence in Ghana is associated with the development of secondary porosity as a result of jointing, shearing, fracturing and weathering. This has given rise to two main types of aquifers: the weathered zone aquifers and the fractured zone aquifers. The weathered zone aquifers usually occur at the base of the thick weathered layer. The weathered layers vary, from 0 m (outcrops) to about 100 m. It is thickest in the wet forested south-western part of the country where it reaches an average thickness of 60 m and thinnest in the semi-arid zone in the extreme northeast where the mean thickness is 10 m. The fractured zone aquifers are normally discontinuous and limited in area. Due to the sandy clay nature of the weathered overburden, the groundwater occurs mostly under semi-confined or leaky conditions. The yield of these aquifers rarely exceeds 6 m^3/h (Obuobie and Boubacar, 2010). Three aquifers occur in the remaining 1% of Ghana, mainly in the extreme south eastern and south western part (with cenozoic and mesozoic sediments formation). The first aquifer is unconfined and occurs in the recent sand very close to the coast. It is between 2 m and 4 m deep and contains fresh meteoric water. The intermediate aquifer is either semi-confined or confined and occurs mainly in the red continental deposits of sandy clays and gravels. The depth of this aquifer varies from 6 m to 120 m, and it contains mostly saline water. The third aquifer is the limestone aquifer which varies in depth between 120 m and 300 m. The groundwater in this aquifer, which often occurs under artesian condition, is fresh. The average yield of the limestone aquifer is about 148 m^3/h (Obuobie and Boubacar, 2010; Dapaah-Siakwan and Gyau-Boakye, 2000).

2.4.5 Groundwater Occurrence in the Voltaian Rock Formation

About 45 percent of the country is underlain by Palaeozoic consolidated sedimentary rocks locally referred to as the Voltaian Formation and consist mainly of sandstones, shale, arkose, mudstone, sandy and pebbly beds and limestones.

Groundwater in the Voltaian Province mainly occurs and flows in fracture zones, and along bedding planes for some areas, since the primary porosity of these rocks are destroyed through consolidation and cementation. The regolith is reported to be unsaturated in many areas and would thus only provide minor amounts of groundwater locally (Acheampong and Hess, 1998). The average thickness of the regolith of the Voltaian sedimentary rocks is approximately 9 m. The relatively thin regolith can be partly explained by the stable clay (shale) or quartz (sandstone) composition or by the fine texture or ductile nature (soft unmetamorphosed mudstone) of sedimentary rocks found in the Voltaian province. Deeper weathering may however occur in some areas, such as those underlain by arkose or arkosic sandstone (e.g. Oti Beds of Middle Voltaian) as K-feldspar weathers more easily than quartz and clay minerals. Underlying fracture zones are generally developed in bedrock at depths greater than 20 m below ground surface but, on average, required yields for rural supplies are obtained above 100 m depth. However, production potential from deeper fractures has not been investigated thoroughly. Fracture characteristics such as frequency, aperture and connectivity can vary substantially over small distances, making it difficult to locate laterally extensive aquifers (Carrier *et al*., 2008).

2.5.0 The Study Area.

The project area is the Kintampo North District of the Brong Ahafo Region of Ghana. The Kintampo North District is one of the 19 districts of the Brong Ahafo region of Ghana as shown in Fig 2.15. It serves as a transit point between the northern and southern sectors of the country because of its location. It is located at the Centre of Ghana, with a population of 96,538 comprising 47,302 male and 48,178 female, with a growth rate of 2.6% (Ghana population census, 2010). The indigenous ethnic groups are the Akans, Bonos and the Mos. Other migrants who are permanently settled in the district include Dagombas, Sissalas, Kokombas, Grushies, Dangbes, Ewes and Fantis. Migrant farmers from the north move to settle on arable lands where they can get enough farm produce because of the fertile nature of the land. Consequently the area has a potential of population explosion.

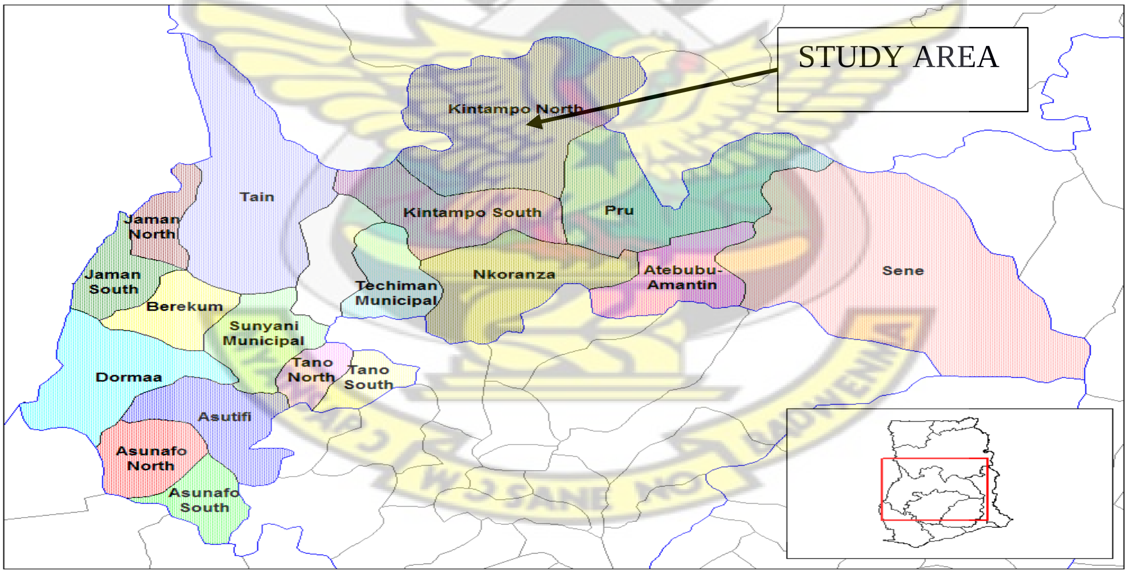

Fig. 2.15. Map of the Brong-Ahafo Region, showing the location of Kintampo North Municipality.

The area is a sparsely populated rural region with underdeveloped infrastructure and services and has been identified as a critical water deficit area based on the water supply coverage

(Unihydro Limited, 2000). Water supply availability is a serious problem and the area relies mostly on dugouts, dams, hand-dug wells and some boreholes. Groundwater is a preferred water supply option in the area because it is generally available even in drought situations and it has relatively good quality. Groundwater is not only feasible but also the most economic source of potable water due to the dispersed nature of the rural settlement (Gyau-Boakye and Dapaah-Siakwan, 1999).

2.5.1 Location and Accessibility

It is located between latitudes 8º45'N and 7º45'N and Longitudes 1º20'W and 2°1'E and shares boundaries with five districts in the Country namely; Central Gonja District to the North; Bole District to the West; East Gonja District to the North-East (all in the Northern Region). The rest are: Kintampo South District to the South; and Pru District to the South-East (all in the Brong Ahafo Region) as shown in Fig. 2.16. The Municipal Capital, Kintampo, is about 130 km away by road from the regional capital and lies east of the Brong Ahafo Regional capital, Sunyani. The Municipal has a surface area of about 5,108 km², thus occupying a land area of about 12.9 % of the total land area of Brong Ahafo Region (39,557 km²).

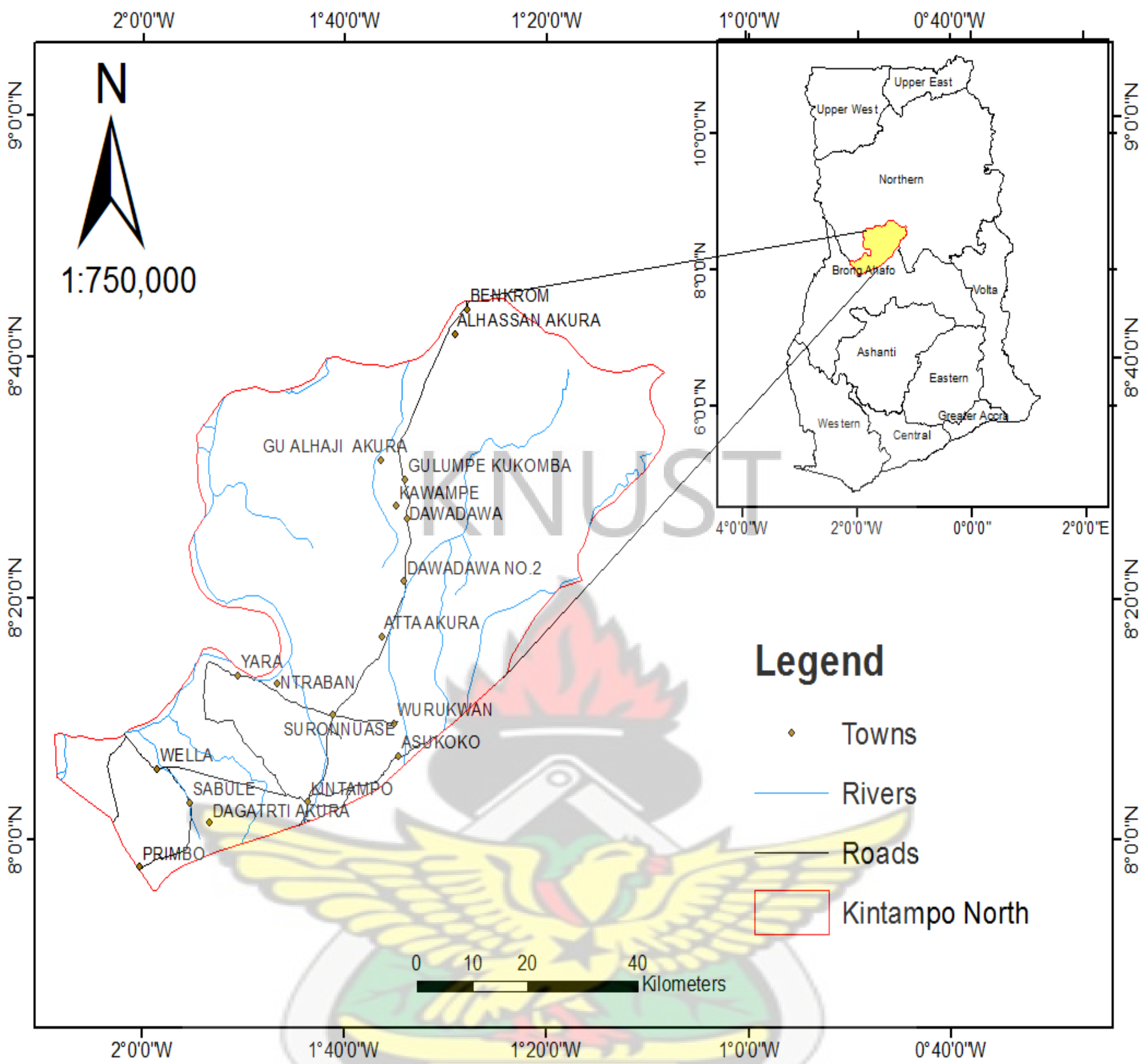

Fig. 2.16 Location map of the Kintampo North Municipality showing communities under study.

2.5.2 The Physical Environment

The Kintampo North Municipality which falls within the Voltaian Basin and the Southern Plateau physiographic regions is a plain with rolling and undulating land surface with a general elevation between 60 - 150 m above sea level. The southern Voltaian plateau occupying the southern part of the Municipality is characterized by series of escarpments.

2.5.3 Drainage Pattern and Topography.

The municipal area is endowed with a lot of water resources. Drainage is enhanced by the Black Volta and finally flows into the Volta Basin. Most of the towns and villages in the district do not have any proper drainage system. The system prevailing is the natural drainage flow, where water finds its own level. Few towns like Kintampo, Babatorkuma, and Kadelso, lying along the Tamale- Kumasi trunk road have drains constructed on each side of their roads that pass through the towns. However, there are streams, which drain into these main rivers. The major water bodies include the Fra, Urukwain, and the Nyamba streams. Others are Oyoko, Nante, Pumpum and Tanfi. These water bodies flow through the west of the district and join the Black Volta at Buipe. The slopes through which the rivers flow have given rise to water falls. The major ones include the Fular Falls on the Oyoko stream and the Kintampo water falls on the Pumpum stream. Most of these streams are intermittent and the large ones like Urukwain and Pumpum fluctuate in volume (http://www.*kintamponorth.ghanadistricts.gov.gh*).

2.5.4 Climate and Rainfall

The Municipality lies within the tropical continental or interior Savannah climatic zone, which is a modified form of the tropical continental or the Wet-semi equatorial type of climate. This is due largely to the fact that the district is in the transition zone between the two major climatic regions in Ghana.

The mean annual rainfall is between 1,400 mm and 1,800 mm; and occurs in two seasons; from May to July and from September to October with the minor season (May – July) sometimes being obscured. However, because of the transitional nature of the area, the distinction between the two peaks is often not so marked.

The mean monthly temperature ranges from 30 °C in March to 24 °C in August with mean annual temperatures between 26.5 °C and 27.2 °C. These conditions give rise to sunny conditions for most parts of the year. Relative humidities are high varying from 90 % - 95 % in the rainy season to 75 % - 80 % in the dry season. The climate of the district has the tendency to change and be inclined more to the drier tropical continental conditions or to the wet semi-equatorial conditions.

2.5.5 Vegetation and Soils

The Municipality comes under the interior wooded savannah or tree savannah. However, owing to its transitional nature, the area does not totally exhibit typical savannah conditions. Thus the savannah here is heavily wooded, though most of the trees are not as tall and gigantic as those in the most deciduous forest.

It is believed that the transitional zone was once forested and that the savannah conditions currently prevailing have been the result of man’s activities. This may be evidenced by the existence of “fringe forest” found along the banks of major rivers and streams and other areas where the impact of man’s activities are minimal.

Trees such as the Mahogany, Wawa, Odum, Onyina, Boabab, Dawadawa, Acacia, and the Sheanut trees, which have adapted to this environment are found in the vegetation zone. They are few and scattered except along the margins of the moist deciduous forest where the trees often grow quite close together. Grass grows in tussocks and can reach a height of about 3.05 m.

Soils in the district belong to two main groups; the ground water lateral soils which cover nearly three fifths of the district in particular and the interior wooded savannah zone in general. The other soil group, covering the rest of the two-fifths of the Municipality is the savannah ochrosols occurring in the south and south- western parts of the district. These soils are formed mainly over Voltaian shale and granites. The ground water lateral soils are generally poor in organic matter and in nutrients. However, the savannah ochrosols are more supplied with organic matter and nutrients. Generally, these soils are good for the cultivation of tubers, cereals, tobacco, vegetable and legumes. Cashew and cotton production have been on a large scale in the Municipality

2.5.6 Geology and Hydrogeology

The Municipality is predominantly underlain by the Voltaian Super group, which covers about two – fifths (2/5) of the surface area of Ghana and about 80 % of the Municipality's land surface. The remaining 20 % of the Municipality's land surface is covered by the Buem formation (Fig. 2.17).

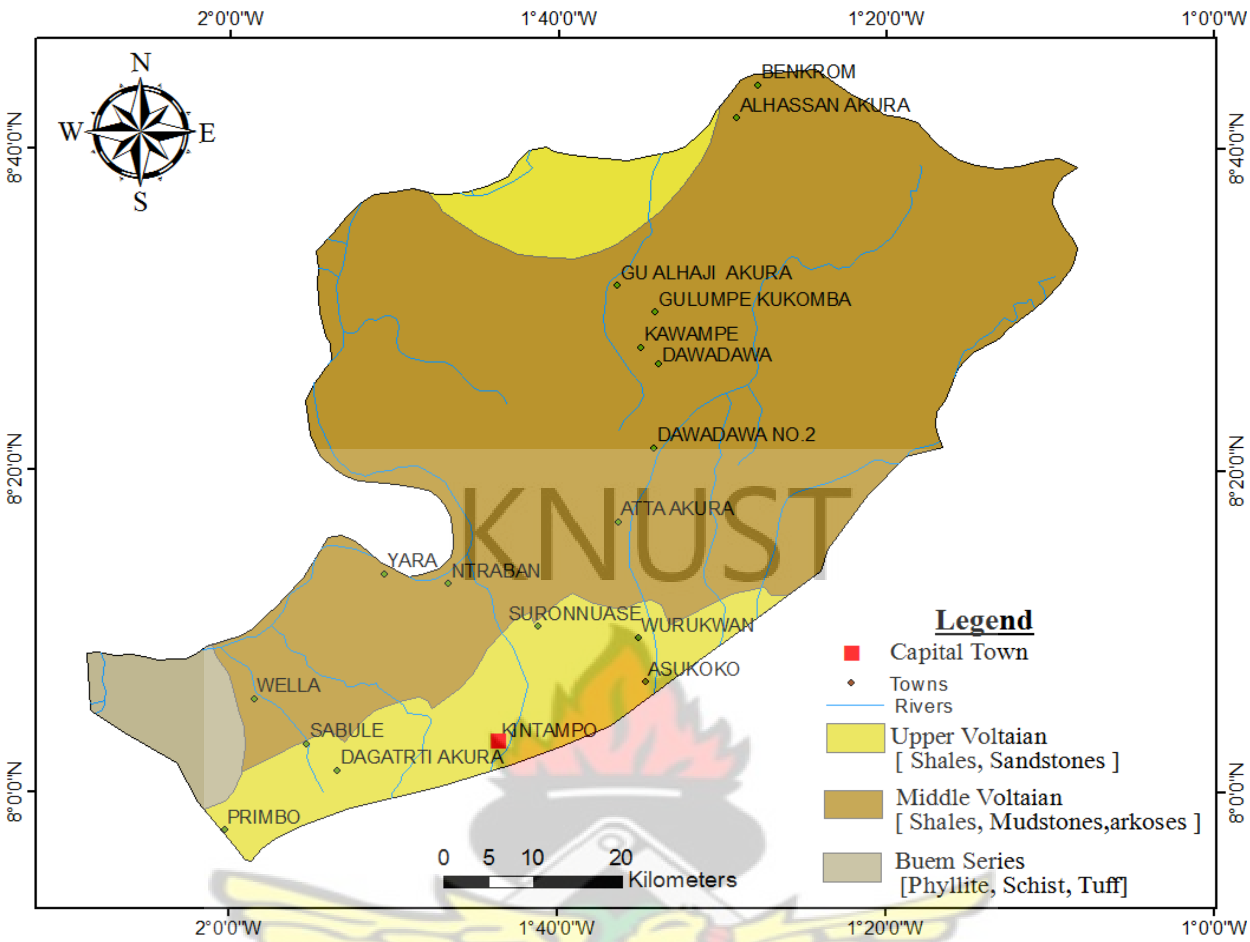

Fig. 2.17 Geological map of the Kintampo North Municipality.

The major lithologic units in the Voltaian Super group include the Lower Voltaian (Panabako formation of Kwahu / Bombouaka group), Middle Voltaian (Oti beds and Obosum / Tamale supergroup) and the Upper Voltaian (Pendjari / Oti super group) as stated in 'The Voltaian Basin, Ghana Workshop and Excursion, March 10-17, 2008'. The Upper Voltaian consist of massive quartz-sandstone containing in places beds of shales and mudstone and thin-bedded sandstones whilst the Middle Voltaian rocks consist of arkoses, mudstones, shales with sandstones, conglomerates, limestone quartz-sandstones and grits and weathers to form residual coarse-sand, shale and clay (see Table 2.4).

Table 2.4 The major lithologic units in the Voltaian (modified after Carrier *et al*., 2008).

system	series	Dominant lithology
Voltaian System	Upper Voltaian	Massive sandstone, conglomerate with thin beds of shale and mudstone locally
	Middle Voltaian	Obosum beds - Mudstone, shale, sandstone, conglomerate, some limestone
		Oti beds - Arkose, sandstone, conglomerate, mudstone, shale, limestone
	Lower Voltaian	Basal quartz sandstone with pebbly grits and grits
-	Buem Series	Shale, sandstone, lava and tuff with some limestone, grit, conglomerate

This study is limited to the Voltaian Group and the study area is not underlain by the Lower Voltaian (Fig. 2.17). The rocks in the Voltaian have almost completely lost their primary porosity through low-grade metamorphism. They are generally well consolidated and are not inherently permeable (Kesse, 1985). The presence of secondary porosity in the rocks such as fractures, joints and fissures, as a result of some amount of tectonic activities, contributes to groundwater storage. Rocks belonging to this formation are mainly sedimentary and exhibit horizontal alignments. Sand stone, shale, mudstone and limestone are the principal examples of these rocks. The Voltaian rocks were formed soon after the Precambrian era when sagging of land occurred resulting in scarp slopes due to different levels of sagging.

2.5.7 Socio-economic Activities

The inhabitants of the area mainly engage in small scale trading and farming. Farmers in the area are into rearing of animals (mostly cattle), cultivation of tubers, cereals, tobacco, vegetable and legumes. Cashew and cotton production has been on a large scale in the

Municipality. The Municipal has a number of water falls which serves as tourist sites for foreign and local tourist.

2.5.8 Previous Groundwater Exploration Projects in the Municipality

The development of groundwater resources of the Voltaian sediments dates back to the 1940s (Kwei, 1997). From 1963–65 the Geological Survey of Ghana and the Volta River Authority (VRA) drilled a number of boreholes to meet the water supply needs of the expanding population (Cobbing and Davies, 2004). Many Governmental, Non-Governmental Organizations (NGOs) and other consultancy firms such as Canadian International Development Agency (CIDA), Water Vision Technology (WVT), Water Sites Limited (WSL) and World Vision Ghana Rural Water Project (WV-GRWP) have also worked in the Voltaian of Northern Ghana to develop the groundwater resources of the area. Geophysical investigations were carried out mostly using the electrical resistivity or the electromagnetic method independently for the selection of sites for borehole drilling. Many of the boreholes drilled were unsuccessful except in isolated areas where the groundwater potentials were good and good drilling results were obtained (Ewusi, 2006).

Generally, groundwater potentials in the study area are structurally controlled and are mostly tapped from fractured / weathered aquifers. The high unsuccessful drilling rate could be attributed mainly to shallow drill depths and inappropriate techniques employed for investigations. The electrical resistivity method is not very good at detecting steeply dipping structures as compared to the electromagnetic method. Hence the combined use of EM and VES survey with detailed interpretation of data in this study can significantly improve on the drilling success rate. Some assessment carried out on existing boreholes within the neighbourhood of the study area indicates that, the success rate of drilling wet well is 68 % with an average yield of 0.90 m^3/h. Limited potable water sources exist in the beneficiary communities necessitating the present intervention. The existing water sources are presented in Table 2.5 below.

Table 2.5 Existing water sources in the beneficiary communities (CSIR-GWP Database, 2013)

Beneficiary Community	Population	Existing Sources of water
Asukoko	500	Stream (Asukoko)
Wurukwan	545	2 Boreholes
Dagarti Akura	450	Stream
Ntraban	600	1 Borehole / Stream
Yaara	1200	Stream / 1 Borehole /Hand dug well
Atta Akura	890	1 Borehole (not functioning) /Stream
Dawadawa No.2	900	Hand dug wells
Kawampe	2000	3 Boreholes (2 functioning; 3 newly drilled are yet to be fitted with hand pump)
Gulumpe Kokomba	450	Depends on Gulumpe borehole
Gu Alhaji Akura	680	Stream
Alhassan Akura	700	Hand dug wells, Black Volta River, 1 BH (no pump fitted)
Benkrom	900	Black Volta River
Kintampo Municipal Hospital		-

CHAPTER 3

INSTRUMENTATION AND FIELD PROCEDURE

3.1.0 Instrumentation

The GEONICS EM34-3 Equipment and the ABEM Terrameter SAS 1000C resistivity equipment were used in the data collection. The GEONICS EM34-3 conductivity meter was used for fast reconnaissance profiling followed by vertical electrical soundings at selected points along the EM profiles using the Terrameter.

3.1.1 Introduction

The EM34-3 is a fast, simple to operate, cost-effective instrument for the engineering geophysicist, geologist and hydrogeologist alike and has been particularly successful for mapping deeper groundwater contaminant plumes and very successful for potable groundwater exploration (Chegbeleh *et al.*, 2009). In the vertical dipole mode specifically, the EM34-3 is particularly sensitive to vertical geologic structure, and is widely used for applications within weathered, fractured and faulted bedrock systems.

Terrameter SAS 1000. SAS stands for Signal Averaging Systems, a method whereby consecutive readings are taken automatically and the results are averaged continuously. This equipment is suitable for all sorts of resistivity surveys. SAS results are more reliable in resistivity surveying mode. A useful facility of the SAS 1000C is its ability to measure in four channels simultaneously. This implies that resistivity, induced potential measurements as well as voltage measurements can be performed up to four times faster. Water exploration survey with the electrical resistivity method is of low cost, easy to operation, faster and accurate (Liu and Yeh, 2004). The Electrical Resistivity (ER) method can be used to obtain, quickly and economically, details about the location, depth and resistivity of subsurface formations (Emenike, 2001).

3.1.2 Description of the GEONICS EM34-3 Equipment

EM 34-3 equipment consists of a battery operated transmitter and receiver unit, transmitter and receiver coils or loops of about 800 mm in diameter. It uses three frequency/coil spacing pairs. The coil spacings are 10, 20, and 40 m, using frequencies of 6400, 1600, and 400 Hz respectively. The operational range of the instrument is 1-1000 mS/m (Sharma, 1997).

The coils are placed at a known distance apart and coupled, either both horizontally or vertically on the ground. The transmitter is turn on, the distance between the transmitter and the receiver is adjusted via the connected intercoil cable and the apparent terrain conductivity is read directly off the receiver. When both coils are placed horizontally on the ground, the transmitter generates an electrical field with a vertical dipole, so this is called the vertical dipole mode. Similarly when the coils are vertical the equipment is in the horizontal dipole mode. The vertical dipole mode has a greater penetration than the horizontal dipole mode (Table 3.0). Where the vertical dipole conductivity exceeds the horizontal dipole mode reading, the main attribution to the ground conductivity is coming from deeper than 39% of the spacing between the coils. This fact allows the instrument to be used quantitatively to interpret the variation of ground conductivity with depth. A search coil is held horizontally (to measure the vertical component) and vertically (to measure the horizontal component). To measure the terrain conductivity the transmitter operator stops at the measurement station, the receiver's operator moves the receiver coil backwards or forwards until his meter indicates correct inter-coil spacing (in this case 20 m). Then he reads the terrain conductivity from a second meter.

Table 3.0: Exploration depths of Geonics EM 34-3 at various intercoil spacing (McNeil and Snelgrove, 1995).

Intercoil spacing (meters)	**Exploration depths (meters)**	
	Horizontal dipoles (HD)	**Vertical dipoles (VD)**
10	7.5	15
20	15	30
40	30	60

3.1.3 Description of ABEM SAS 1000C TERRAMETER

It comprises a battery powered, deep penetration resistivity meter with an output sufficient for a current electrode separation of 200 m under good survey conditions. The Terrameter is powered by a 12.5V DC power source. Other accessories to the equipment include the booster, four metal electrode, cables and hammers (Fig. 3.1).

Fig. 3.1 ABEM SAS 1000C Terrameter and cables.

3.1.4 Principle of Operation of ABEM SAS 1000C TERRAMETER

The field equipment employed for the resistivity field data measurement is the ABEM SAS 1000C Terrameter. The equipment measures resistivity values digitally as computed from Ohm's law. Schlumberger array was employed. Generally the array consists of a pair of potential electrodes ($P_1P_2/2$) and a pair of current electrodes ($C_1C_2/2$). These are driven into the earth in a straight line to make a good contact with the ground. The Schlumberger VES method involved moving electrodes progressively and symmetrically apart. This was followed by taking and recording of the resistivity data at certain electrodes spacing. Two distinct advantages of taking readings by moving the current electrodes were considered in preference to other methods. These are: (1) there are fewer electrodes to move and (2) the readings are less affected by any lateral variations that may exist (Mussett and Khan, 2000). At some points, the expansions of the current electrodes resulted in a too small potential difference values, which became difficult to precisely measure. This problem was overcame by moving Potential electrodes further apart, while keeping the current electrodes fixed. Further readings were then taken by expanding the current electrodes, using the new potential electrode positions. This also allowed an increase in the depth of the investigation. The current electrode separation $C_1C_2/2$ was from 1.5 m to 83 m, while the potential electrode separation $P_1P_2/2$ was either 0.5 m or 5 m with a view to determining the subsurface layering, overburden thickness and thickness of the aquifer. A total of fifty three (53) Vertical Electrical Sounding points were investigated.

3.1.5 Equipment Handling and Operation

The EM34-3 transmitter and receiver units are contained in small shoulder bags and handled together with their individual separate coils. The principal coil spacing must be determined.

Where the depth to static water level is less than 15 m, a 20 m coil spacing should be used, but where greater than 15 m, the coil spacing should be 40 m (Beeson and Jones, 1988). Hence, the former was used because the depth to static water level was less than 15 m for most of the areas under study (Appiah and Momade, 2012).

The transmitter and receiver are connected by a cable, whose length is that of the required coil spacing. The traverse is carried out with the receiver ahead of the transmitter, in the direction of the traverse. The transmitter operator stops at the measurement station and the receiver operator moves the receiver coil backward or forward until his meter indicates correct inter-coil spacing. He then marks this position and reads the terrain conductivity from a second meter also on the receiver. The conductivity read is an apparent value because the subsurface is non-homogenous.

During traversing, attention is paid to areas which have adequate conductance at depth; this is normally indicated by values of the vertical dipole being greater than those of the horizontal dipole (Beeson and Jones, 1988). When such an anomalous feature is located, the centre point is marked and recorded on field sheets. The concept is that, when used in the vertical dipole mode (horizontal coil system) the device is responsive to the presence of relatively low-conductivity of steeply- dipping structures such as water-bearing fracture zones. However, in the horizontal dipole mode (vertical coil system) the device is quite insensitive to such structures and give fairly accurate measurements of ground conductivity in close proximity to them (Sharma, 1997). When the EM survey is completed, the various anomaly patterns are analysed and the most promising sites selected for further VES investigations.

3.2.0 Field Procedure

3.2.1 Introduction (Methodology)

The methodology consisted of a desk study and field investigations.

The assessment of groundwater potentials was carried out in five stages; (a) desktop study of physical and geological maps of the study area; previous literature on static water level measurements from hand dug wells (b) field reconnaissance survey; (c) EM profiling and Vertical Electrical Soundings; (d) Processing, Analysis and Interpretation of Data.

3.2.2 Desk Study & Data Compilation

The desk study involved compiling and assessing the following data sets:

- Topographic and geological maps
- Existing borehole information and
- Previous hydrogeological work undertaken in the study area.

The purpose of this study was to establish the current knowledge about lineament and fracture patterns, the presence of suitable aquifers and their thickness, groundwater quality, the mean aquifer depth and the expected lithological sequence. The mean depth to aquifer and water table and the expected lithological sequences and Climatic information for the area was obtained from existing literature. The average mean depth to water table in the municipality was found to be 15 m (Appiah and Momade, 2012).

3.2.3 Field Reconnaissance Survey

This involved ground truthing to ascertain findings during the desk study. The reconnaissance survey was meant to locate and target areas for geophysical investigations to detect sufficiently permeable strata that could be considered water- bearing by means of topography, geology, hydrogeology, structural features, water points and soil surveys. Furthermore, accessibility considerations were also taken into account. It also included setting out traverse lines in the selected target areas and identification of pollution sources.

3.2.4 Terrain Evaluation

The terrain in the various communities was assessed to have a fair idea of the working environment. Terrain evaluation is an inherent part of every groundwater exploration programme. It precedes all geophysical investigations and its main objective is to locate the best site for carrying out geophysical surveys, by identifying surface features, which are characteristic indicators of the presence of subsurface water-bearing formations.

It involves a very careful observation of the surface physiographic and geologic features in the survey area such as vegetation, outcrops, stream patterns, springs, and the location of any previous boreholes or wells, exposed fractures and the direction of runoffs or the slope of the terrain. Much information is also sought from members of the community, on environmentally prohibitive locations such as rubbish dumps, cemeteries and toilets. After collating all these information, suitable locations are then earmarked for geophysical surveys.

3.2.5 Geophysical Measurements

The Electromagnetic (EM) Profiling and Vertical Electrical Sounding (VES) techniques were employed in the survey, aiming at detecting both narrow and large fracture zones, as well as thicknesses of weathered zones, which control groundwater occurrence in the study area.

3.2.0 3.2.6 Electromagnetic (EM) Profiling

EM 34-3 electromagnetic equipment was employed in the survey. The Electromagnetic equipment provides a direct measurement of apparent conductivity in the region of the measuring coil based upon the principle of electromagnetic induction.

The principle basically involves the generation of primary electromagnetic field by a transmitter, which induces a secondary magnetic field in the sub-surface. A receiver that is linked to the transmitter by either the 20 m or 40 m inter-coil cable receives the induced secondary magnetic field. When linked by the 20 m inter-coil separation cable, the maximum depth of investigation is 15 m below ground level when the equipment is operated in the Horizontal dipole (HD) mode, and it is 30 m deep when it operates in the vertical dipole (VD) mode. However, when connected to the 40 m cable, the depths of investigation are 30 m and 60 m when operated in the horizontal and vertical dipole modes respectively.

Due to the fact that the water-bearing zone within the study areas is within a depth of 15 - 30 m (Appiah and Momade, 2012), measurements were made using the 20 m inter-coil separation cable in both the horizontal (HD) and vertical dipole modes (VD). EM measurements were taken at 10 m stations along each of the traverse lines. Field measurements and their interpretation are presented by communities in chapter four (4).

3.2.6 Vertical Electrical Sounding (VES)

The ABEM Terrameter SAS 1000C direct current electrical resistivity equipment was used to perform VES. Stainless steel electrodes were used, since they are strong and are resistant to corrosion (Telford *et al.*, 1990). Vertical electrical soundings were done on the anomalous points observed in the EM profile lines in communities where EM profiling was done.

However only VES was conducted in communities where EM profiling was not done (Kintampo Municipal Hospital and Wurukwan).

Vertical Electrical Sounding (VES) was carried out at each of the selected points within the beneficiary communities. Field data was analyzed using the 'RESIST1D' software program. The Model outputs include the number of geological layers in the sub-surface, and their corresponding resistivity and thickness. The results of the field measurements, i.e. the data, interpretation and recommendations are presented by communities in chapter four (4).

CHAPTER 4

DATA PRESENTATION AND INTERPRETATION

4.1 Introduction

The success of resistivity survey for groundwater is hinged on a good data presentation which may lead to a correct interpretation to achieve the desired results. The herculean task has always been how to detect groundwater or an aquifer from the resistivity values. To identify the presence of groundwater from resistivity measurements, one can look to the absolute value of the ground resistivity, through the Archie's law:

$$S_w = [\ (a\ / F^m) * \left(R_w /\ R_t\right)\ ]^{(1/n)}$$

Where S_w: water saturation, F: porosity, R_w: formation water resistivity, R_t: observed bulk resistivity, a: a constant (often taken to be 1), m: cementation factor (varies around 2), n: saturation exponent (generally 2).

For a practical range of fresh water resistivity of 10 to 100 Ω.m, a usual target for aquifer resistivity can be between 50 and 2000 Ω.m. Most of the time it is the relative value of the ground resistivity which is considered for detecting groundwater: in a hard rock (resistant) environment, a low resistivity anomaly will be the target, while in a clayey or salty (conductive) environment, it is a high conductivity anomaly which will most probably correspond to (fresh) water. In sedimentary layers, the product of the aquifer resistivity by its thickness can be considered as representative of the interest of the aquifer (Bernard, 2003). This approach has been adopted in this interpretation (Fig. 4.1).

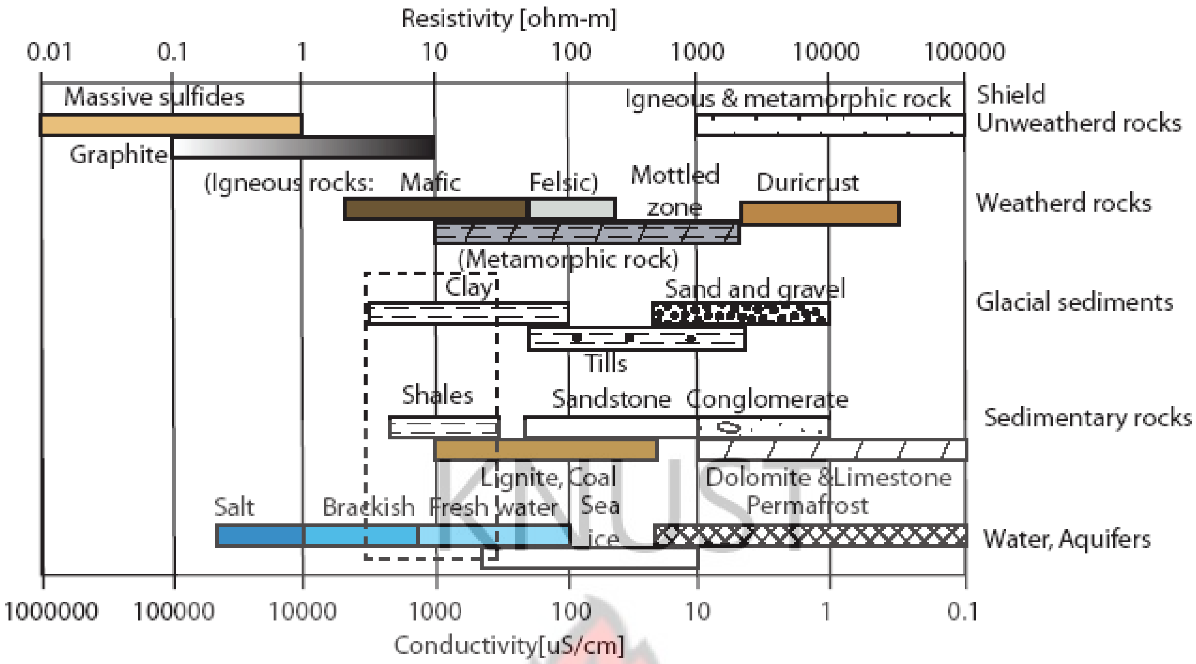

Fig. 4.1 Typical ranges of electrical resistivities of earth materials (modified after Palacky, 1987)

4.2 Data Presentation

The EM data (vertical and horizontal coil resolutions) were presented as plots of conductivity profiles against station intervals.

The apparent resistivity data obtained from the VES survey were presented as depth sounding curves by plotting the apparent resistivities along the ordinate axis and the half current electrode spacing along the abscissa axis.

4.3 Interpretation of Data

The EM profiles were qualitatively analyzed. The qualitative analysis enabled the identification of anomaly points of both the HD and VD dipoles, which were considered as priority areas for vertical electrical sounding. Crossover patterns occurring in conductivity peaks were mostly selected as VES points. Though they may yield wet boreholes, classic crossover patterns do not necessarily indicate water-bearing fractures. It is therefore very important to recognize and interpret fracturing systems carefully (Chegbeleh *et al.*, 2009). The nature of a peak was observed to have a relation with a buried depth of a conductive body. A sharp rising peak was an indication of a superficial buried conducting body and a gentle rising peak indicated a deeply situated conductive body. A vertical fracture is suggested by a symmetrical signature of the EM data. More information about vertical fractures is described elsewhere (McNeil, 1980).

RESIST1D software was used for the 1-D computer modelling. The VES curves were interpreted with a minimum number of layers that were deemed necessary, and that were qualitatively recognizable on the modelled curves. The layer resistivity, thickness and depth were taken into consideration in selecting a potential drill site.

4.3.1 Bases for Selecting Drilling Sites

The interpretation technique takes advantage of the sensitivity of the EM equipment to detect fractures for the delineation of geological features or water bearing zones. Once these anomalous zones are recognized, modelled VES sounding curves are produced for these points. The curves display the number of layers, the apparent resistivity, thickness and depth of each layer. The apparent resistivity, thickness and depth of a layer are considered to draw an inference on whether the layer is weathered and fractured, a condition for groundwater accumulation. This is done by comparing the resistivity values of each layer with the standard fresh groundwater resistivity values. The resistivity of ground water varies from 10 to 100 Ω.m, depending on the concentration of dissolved salts (Loke, 1999).

By comparing, the VES point housing a layer with resistivity range within 10 to 100 Ω.m, high layer thickness and at a depth beyond 40 m is then selected taking the water table and existing bore/hole depths in the study community into consideration.

4.3.2 Crossover Anomaly

Interpretations of EM graphs (plots of HD and VD responses) were carried out qualitatively. Points of sharp positive peaks of a deeper electromagnetic response on the vertical dipole (VD) crossing over the peak of a shallower response on the horizontal dipole (HD) along the EM profile are likely fractured and weathered subsurface zones, which have a high potential for groundwater accumulation. This kind of anomaly is referred to as a ‘’cross-over’ ’anomaly. It is indicated by values of the vertical dipole mode being greater than those of the horizontal dipole mode. Such anomalies may indicate the presence of weathered or fractured subsurface zones, with possible groundwater potential. The response of the conductivity meter to fracture and weathered zones are characterized by high electrical conductivities in both the vertical and horizontal dipole modes relative to background levels, and a higher conductivity for the vertical dipole than for the horizontal dipole.

4.3.3 Analyses of Terrain Conductivity Profiles and modelled VES Curves

4.3.3.1 Alhassan Akura EM Profiles And modelled VES curves

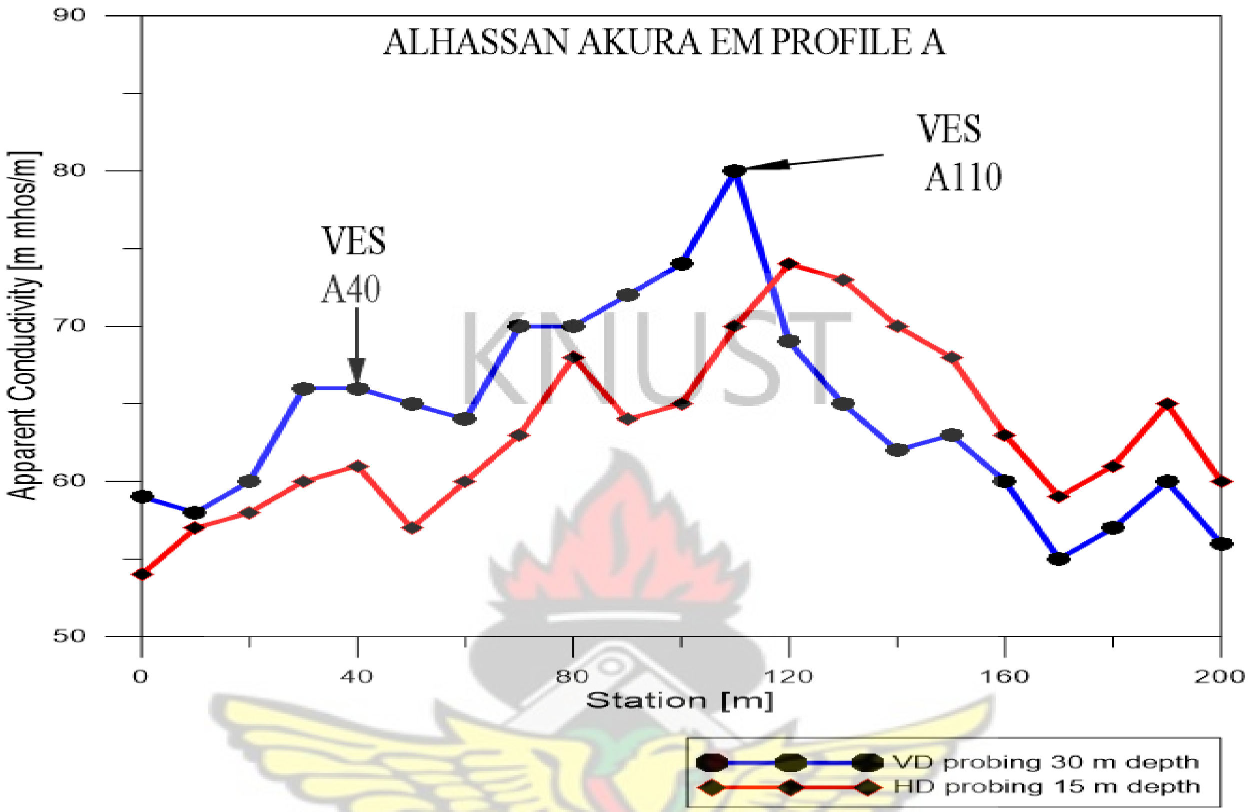

Fig 4.2 EM Profile along Traverse A, Alhassan Akura

Figure 4.2 shows the EM profile of subsurface apparent conductivity along traverse A over a distance of 200 m in Alhassan Akura community. The profile depicts a varying apparent conductivity at the subsurface at both shallower (15 m) and deeper (30 m) depths. Most part of the profile shows higher apparent conductivity values for VD mode than the HD mode at the subsurface up to station 110 m. However, from station 120 m to 200 m the profile shows higher apparent conductivity values for HD mode than the VD mode. At 110 m point on the traverse there is a crossover of sharp positive peak (transition), indicating a significant anomaly. This and station A40 m may be a deep fractured zones beneath the subsurface with station A110 m having relatively higher apparent conductivity. Thus, the two points were selected for further VES investigation.

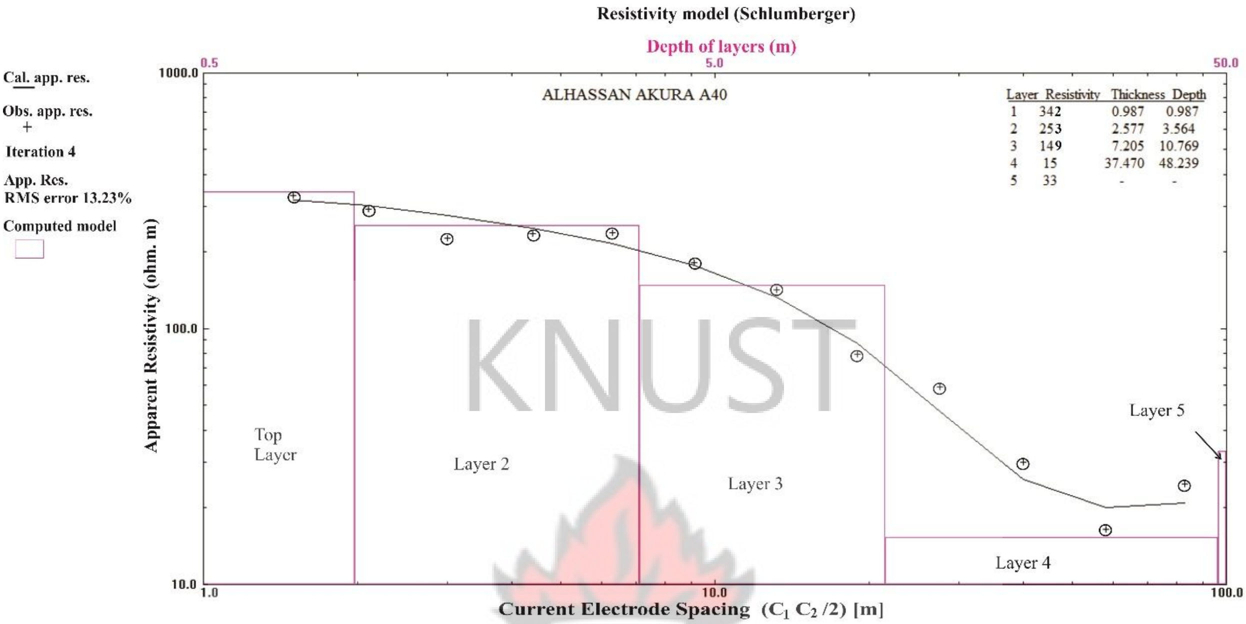

Fig. 4.3 VES Model Curve at station A40 m, Alhassan Akura.

Figure 4.3 shows the apparent resistivity VES model curve at the station, 40 m or VES point A40 m on the traverse. The model depicts a thin overburden of approximately 1.0 m. Quantitatively, it shows a five-layered model with decreasing apparent resistivity from about 342 Ωm at the first layer (topsoil) to 15 Ωm at the fourth layer at a depth of about 48.0 m. The layer parameters of apparent resistivity, thickness and depth of the various layers show that there may be a deep weathered zone ranging from the third to the fourth layer at depth from about 37 m to 48 m. Thus the VES point A40 was chosen and recommended for drilling up to a depth of about 50 m.

Fig. 4.4 VES Model Curve at station A110 m, Alhassan Akura

Figure 4.4 shows the apparent resistivity VES model curve for station 110 m or VES point A110 m on the traverse. Quantitatively the model on the same traverse rather shows a four layered model with increasing apparent resistivity from about 241 Ωm for the first layer (topsoil) to 4341 Ωm in the second; then a drastic decrease to about 4 Ωm at the third layer and an increase again to about 386 Ωm in the fourth layer. The layer parameters of apparent resistivity, thickness and depth of the various layers show that the overburden is thin and the subsurface may be underlain by deep fractured zone at a depth of about 14.0 m. Therefore, VES point A110 was recommended for drilling up to a depth of about 20 m.

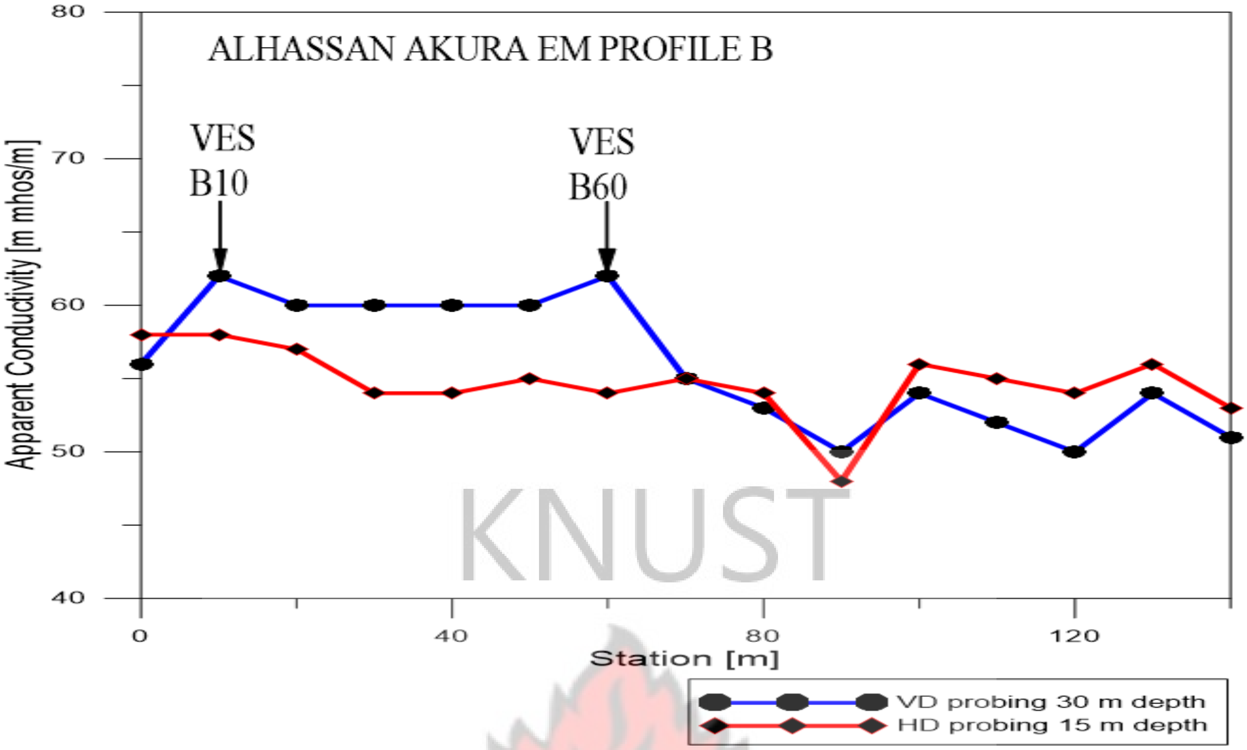

Fig 4.5 EM Profile along Traverse B, Alhassan Akura.

Figure 4.5 shows the EM profile of subsurface apparent conductivity along traverse B over a distance of 140 m in the community, Alhassan Akura. The profile exhibits a varying apparent conductivity at the subsurface at both shallower (15 m) and deeper (30 m) depths. About half of the profile length shows higher apparent conductivity values for VD mode than the HD mode at the subsurface up to station point at 60 m. However, from station points 0 m to 5 m and 70 m to 85 m, the profile shows higher apparent conductivity values for HD mode than the VD mode. At 10 m, 60 m and 90 m points on the traverse, there are crossovers indicating a significant anomaly. Stations B10 m and B60 m may be a deep fractured zones, with relatively higher apparent conductivity values. Thus, the two points were selected for further VES investigation.

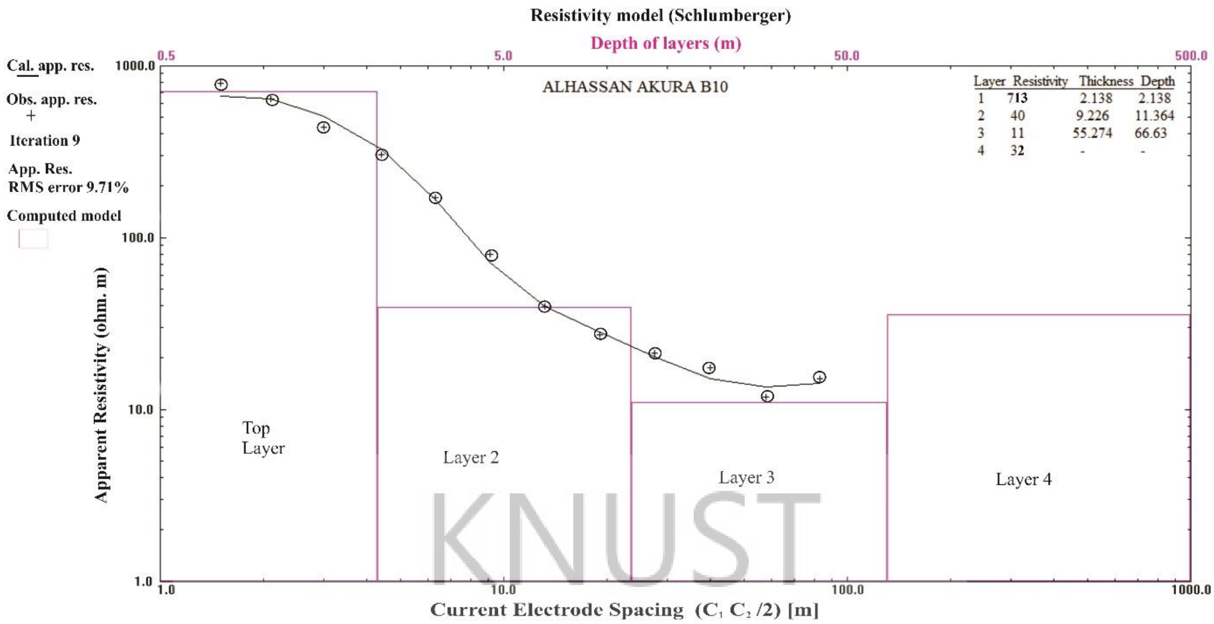

Fig 4.6 VES Model Curve at station B10 m, Alhassan Akura

Quantitatively, the apparent resistivity VES model curve for station B10 m in the Alhassan Akura community (Figure 4.6) shows a four layer subsurface structure. There is a drastic decrease in apparent resistivity from about 713 Ωm at the first layer (topsoil) to 40 Ωm at the second; then another decrease to about 11 Ωm at the third layer and an increase to about 32 Ωm at the fourth layer. The layer parameters of apparent resistivity, thickness and depth of the various layers show that the overburden is thick and the subsurface may be underlain by deep fractured zone at a depth of about 67.0 m. Therefore, VES point A110 m was recommended for drilling up to a depth of about 70 m.

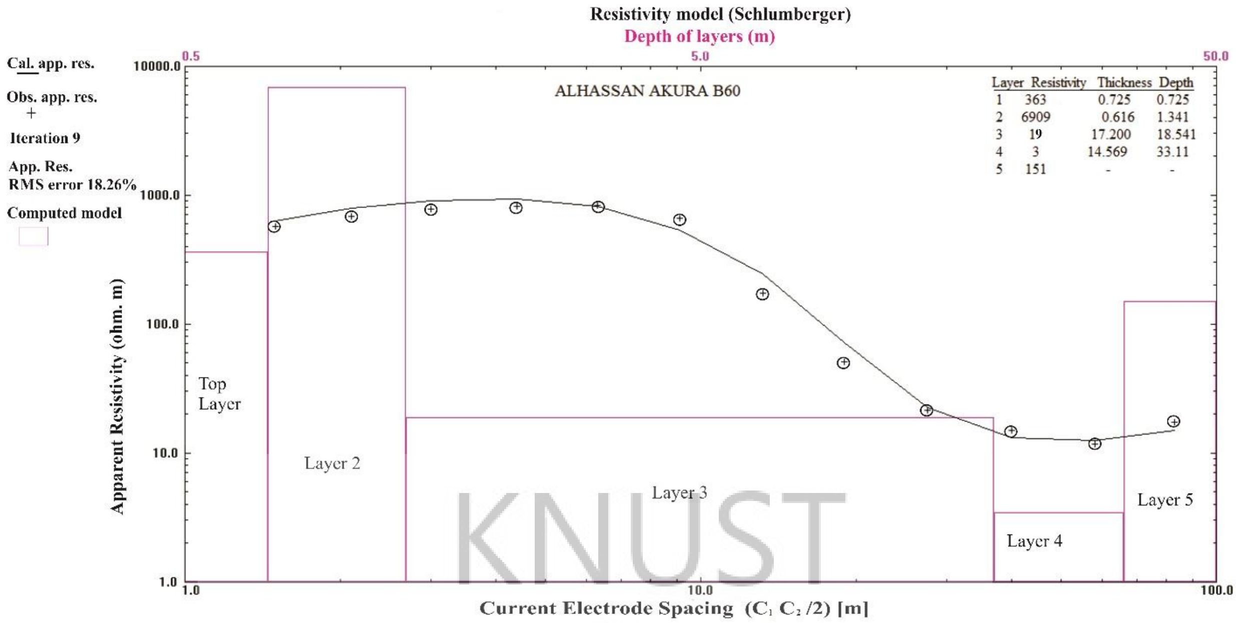

Fig 4.7 VES Model Curve at station B60 m, Alhassan Akura

A five-layer subsurface structure was revealed at VES station B60 m in the Alhassan Akura community as shown in Figure 4.7 above. There is a sharp increase in apparent resistivity of 363 Ωm of the top soil to 6909 Ωm in the second layer, then a drastic drop to about 19 Ωm in the third layer and a further decrease to 4 Ωm in the fourth layer. However, the apparent resistivity of the fifth layer increased to about 151 Ωm. The apparent resistivity, thickness and depth of the various layers show that the overburden is thin and the subsurface may be underlain by weathered and fractured zone at a depth of about 34.0 m. Therefore, VES point B60 m was recommended for drilling up to a depth of about 40 m.

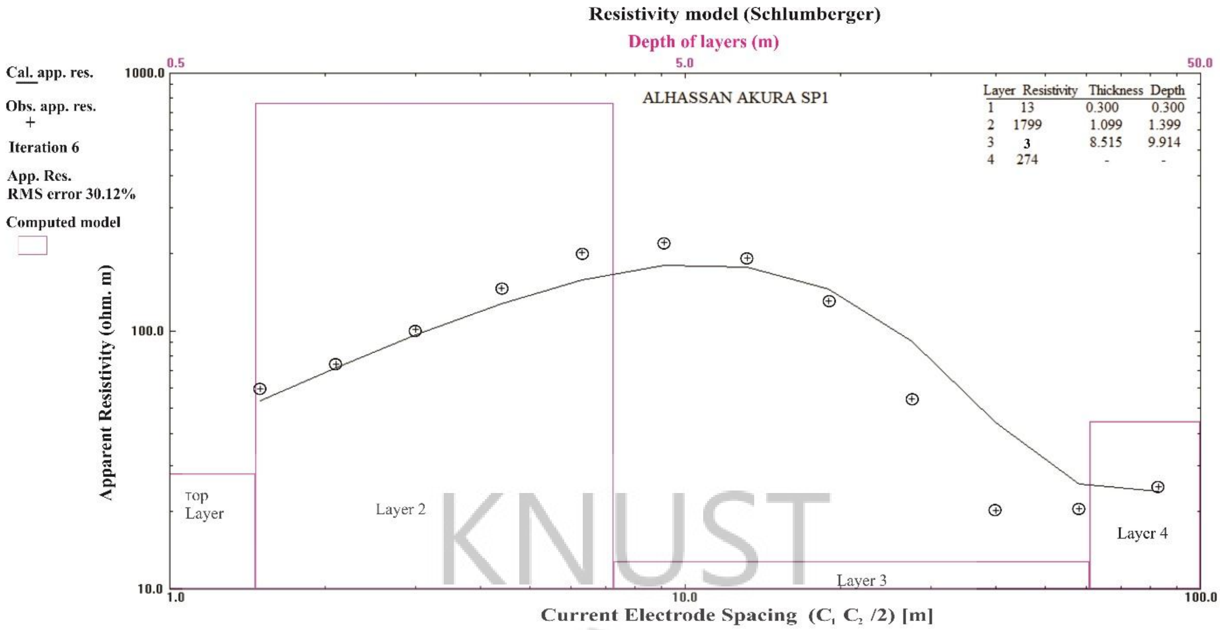

Fig 4.8 VES Model Curve at station SP1, Alhassan Akura

A four-layer subsurface structure was revealed at VES station point SP1 in the Alhassan Akura community as shown in Figure 4.8. The modeled curve shows a sharp increase in apparent resistivity of about 13 Ωm in the top soil to about 1799 Ωm in the second layer. Then a drastic drop to about 3 Ωm in the third layer and an increase to about 274 Ωm in the fourth layer. The layer parameters, apparent resistivity, thickness and depth of the various layers show that the overburden is thin and the subsurface may be underlain by clay at a depth of about 10.0 m. Therefore, VES point SP1 is inferred not to be a good point for groundwater exploration.

Table 4.1 Ranked VES points in Alhassan Akura community.

Community	VES Point	Layer	Resistivity (Ωm)	Thickness (m)	Depth (m)	Rank
Alhassan Akura	A40	1	342	0.987	0.987	**2nd**
		2	253	2.577	3.564	
		3	149	7.205	10.768	
		4	15	37.470	48.239	
		5	33	-	-	
	A110	1	241	0.625	0.625	**4th**
		2	4341	2.072	2.697	
		3	4	11.350	14.047	
		4	386	-	-	
	B60	1	363	0.725	0.725	**3rd**
		2	6909	0.616	1.341	
		3	19	17.200	18.541	
		4	3	14.569	33.11	
		5	151	-	-	
	B10	1	713	2.138	2.138	**1st**
		2	40	9.226	11.364	
		3	11	55.274	66.63	
		4	39	-	-	
	SP1	1	13	0.300	0.300	**5th**
		2	1799	1.099	1.399	
		3	3	8.515	9.914	
		4	274	-	-	

4.1.1.1 4.3.3.2 ASUKOKO EM PROFILES AND MODELLED VES CURVES

A total of 200 m long traverse was profiled in the Asukoko community to delineate conductance anomaly in the terrain, figure 4.9. The apparent conductivity of the area ranges from 6 - 19 m mhos/m. The average apparent conductivity contributed by the Vertical Dipole (VD) is 12.50 m mhos/m and that by the Horizontal Dipole (HD) is 12.00 m mhos/m.

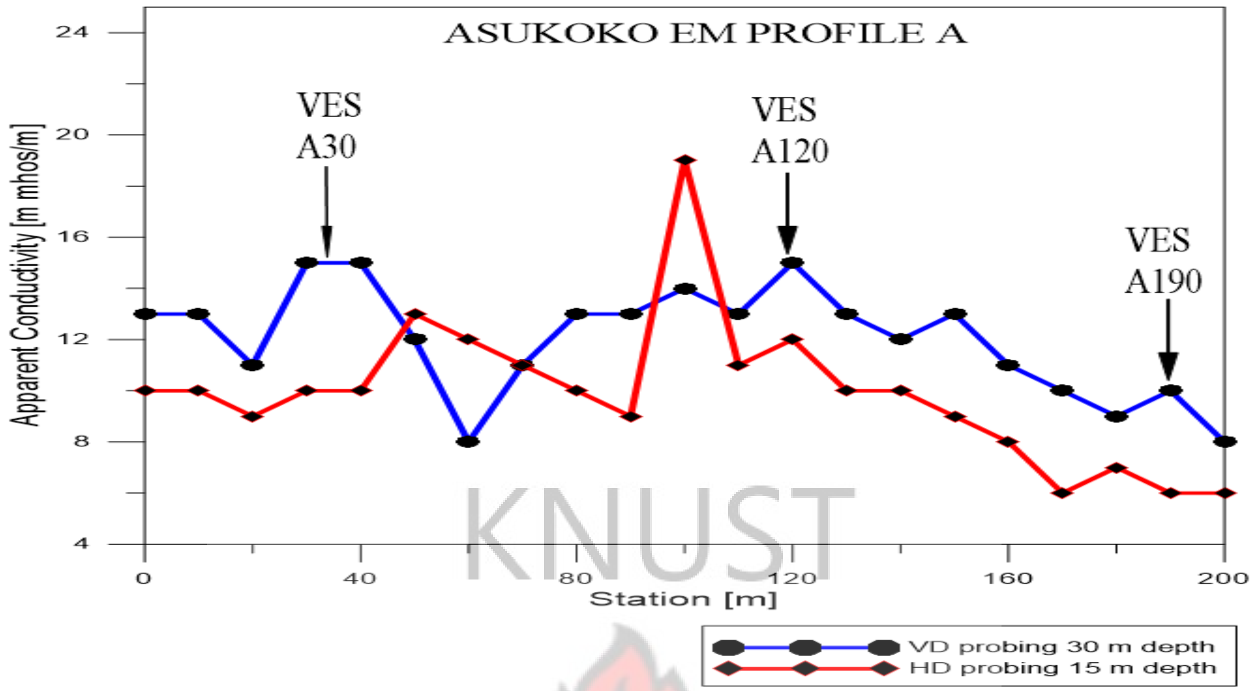

Fig 4.9 EM Profile along Traverse A at Asukoko.

The profile figure 4.9 above depicts a varying apparent conductivity at the subsurface at both shallow (15 m) and deeper (30 m) depths. The profile shows higher apparent conductivity values for VD mode than the HD mode at the subsurface up to station A30 m. However, from station point 50 m to 70 m and also from station points 90 m and 110 m, the profile shows higher apparent conductivity values for HD mode than the VD mode. The stations A30 m, A120 m and A190 m points on the traverse recorded relatively higher apparent conductivity values for VD mode than the corresponding HD mode. These stations may be deeply fractured zones, and were selected for further VES investigation.

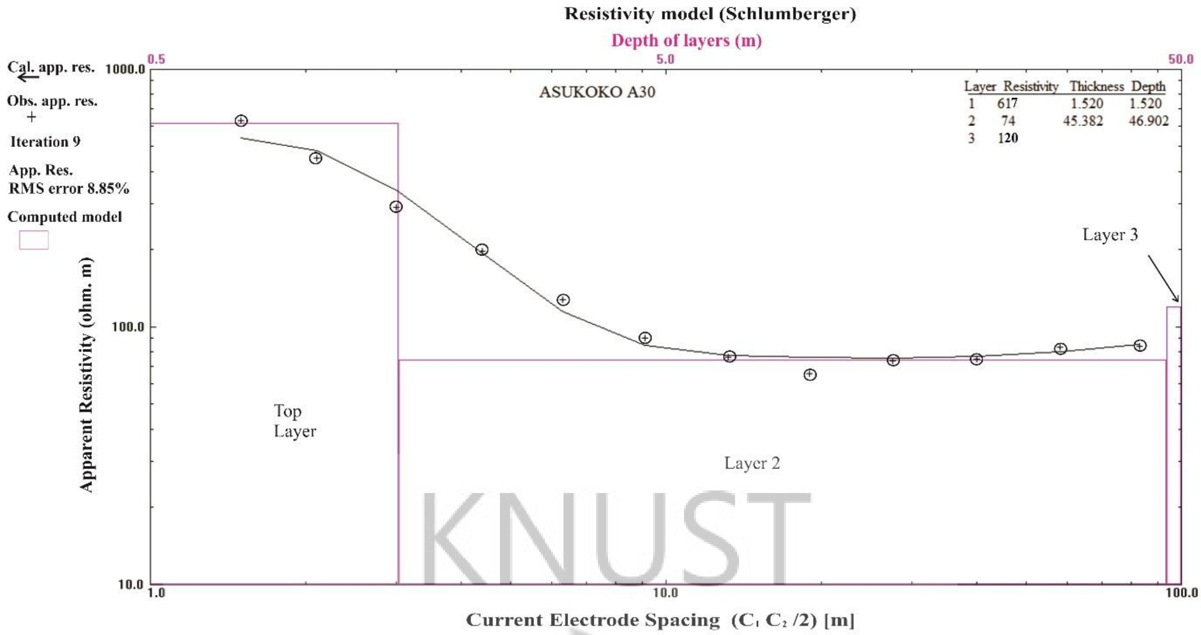

Fig 4.10 VES Model Curve at station A30 m, Asukoko

Figure 4.10 shows the apparent resistivity VES model curve at station A30 m. Quantitatively the model on the traverse shows a three layered model with decreasing apparent resistivity from about 617 Ωm at the first layer (topsoil) to 74 Ωm in the second layer; then an increase again to about 120 Ωm in the third layer. The layer parameters of apparent resistivity, thickness and depth of the various layers show that the overburden is averagely thick and the subsurface may be underlain by deep fractured zone at a depth of about 47 m. Therefore, VES point A30 m was recommended for drilling up to a depth of about 50 m.

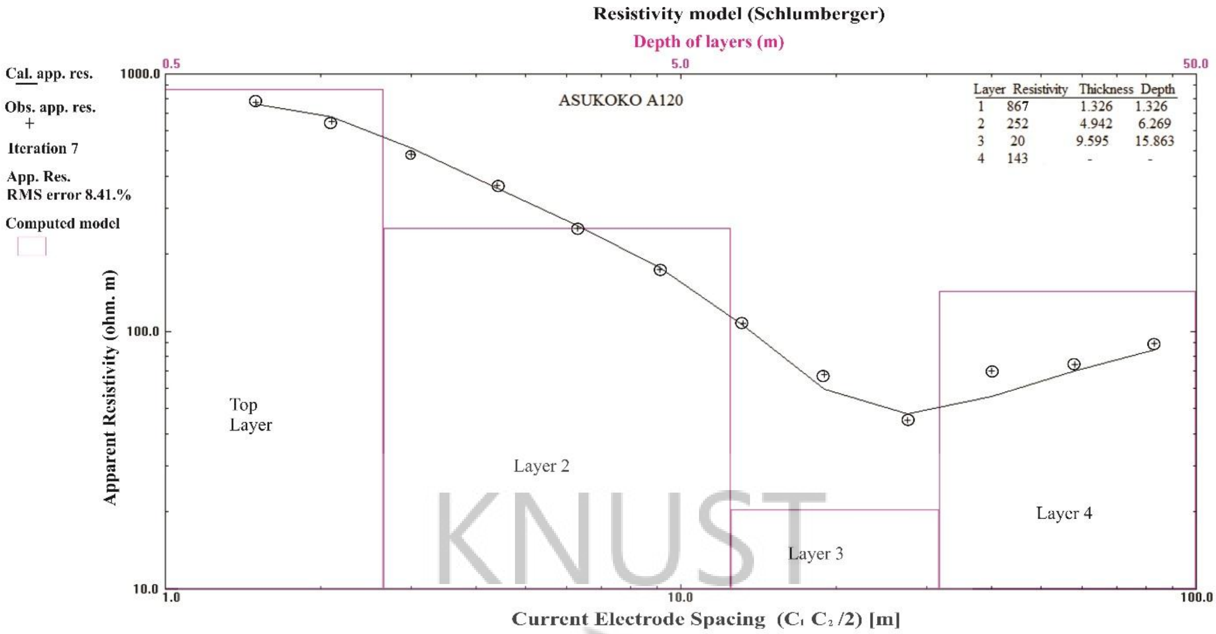

Fig 4.11 VES Model Curve at point A120 m, Asukoko.

A four-layer subsurface structure was revealed at point A120 m as shown in figure 4.11 above. The apparent resistivity dropped significantly from 867 Ωm in the top layer to 252 Ωm in the second layer and a further drop to about 20 Ωm in the third layer. However, the fourth layer's apparent resistivity rather increased to 143 Ωm at a depth below 16 m and of infinite thickness. The third layer of low apparent resistivity 20 Ωm is inferred to be clay. This point might not be recommended for drilling because of the shallow depths and their layer thickness.

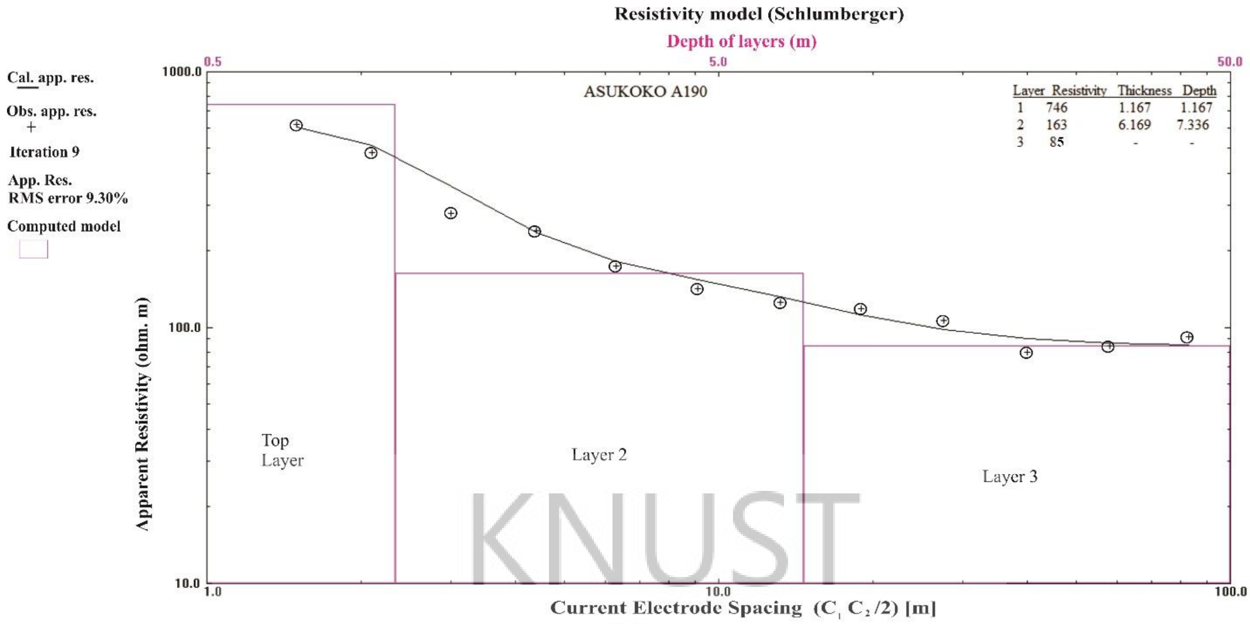

Fig 4.12 VES Model Curve at point A190 m, Asukoko.

Figure 4.12 shows the apparent resistivity VES model curve for station A190 m on the traverse in the Asukoko community. Quantitatively, the model showed three layers. The top layer's (topsoil) apparent resistivity is about 746 Ωm at a shallow depth of about 1.2 m. The apparent resistivity of the second layer decreased to about 163 Ωm and a further decreased to 85 Ωm in the third layer. The layer resistivity, thickness and depth of the various layers showed that the overburden might not be thick and the subsurface may be underlain by fractured zone at a shallow depth of about 10 m. Therefore, VES point A190 m is not recommended for drilling.

Table 4.2 Ranked VES points in Asukoko community.

Community	VES Point	Layer	Resistivity (Ωm)	Thickness (m)	Depth (m)	Rank
Asukoko	A30	1 2 3	617 74 120	1.520 45.382	1.520 46.902	1st
	A120	1 2 3 4	867 252 20 143	1.326 4.942 9.595 -	1.326 6.269 15.863 -	2nd .
	A190	1 2 3	746 163 85	1.167 6.169 -	1.167 7.336 -	3rd

4.3.3.3 ATTA AKURA EM PROFILES AND MODELLED VES CURVES

Two (2) traverses of total length 260 m were profiled (Profile A on the right side of community and Profile B at the Primary/JHS School) to delineate the apparent conductive anomaly. The apparent conductivity response values ranged between 60 and 90 m mhos/m with an average of 75 m mhos/m. Two spot soundings SP1 and SP2 were also probed.

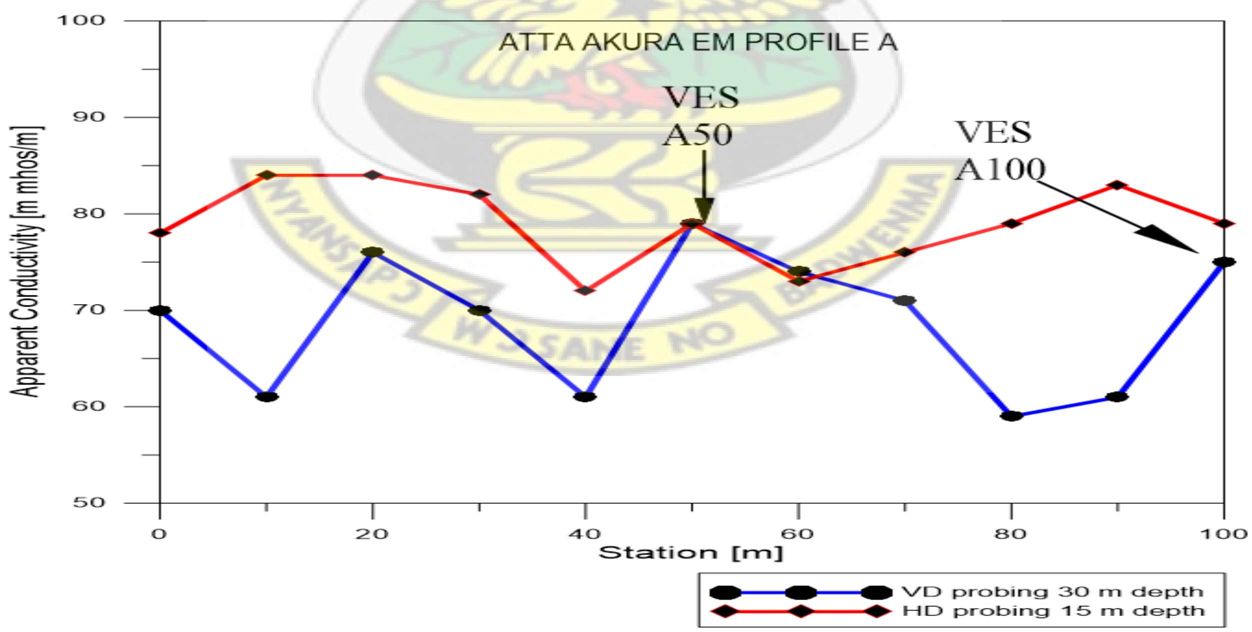

Fig 4.13   EM Profile along Traverse A at Atta Akura.

The profile (figure 4.13) above shows apparent conductivity at the subsurface at both shallow (15 m) and deeper (30 m) depths for EM profile A in the Atta Akura community. The profile shows higher apparent conductivity values for HD mode than the VD mode at the subsurface except at station points A50 m and A60 m, where an anomaly occurred. Apart from these two stations mentioned, the apparent conductivity, VD mode of A100 m is also high. These stations may be deeply fractured and weathered zones. Therefore, A50 m and A100 m where selected for further VES investigations.

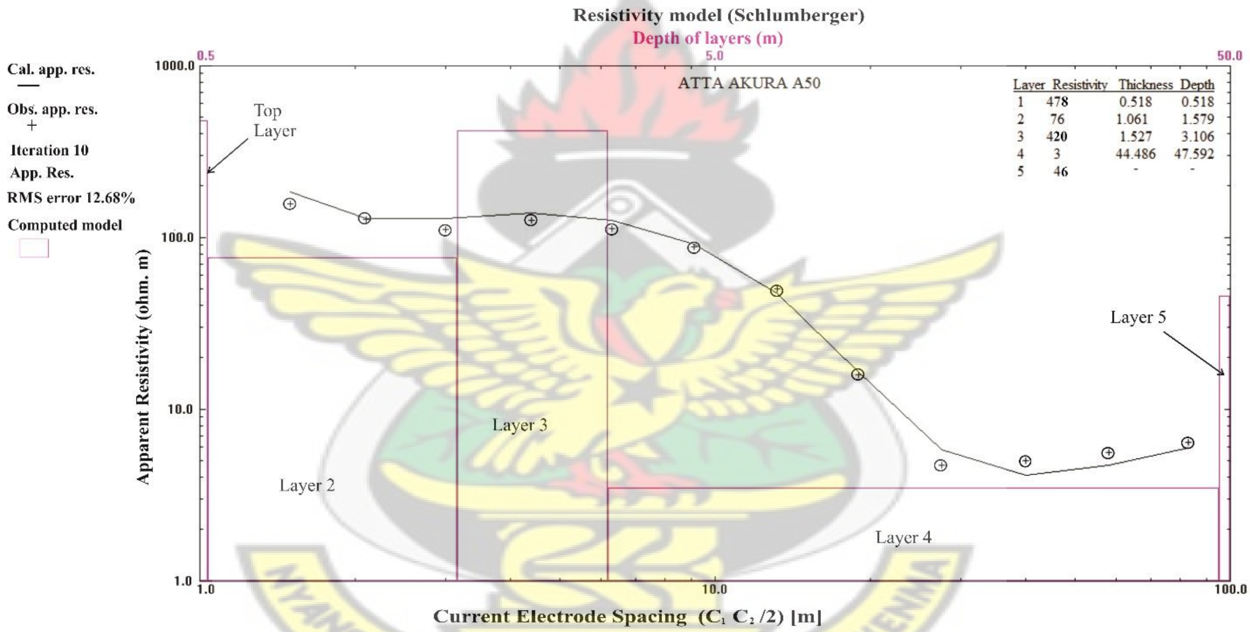

Fig 4.14 VES Model Curve at station A50 m, Atta Akura.

The VES modelled curve, figure 4.14 above delineated five subsurface layers for sounding spot A50 m within the Atta Akura community. The apparent resistivity changed significantly from 478 Ωm in the first layer to as low as 76 Ωm in the second layer. However, the apparent resistivity increased to 420 Ωm in the third layer before dropping to as low as 4 Ωm in the fourth layer and again increased to about 46 Ωm in the fifth layer. The layer resistivity, thickness and depth suggest that, the subsurface is thick and could be fractured and weathered. This VES point is thus recommended for drilling up to a depth of 50 m.

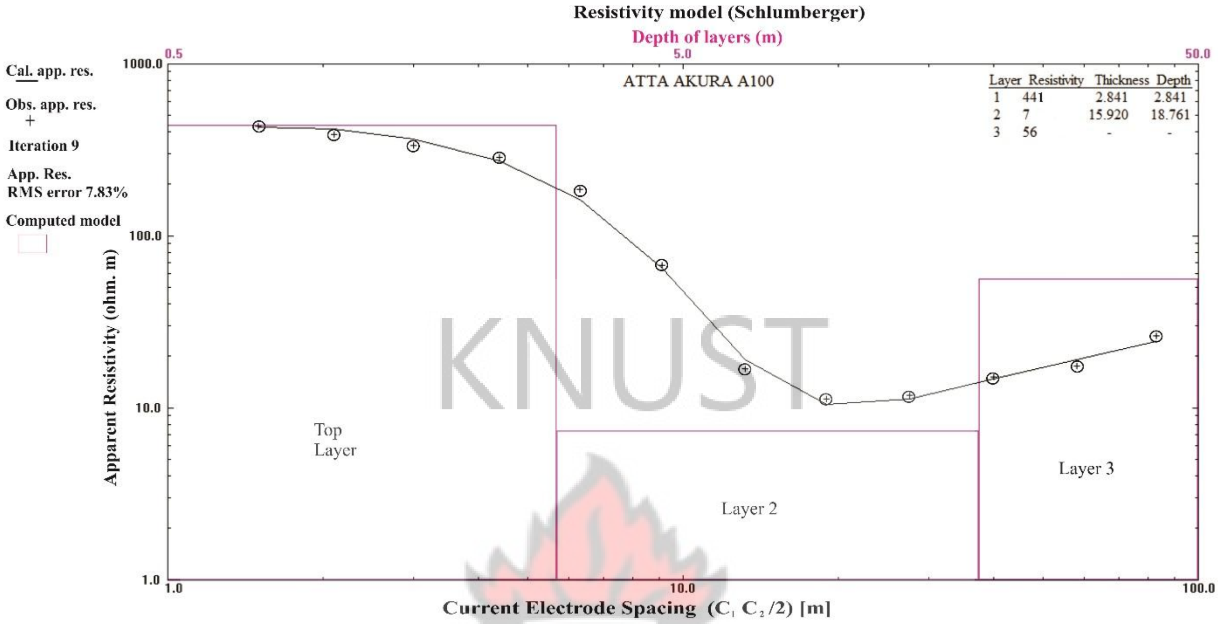

Fig 4.15 VES Model Curve at station A100 m, Atta Akura.

Figure 4.15 shows the apparent resistivity VES model curve for station A100 m on the traverse in the Atta Akura community. Quantitatively, the model showed three layers. The top layers' (top soil) apparent resistivity is about 441 Ωm at a shallow depth of about 3 m. The apparent resistivity of the second layer decreased to about 7 Ωm. It then increased to 56 Ωm in the third layer. The layer parameters (apparent resistivity, thickness and depth of the various layers) showed that the overburden might be averagely thick and the subsurface may be underlain by fractured zone at a depth beyond 20 m. Therefore, VES point A100 m is recommended for drilling up to a depth of 30 m.

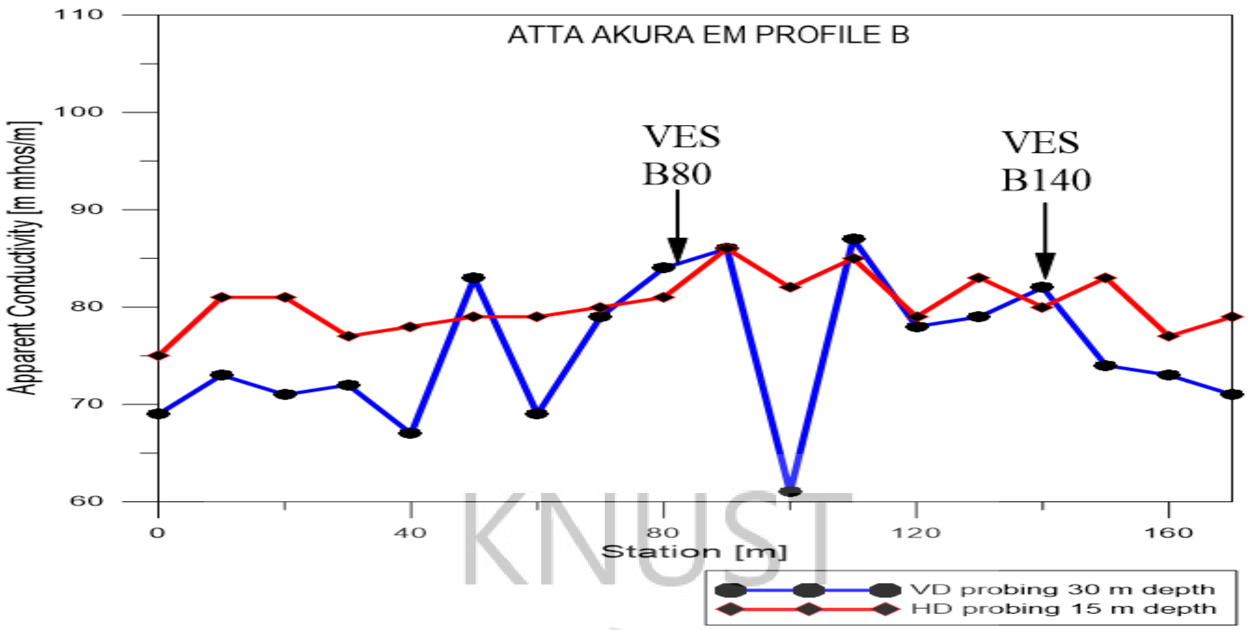

Fig 4.16 EM Profile along Traverse B in Atta Akura.

Figure 4.16 shows the EM profile along traverse B over a distance of about 170 m in Atta Akura community. The profile exhibits a varying apparent conductivity at the subsurface at both shallower (15 m) and deeper (30 m) depths. The profile length shows higher apparent conductivity values for HD mode than the VD mode at almost all the entire profile except only at the crossovers, where the VD mode shows higher conductivity values than the HD mode. The crossovers occurred at B50 m, B80 m, B110 m and at B140 m. These crossovers indicate significant anomaly at the subsurface, which are likely deep fractured zones, with relatively higher apparent conductivity values. However, only two points B80 m and B140 m were selected for further VES investigation.

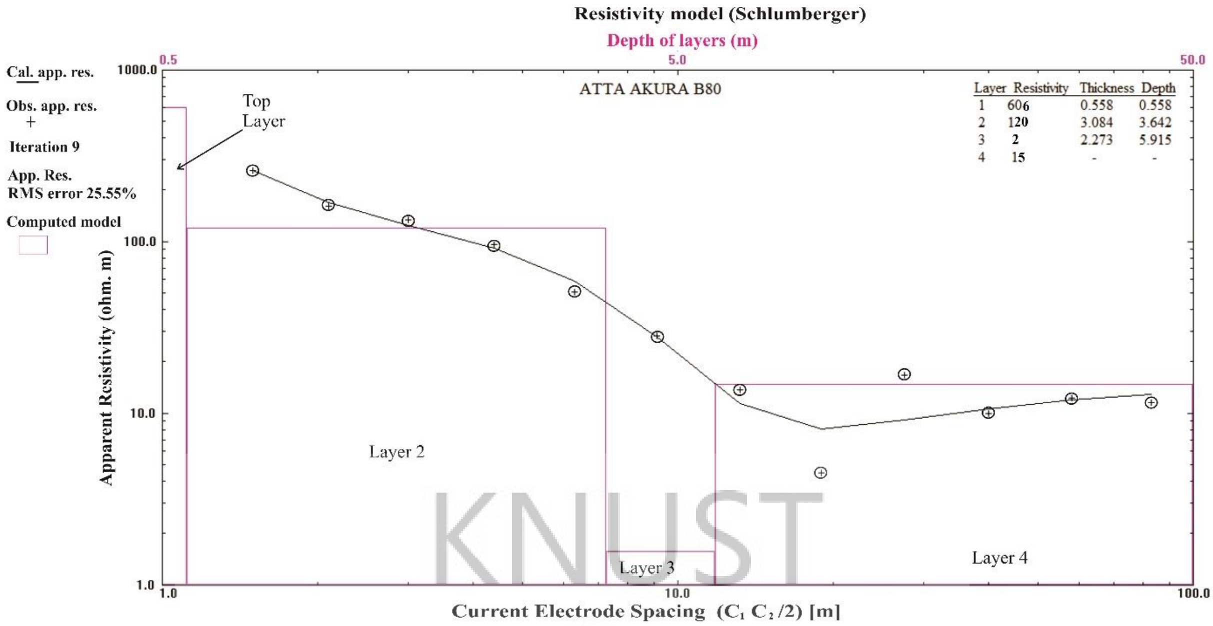

Fig 4.17 VES Model Curve at point B80 m, Atta Akura.

From the modelled VES curve at station B80 m, the subsurface consists of four layers as shown in figure 4.17 above. The apparent resistivity value of 606 Ωm of the top layer decreases to 120 Ωm in the second layer and further drop drastically to 2 Ωm in the third layer. It then increased to about 15 Ωm at a depth beyond 6 m in the fourth layer. The layer parameters (apparent resistivity, thickness and depth), suggest a very thin overburden at shallow depth of about 6 m with a very low resistivity suspected to be clay. This VES point might not contain a fracture with groundwater storage potential. Hence is not recommended for drilling.

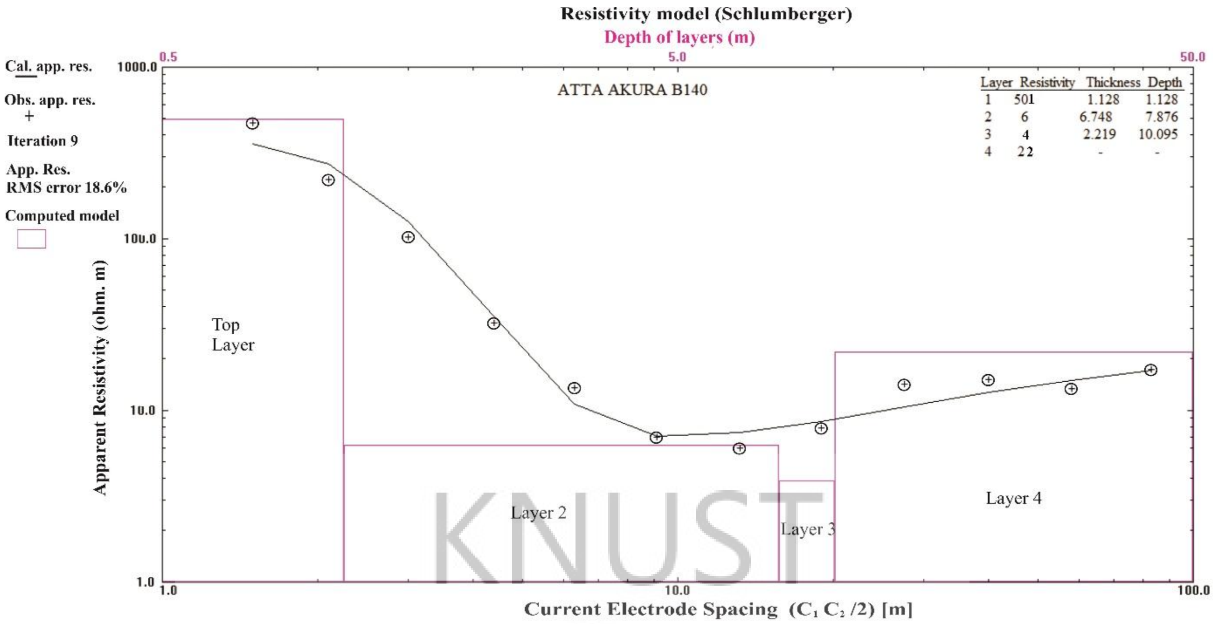

Fig 4.18 VES Model Curve at station B140 m, Atta Akura.

At station B140 m, the subsurface consists of four layers as shown in figure 4.18 above. The apparent resistivity dropped significantly from about 501 Ωm in the top layer to about 6 Ωm in the second layer and a further drop to about 4 Ωm in the third layer. However, the fourth layer's apparent resistivity rather increased to 22 Ωm at a depth below 11 m and of infinite thickness. The third layer of low apparent resistivity 4 Ωm is inferred to be clay. This point is not recommended as a test drilling point.

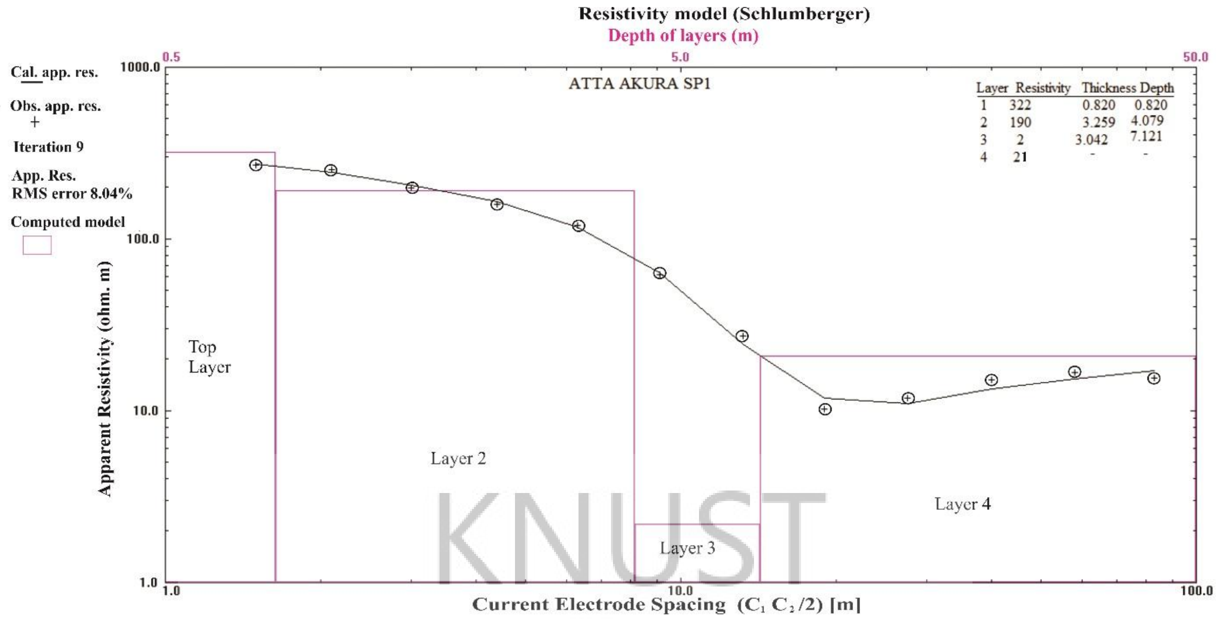

Fig 4.19 VES Model Curve at point SP1, Atta Akura.

At spot station SP1, the subsurface consists of four layers as shown in figure 4.19 above. The apparent resistivity of the first layer is about 322 Ωm at a very shallow depth of about 0.8 m. The apparent resistivity of the second layer decreased to 190 Ωm. It further decreased to about 2 Ωm in the third layer. Conversely, the fourth layers apparent resistivity rather increased to 21 Ωm at a depth beyond 8 m. The third layer of low apparent resistivity 2 Ωm is inferred to be clay. However, that of the fourth layer could be a fractured zone at a very shallow depth. The layer parameters involving the apparent resistivity, thickness and depth of the various layers showed that the overburden is not thick and the subsurface may be underlain by a fractured zone at a depth of about 10 m. Therefore, VES point SP1, was not recommended for drilling.

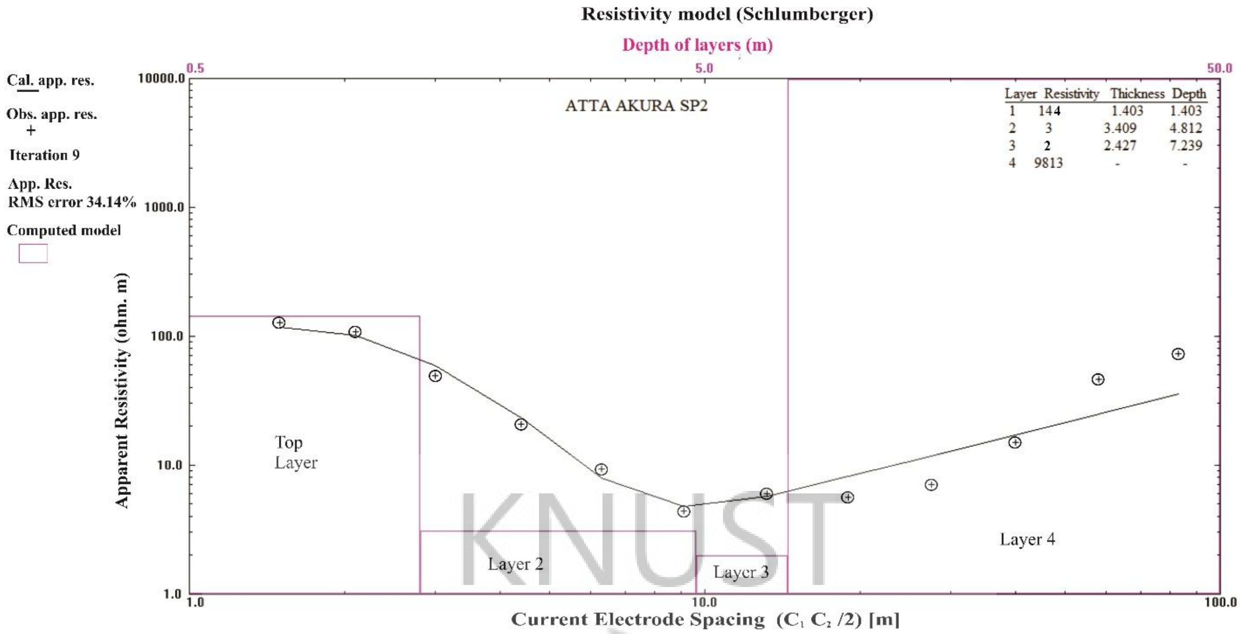

Fig 4.20 VES Model Curve at SP2, Atta Akura community.

At SP2, the modelled curve of the subsurface depicts four layers as shown in figure 4.20 above. The top layers apparent resistivity is about 144 Ωm at a depth of about 1.4 m. The apparent resistivity of the second layer decreased to 3 Ωm. It further decreased to about 2 Ωm in the third layer. The fourth layers apparent resistivity increased to about 9813 Ωm at a depth below 8 m and of infinite thickness. The low apparent resistivity of the third layer is suspected to be clay. However, that of the fourth layer could be an un-fractured dolomite or limestone at a very shallow depth of about 10m. The layer parameters of apparent resistivity, thickness and depth of the various layers showed that the overburden is not thick and possibly un-fractured, which is not suitable for groundwater accumulation and storage. Therefore, VES point SP2, is also not recommended for drilling.

Table 4.3 Ranked VES points in Atta Akura community.

Community	VES Point	Layer	Resistivity (Ωm)	Thickness (m)	Depth (m)	Rank
Atta Akura	A50	1 2 3 4 5	478 76 420 3 46	0.518 1.061 1.527 44.486 -	0.518 1.579 3.106 47.592 -	1st
	A100	1 2 3	441 7 56	2.841 15.920 -	2.841 18.761 -	**2nd**
	B80	1 2 3 4	606 120 2 15	0.558 3.084 2.273 -	0.558 3.642 5.915 -	**5th**
	B140	1 2 3 4	501 6 4 22	1.128 6.748 2.219 -	1.128 7.876 10.095 -	**3rd**
	SP1	1 2 3 4	322 190 2 21	0.820 3.259 3.042 -	0.820 4.079 7.121 -	4th
	SP2	1 2 3 4	144 3 2 9813	1.403 3.409 2.427 -	1.403 4.812 7.239 -	6th

4.3.3.4 BENKROM EM PROFILES AND MODELLED VES CURVES

One EM traverse of length 160 m was run within the school premises to obtain anomalous points for further investigations, (figure 4.21 below).

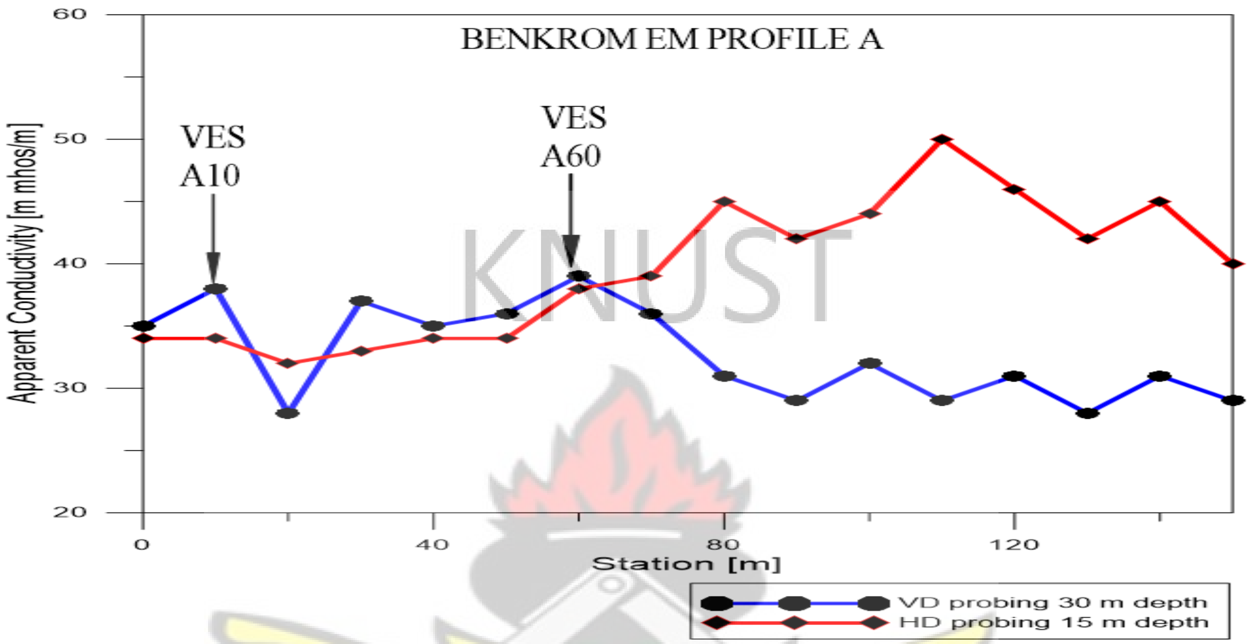

Fig 4.21 EM Profile along Traverse A, Benkrom

The apparent conductivity curve as shown in figure 4.21 above depicts higher HD mode values than VD mode along the traverse except at the station 0 m, 10 m, 20 m, 40 m, 50 m and 60 m, where the VD values are higher than the HD values. The crossovers at station points A10 m and A60 m were selected for further VES investigations. In addition to these two, three other VES station points, SP1, SP2 and SP3 were investigated.

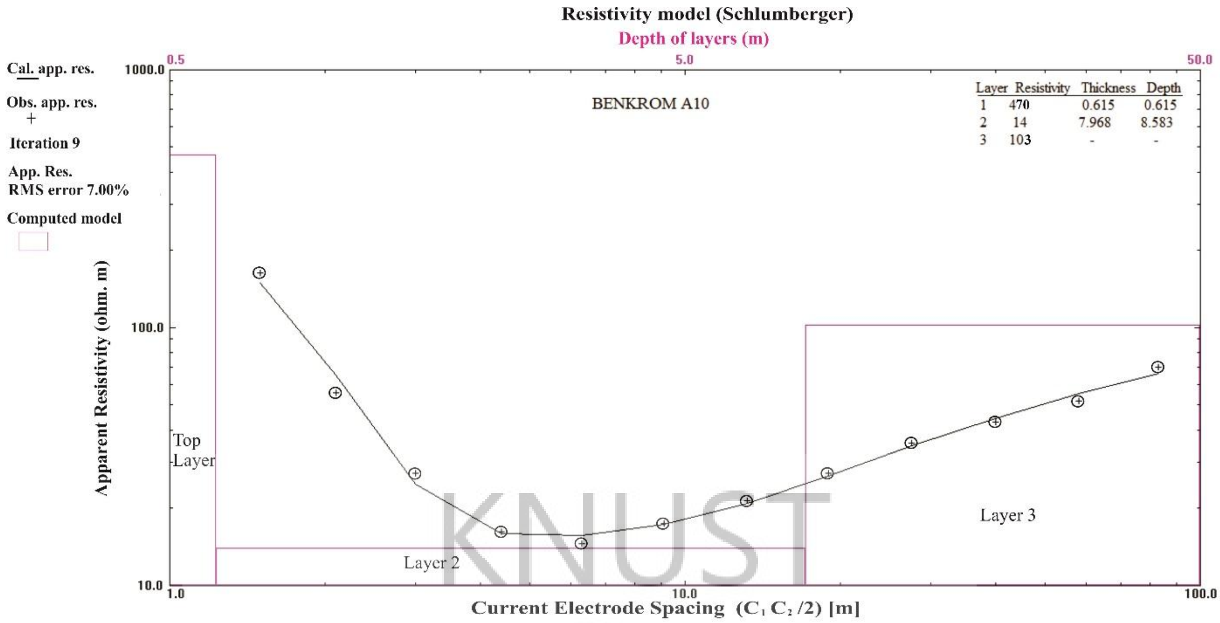

Fig 4.22 VES Model Curve at station A10 m, Benkrom community.

Figure 4.22 is the VES modelled curve for station A10 m in the Benkrom community. It portrays a three layer subsurface structure with varying apparent resistivities. The top soil has a resistivity of about 470 Ωm, which drops to about 14 Ωm in the second layer. The apparent resistivity however increases to about 103 Ωm in the third layer at a depth deeper than 10 m. The resistivity of the third layer is 103 Ωm and it could be an indication of a fracturing of the basement rock, which could potentially contain some ground water. However, the depth of about 10 m at which this occurred in the Voltaian makes it unsuitable point for drilling. Hence, the point A10 m in Benkrom was thus not recommended for drilling.

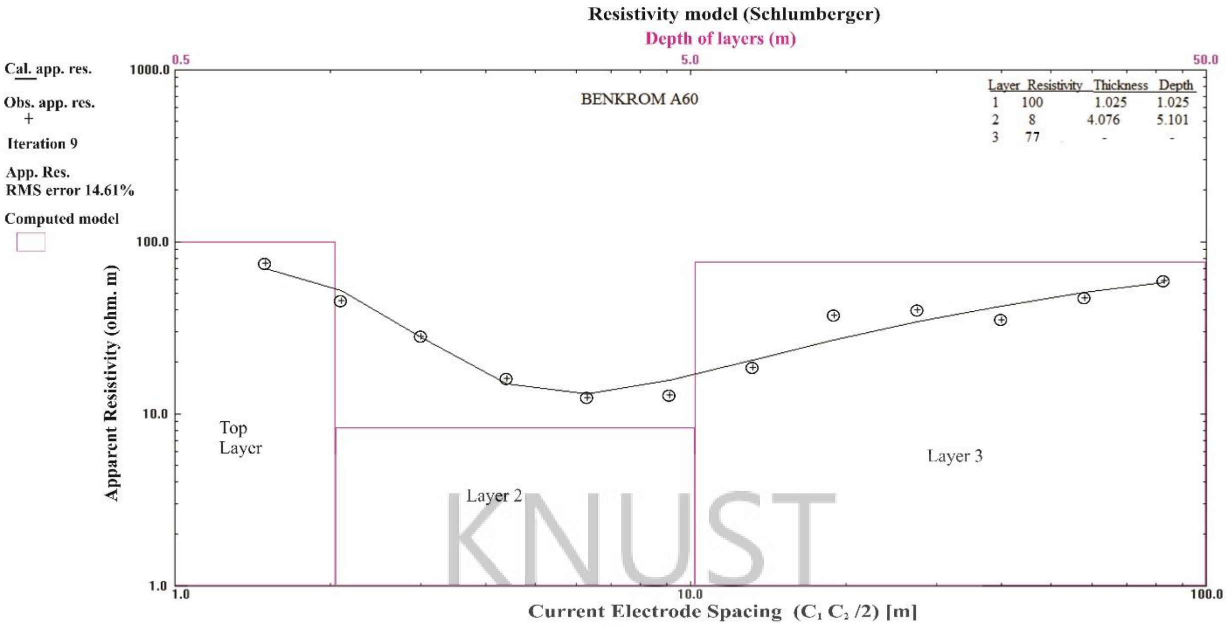

Fig 4.23 VES Model Curve at station A60 m, Benkrom community.

Figure 4.23 above shows a VES model curve at station A60 m in the Benkrom community. It reveals a three layer subsurface structure with varying apparent resistivities. The top soil has a resistivity of about 100 Ωm, which falls to about 8 Ωm in the second layer. The apparent resistivity however increases to about 77 Ωm in the third layer at a depth deeper than 6 m. Layer three of resistivity of about 77 Ωm could be a fractured zone in the subsurface which could contain ground water. However, the shallow depth of about 6 m at which this occurred in the Voltaian makes it unsuitable for bore hole drilling. Therefore, this point A60 m in Benkrom was thus not recommended for drilling.

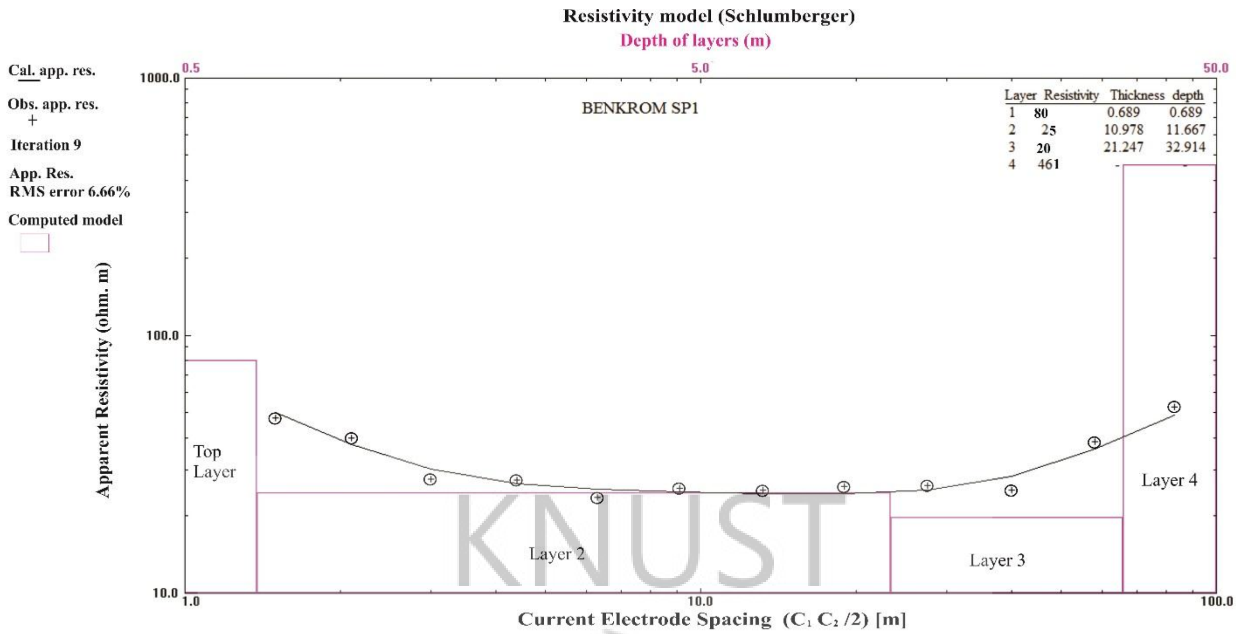

Fig 4.24 VES Model Curve at station SP1, Benkrom community.

At spot sounding SP1 in the Benkrom community, the subsurface consists of four layers as shown in figure 4.24 above. The top layers apparent resistivity is about 80 Ωm at a very shallow depth of about 0.7 m. The apparent resistivity of the second layer decreased to about 25 Ωm. It further decreased to about 20 Ωm in the third layer. On the contrary, the fourth layers apparent resistivity rather increased to 461 Ωm at a depth deeper than 35 m. The third layer resistivity of about 20 Ωm is inferred to be a fractured rock which could contain ground water. The layer parameters (apparent resistivity, thickness and depth of the various layers) showed that the overburden is thick and the subsurface may be underlain by a fractured zone at a depth of about 33 m. Therefore, VES point SP1, is recommended for drilling up to a depth of about 35 m.

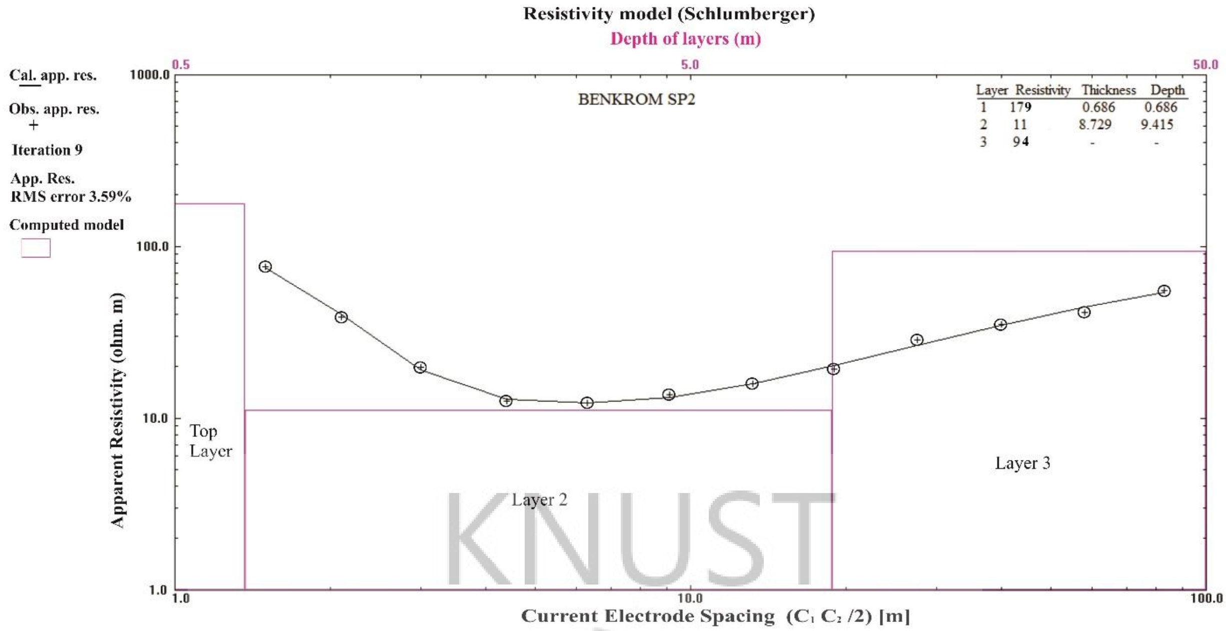

Fig 4.25 VES Model Curve at station SP2, Benkrom community.

Figure 4.25 above depicts a VES modelled curve for sounding spot SP2 in the Benkrom community. It indicates a three layer subsurface structure with varying apparent resistivities. The top soil has a resistivity of about 179 Ωm, which decreases to about 11 Ωm in the second layer. The apparent resistivity however increased to about 94 Ωm in the third layer at a depth deeper than 10 m. The layer parameters involving apparent resistivity, thickness and depth indicates that the overburden is fractured and thin. Layer three of resistivity of about 94 Ωm could potentially be an indication of a fractured and weathered zone in the subsurface, which could contain ground water. However, the depth of about 10 m at which this occurred in the Voltaian could possibly be perched water. Therefore, the point SP2 in Benkrom is thus not recommended for drilling.

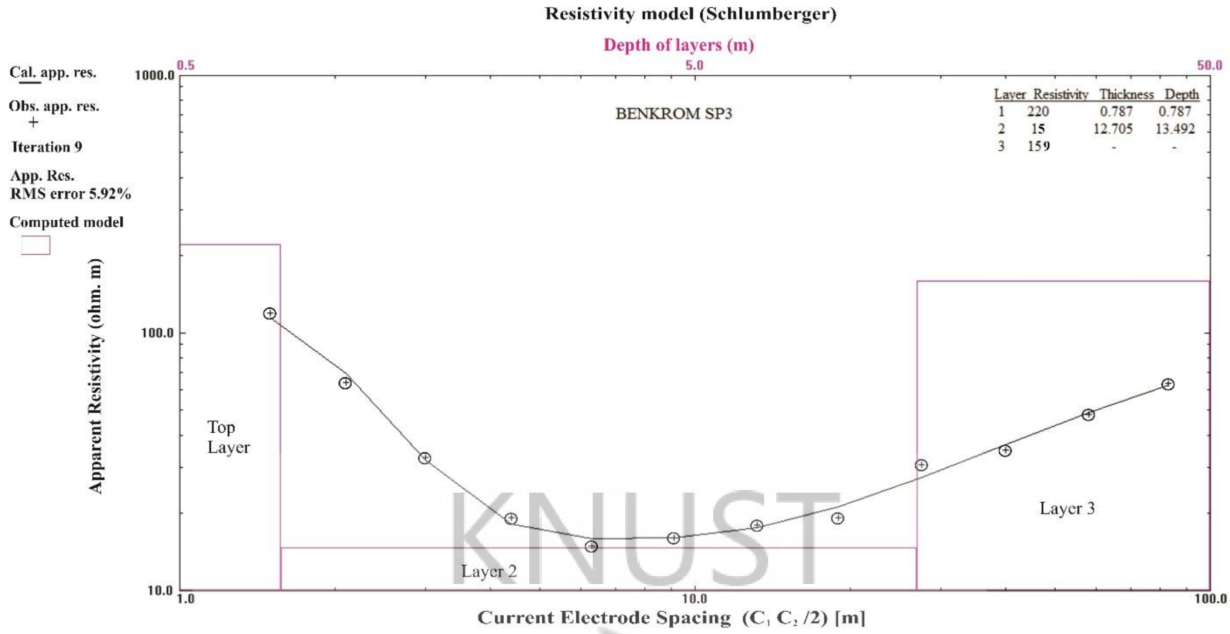

Fig 4.26 VES Model Curve at SP3, Benkrom community.

Figure 4.26 above is a VES modelled curve at the spot SP3 in the Benkrom community. It depicts a three layer subsurface with varying apparent resistivities at varying depths. The top soil has a resistivity of about 220 Ωm, which decreases to about 15 Ωm in the second layer at a depth of about 14 m. The apparent resistivity however increased to about 159 Ωm in the third layer at a depth deeper than 15 m. The layer parameters involving apparent resistivity, thickness and depth indicates that the overburden is fractured and thin. However, the depth of about 15 m at which this occurred could possibly be clay. Therefore, the point SP3 in Benkrom is thus not recommended for drilling.

Table 4.4 Ranked VES points in Benkrom community.

Community	VES Point	Layer	Resistivity (Ωm)	Thickness (m)	Depth (m)	Rank
Benkrom	A10	1 2 3	470 14 103	0.615 7.968 -	0.615 8.583 -	3rd
	A60	1 2 3	100 8 77	1.025 4.076 -	1.025 5.101 -	4th
	SP1	1 2 3 4	80 25 20 461	0.689 10.978 21.247 -	0.689 11.667 32.914 -	1st
	SP2	1 2 3	179 11 94	0.686 8.729 -	0.686 9.415 -	2nd
	SP3	1 2 3	220 15 159	0.787 12.705 -	0.787 13.492 -	5th

4.3.3.5 DAGARTI AKURA EM PROFILES AND MODELLED VES CURVES

Two Electromagnetic Profiles A and B of 130 m and 100 m length respectively were carried out.

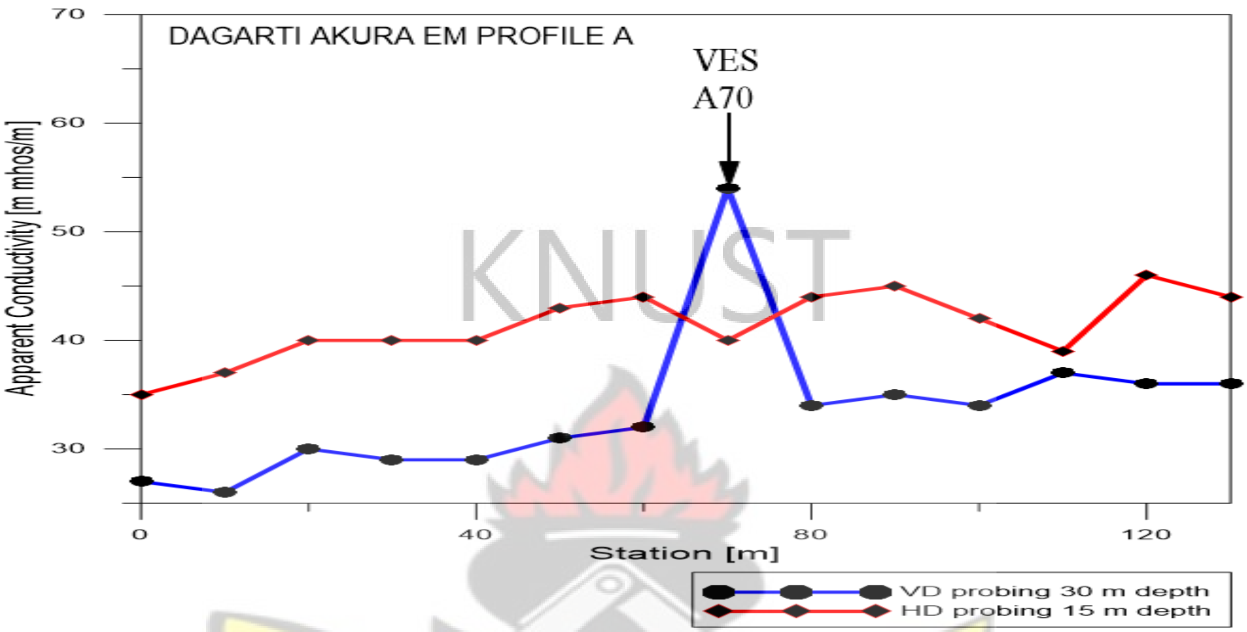

Fig 4.27 EM Profile along Traverse A, Dagarti Akura.

Figure 4.27 above shows the EM profile of the apparent conductivity along traverse A, over a distance of about 130 m in Atta Akura community. The profile shows higher apparent conductivity values for HD mode (15 m) than the VD mode (30 m) at almost all the entire profile length except only at the crossover point A70 m, where the VD mode shows higher conductivity values than the HD mode. This crossover indicates significant anomaly at the subsurface, which is likely a deep fractured and weathered zone. Hence, this point A70 m, was selected for further VES investigation.

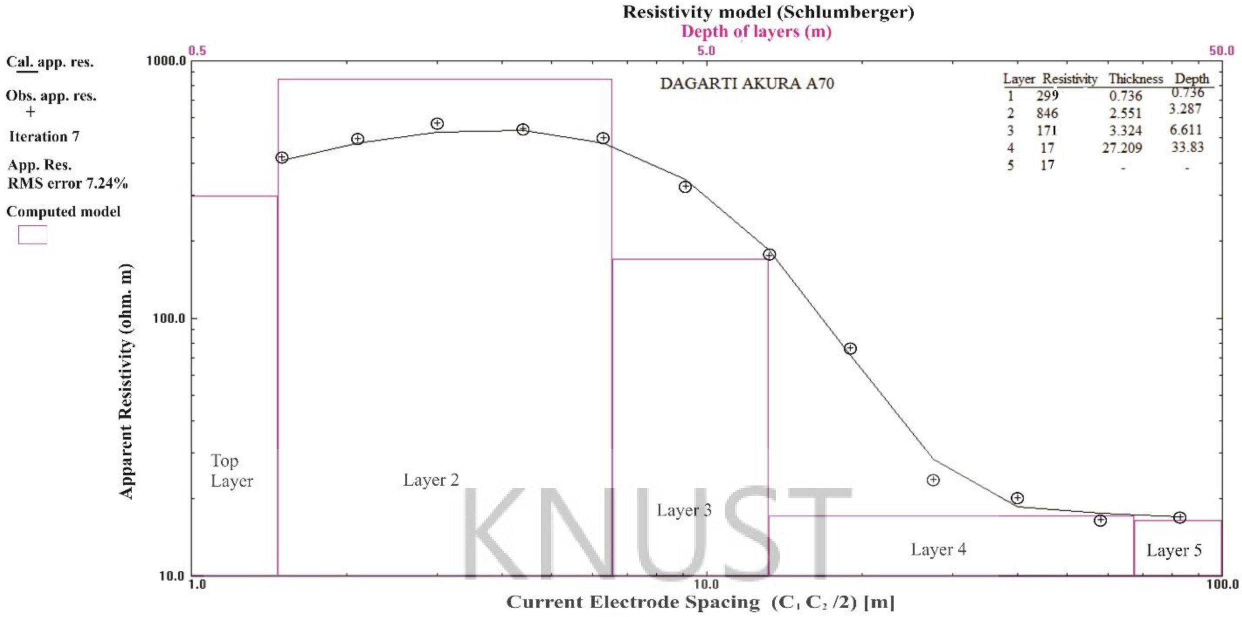

Fig 4.28 VES Model Curve at A70 m, Dagarti Akura community.

A five-layer subsurface structure was revealed at VES station A70 m in the Dagarti Akura community as shown in figure 4.28. There is an increase in apparent resistivity of about 299 Ωm in the top soil to about 846 Ωm in the second layer. There is a resistivity drop to about 171 Ωm in the third layer and a further decrease to 17 Ωm in the fourth layer. There was however a marginal decrease in apparent resistivity in the fifth layer to about 16 Ωm occurring at a depth of about 36 m. The apparent resistivity, thickness and depth of the various layers show that the overburden is thick and the subsurface may be underlain by weathered and fractured zone at a depth of about 36.0 m. Therefore, VES point A70 m was recommended for drilling up to a depth of about 40 m.

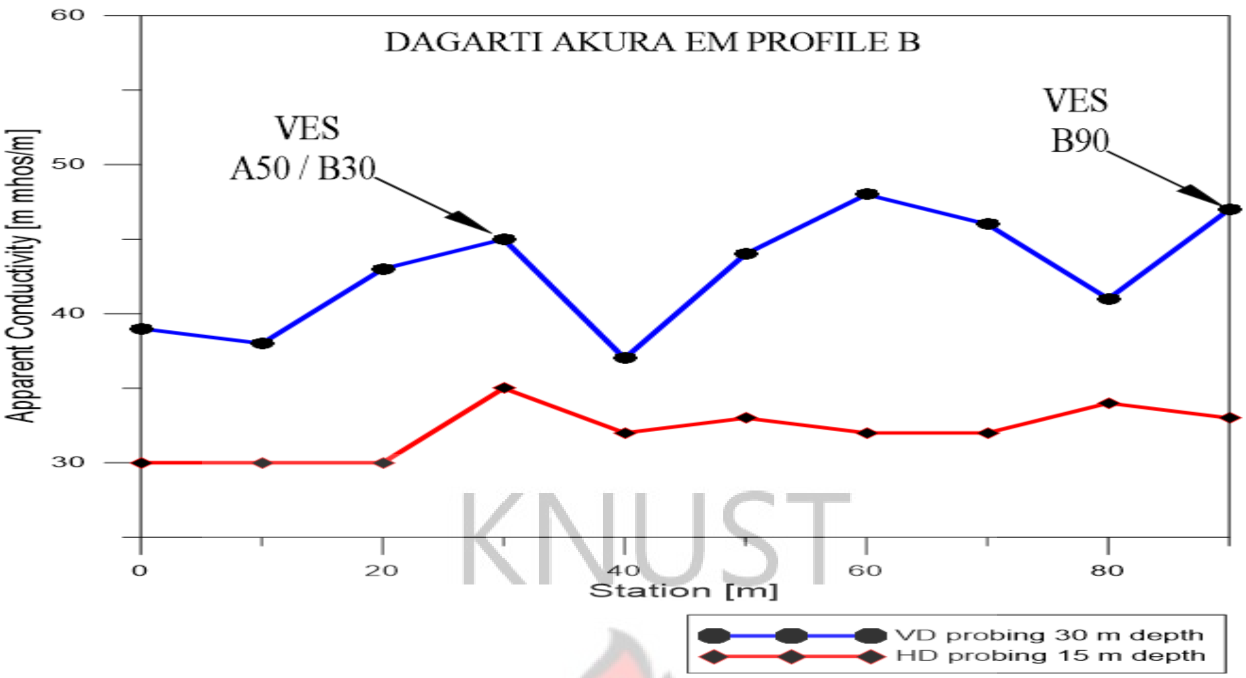

Fig 4.29 EM Profile along Traverse B, Dagarti Akura.

Figure 4.29 above is the EM profile indicating the variation of apparent conductivity along traverse B over a distance of about 100 m in Dagarti Akura community. The profile shows higher apparent conductivity values for the VD mode (30 m) than the corresponding HD mode (15 m) along the entire profile length. There were no crossovers. However, two peaks along the VD mode curve, A50/B30 and B90, which are likely fractured and weathered zones were further probed using VES.

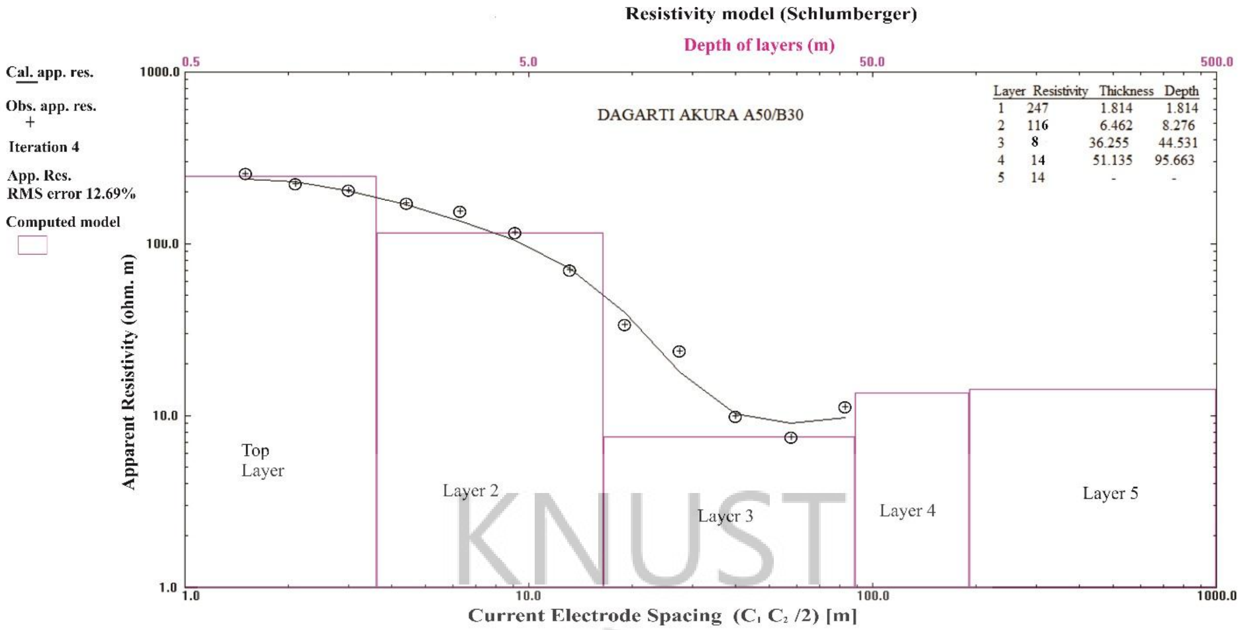

Fig 4.30 VES Model Curve at station A50/B30 m, in the Dagarti Akura community.

Figure 4.30 above shows a five-layer subsurface structure at VES station A50/B30 m in the Dagarti Akura community. The apparent resistivity decreases from about 247 Ωm in the top layer to about 116 Ωm in the second layer. Then, a further resistivity drop to about 8 Ωm in the third layer. However, the apparent resistivity of the fourth layer rather increased to about 14 Ωm, and a further slightly increased to about 14 Ωm in the fifth layer. The apparent resistivity, thickness and depth of the various layers show that the overburden is thick and the subsurface may be underlain by a very thick weathered and fractured zone occurring at a depths between 45 m to about 96.0 m. Hence, VES point A50/B30 m is highly recommended for drilling up to a depth of about 100 m.

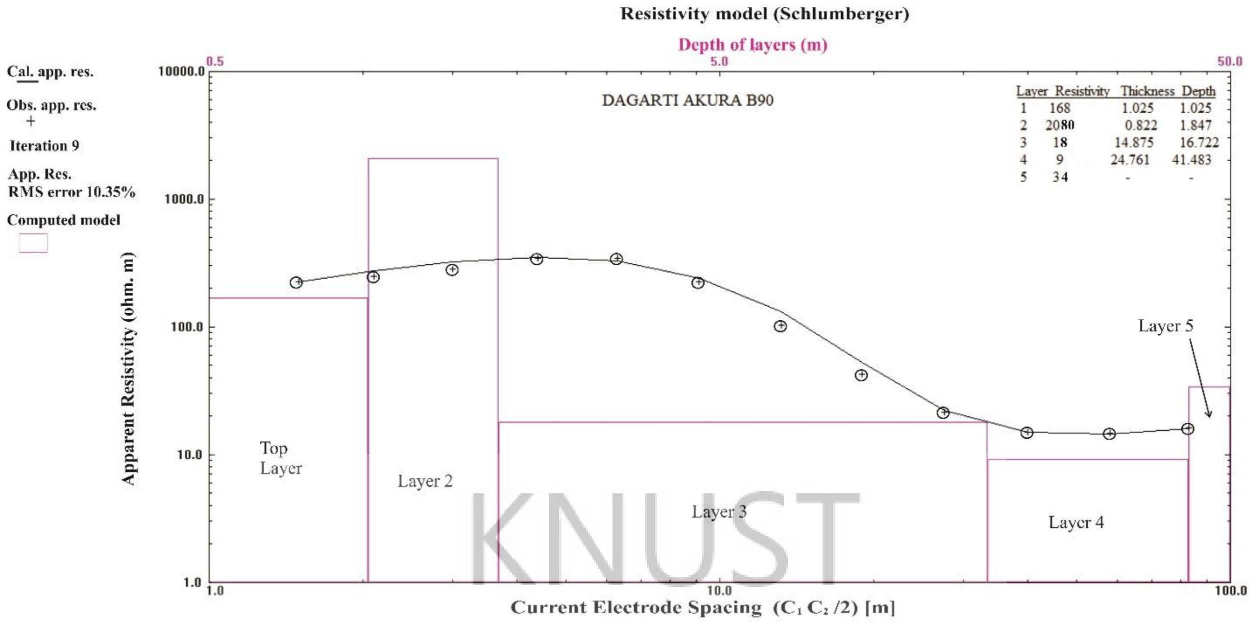

Fig 4.31 VES Model Curve at station B90 m, in the Dagarti Akura community.

A five-layer subsurface was revealed at VES station A90 m in the Dagarti Akura community as shown in figure 4.31 above. The apparent resistivity of about 168 Ωm in the first layer increases significantly to about 2080 Ωm in the second layer. Then a very steep resistivity drop to about 18 Ωm in the third layer and a further decrease to 9 Ωm in the fourth layer. There was however a slight increase in apparent resistivity to about 34 Ωm in the fifth layer, occurring at a depth beyond 42 m. The layer parameters, (apparent resistivity, thickness and depth of the various layers) show that the overburden is thick and the subsurface may be underlain by weathered and fractured zone at a depth of about 45.0 m. Therefore, VES point B90 m is recommended for drilling up to a depth of about 50 m.

.

Table 4.5 Ranked VES points in Dagarti Akura community.

Community	VES Point	Layer	Resistivity (Ωm)	Thickness (m)	Depth (m)	Rank
Dagarti Akura	A70	1	299	0.736	0.736	**1st**
		2	846	2.551	3.287	
		3	171	3.324	6.611	
		4	17	27.209	33.83	
		5	17	-	-	
	A50/B30	1	247	1.814	1.814	**2nd**
		2	116	6.462	8.276	
		3	8	36.255	44.531	
		4	14	51.135	95.663	
		5	14	-	-	
	B90	1	168	1.025	1.025	**3rd**
		2	2080	0.822	1.847	
		3	18	14.875	16.722	
		4	9	24.761	41.483	
		5	34	-	-	

4.3.36 DAWADAWA NO.2 EM PROFILE AND MODELLED VES CURVES

A total of 260 m long traverse was profiled to delineate the conductive anomaly using the EM method within Dawadawa No. 2. Community.

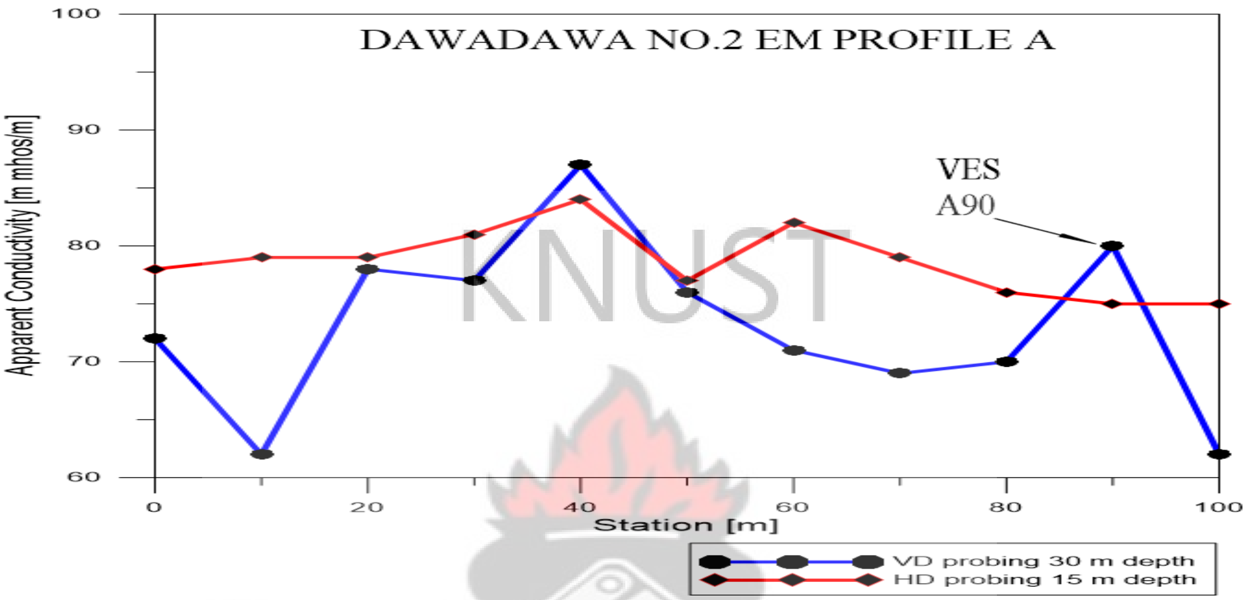

Fig 4.32 EM *Profile* along Traverse A, Dawadawa No. 2 community.

Figure 4.32 shows the EM profile of apparent conductivity along traverse A over a distance of about 100 m in Dawadawa No. 2. Community. The profile depicts a varying apparent conductivity at the subsurface at both shallower (15 m) and deeper (30 m) depths. Most part of the profile shows higher apparent conductivity values for HD mode than the VD mode at the subsurface. But at station points A40 m and A90 m on the traverse, crossovers occurred, where the VD mode shows higher apparent conductivity values than the HD mode. These crossovers of sharp positive peaks (transition), indicate significant anomalies. These stations A40 m and A90 m may be deep fractured zones. Thus, station A90 m was selected for further VES investigation.

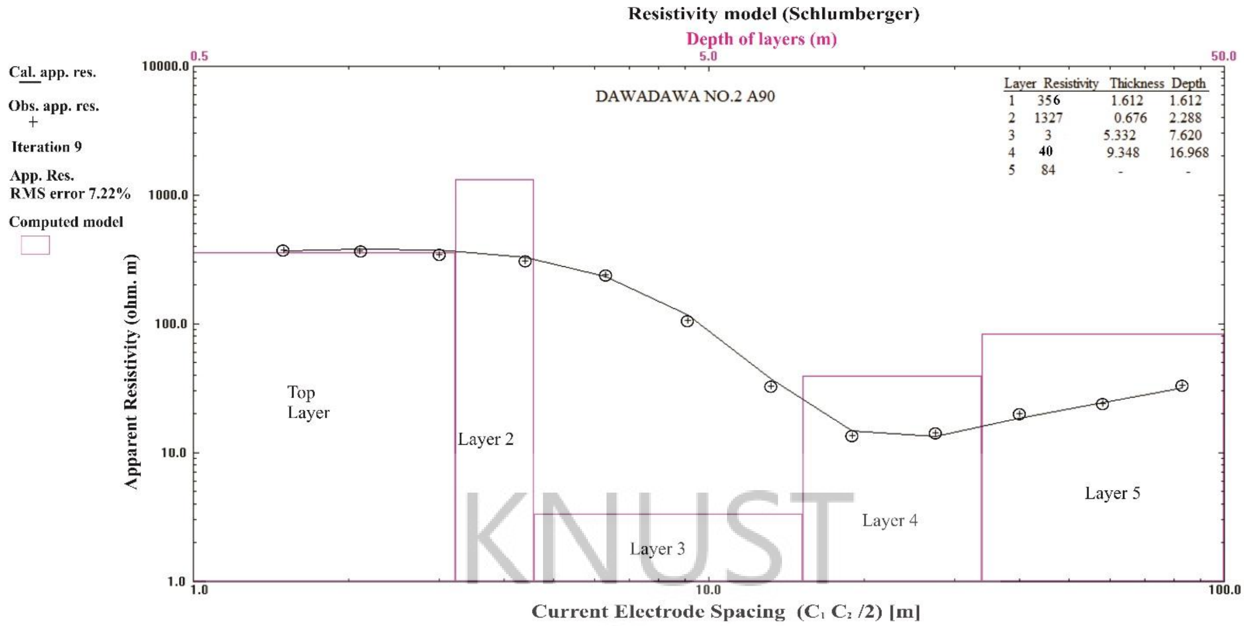

Fig 4.33 VES Model Curve at station A90 m, in Dawadawa No. 2 community.

Figure 4.33 shows a five-layer subsurface structure at VES station A90 m in Dawadawa No. 2 community. The apparent resistivity increases from about 356 Ωm at the top layer to about 1327 Ωm in the second layer, followed by a drastic resistivity drop to about 3 Ωm in the third layer. However, the apparent resistivity of the fourth layer rather increased to about 40 Ωm, and it further increased to about 84 Ωm in the fifth layer. The apparent resistivity, thickness and depth of the various layers show that the overburden is likely to be thin, and the subsurface may be underlain by a weathered and fractured zone occurring at a depth of about 18.0 m. This VES point A90 m is not recommended for drilling.

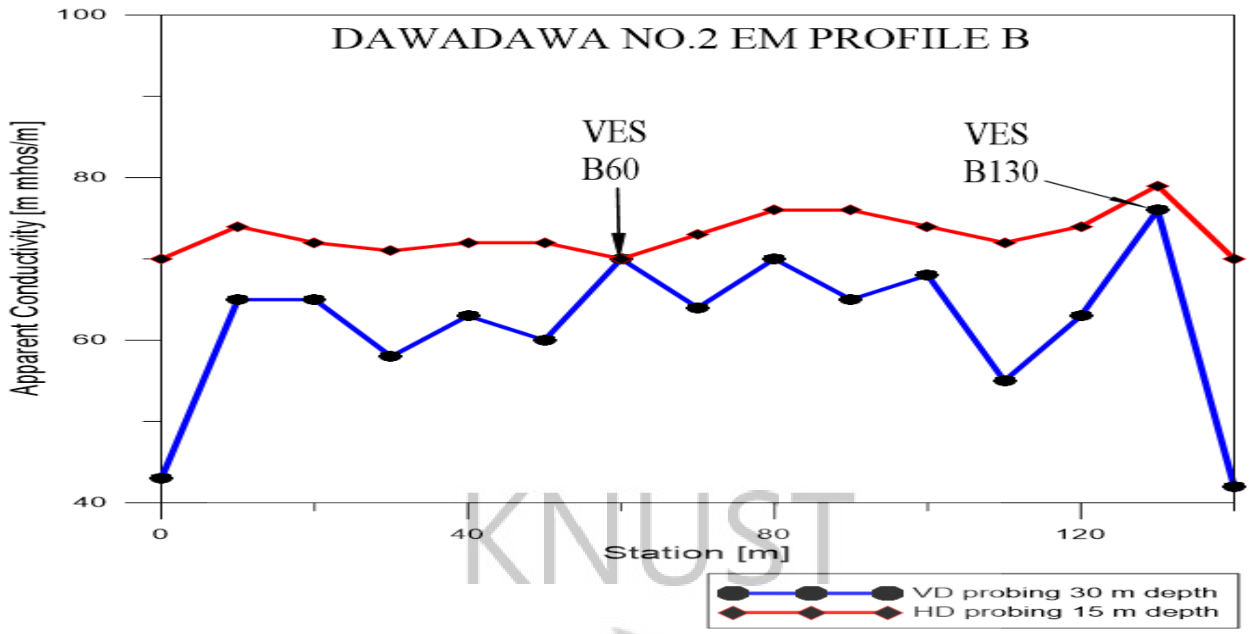

Fig 4.34 EM Profile along Traverse B, Dawadawa No. 2 community.

Figure 4.34 shows the EM profile of apparent conductivity along traverse B over a distance of about 140 m in Dawadawa No. 2 community, primary school. The profile describes varying apparent conductivity at the subsurface at both shallower (15 m) and deeper (30 m) depths. Almost all the entire section of the profile show higher apparent conductivity values for the HD mode than the corresponding VD mode at the subsurface except at station where B60 m where an anomaly occurred. This anomaly could be a fractured and weathered zone. Hence, station B60 m and B130 m which show the highest VD mode reading were selected for further VES investigation.

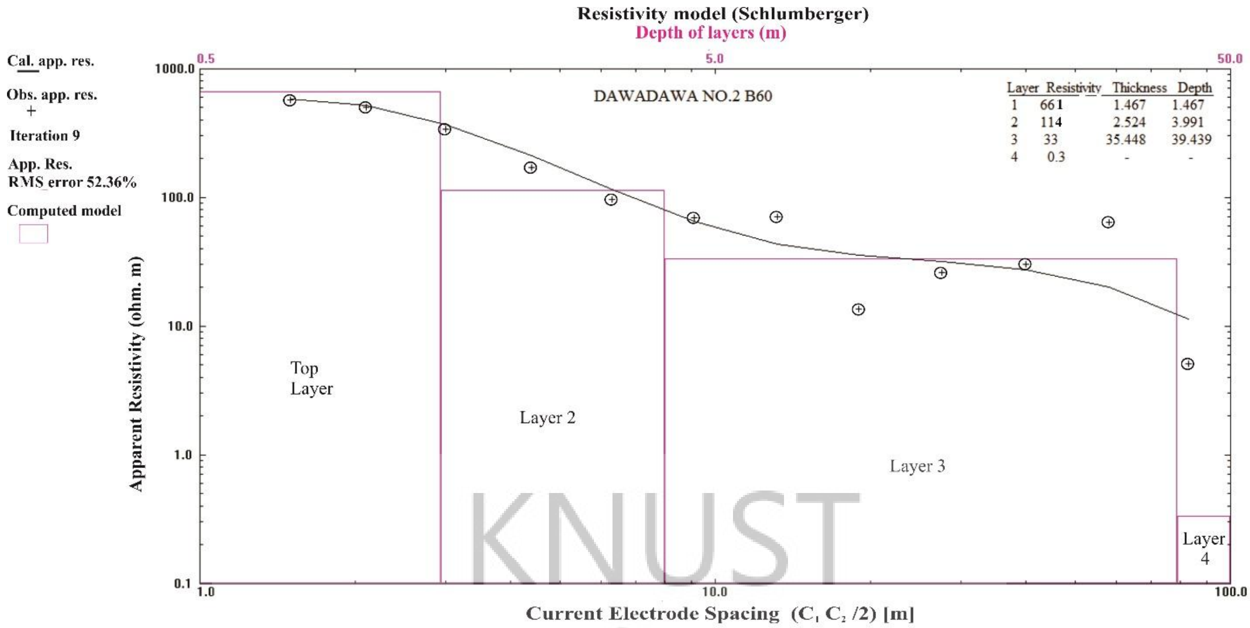

Fig 4.35 VES Model Curve at station B60 m, in Dawadawa No. 2 primary.

At station B60 m in the Dawadawa No. 2 community, the VES modelled curve of the subsurface depicted four layers as shown in Figure 4.35. The top layer apparent resistivity is about 661 Ωm at a depth of about 1.5 m. The apparent resistivity of the second layer decreased to about 114 Ωm. It further decreased to about 33 Ωm in the third layer and reduced drastically to as low as 0.3 Ωm in the fourth layer. The layer parameters of the apparent resistivity, thickness and depth of the various layers showed that the overburden is quite thick. It is possibly fractured and weathered which is a condition for groundwater accumulation and storage. Therefore, VES point B60 m was recommended for drilling up to a depth of about 42 m.

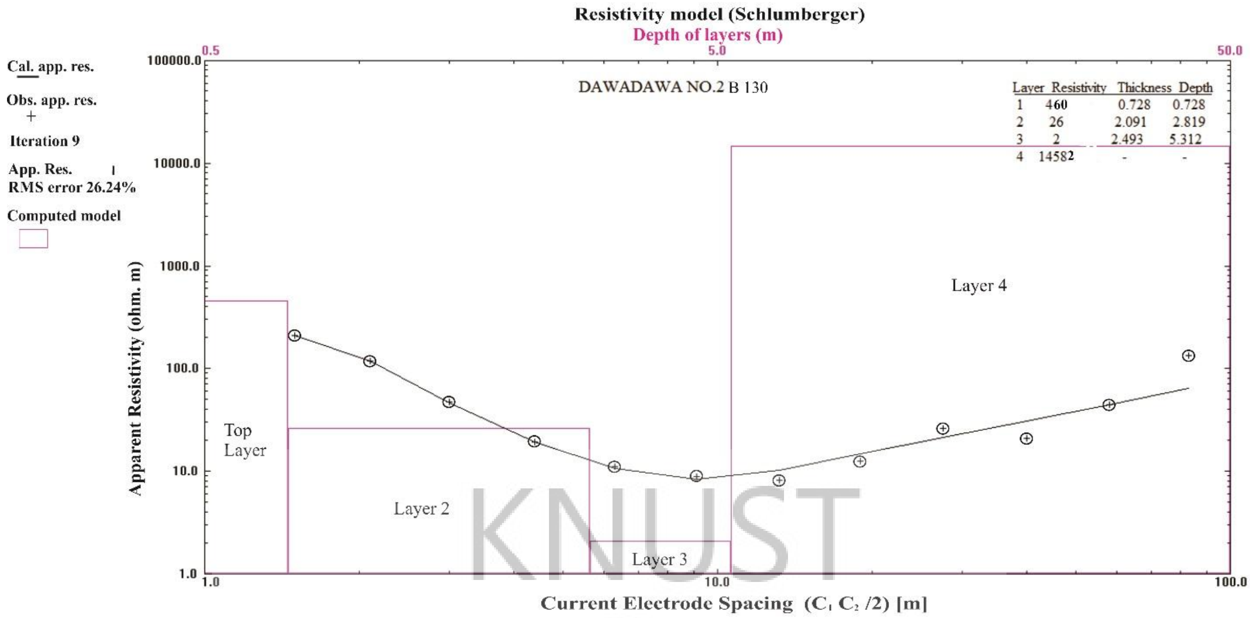

Fig 4.36 VES Model Curve at station B130 m, in the Dawadawa No. 2 primary school.

From the modelled VES curve of station B130 in the Dawadawa No. 2 primary school, the subsurface consisted of four layers as shown in Figure 4.36. The apparent resistivity of 460 Ωm in the top layer decreases to about 26 Ωm in the second layer and further dropped to as low as 2 Ωm in the third layer. It then shot to about 14,582 Ωm in the fourth layer at a depth beyond 7 m. The layer parameters involving the apparent resistivity, thickness and depth, suggest a very thin overburden at shallow depth of about 7 m. This VES point might not contain any fracture to store groundwater. Hence it was not recommended for drilling.

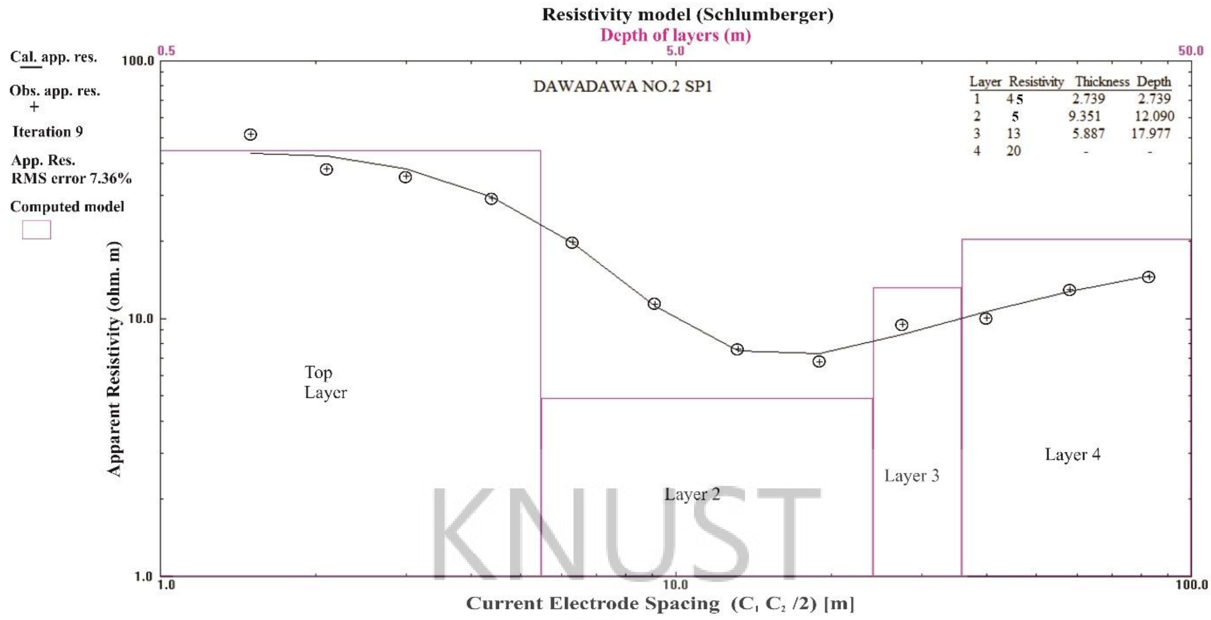

Fig 4.37 VES Model Curve at station SP1, in the Dawadawa No. 2 community.

The modelled VES curve at station SP1 in the Dawadawa No. 2 community revealed a four layer subsurface structure as shown in figure 4.37 above. The apparent resistivity of the top layer decreased from about 45 Ωm to about 5 Ωm in the second layer. But the apparent resistivity of the third layer rather increased to 13 Ωm in the third layer. Continuing in that trend, it further increased to about 20 Ωm in the fourth layer at a depth beyond 18 m. The layer parameters (apparent resistivity, thickness and depth), suggest a thin overburden at shallow depth of about 18 m. This VES point might not contain any fracture with groundwater storage potential for borehole drilling. Hence it is not recommended for drilling.

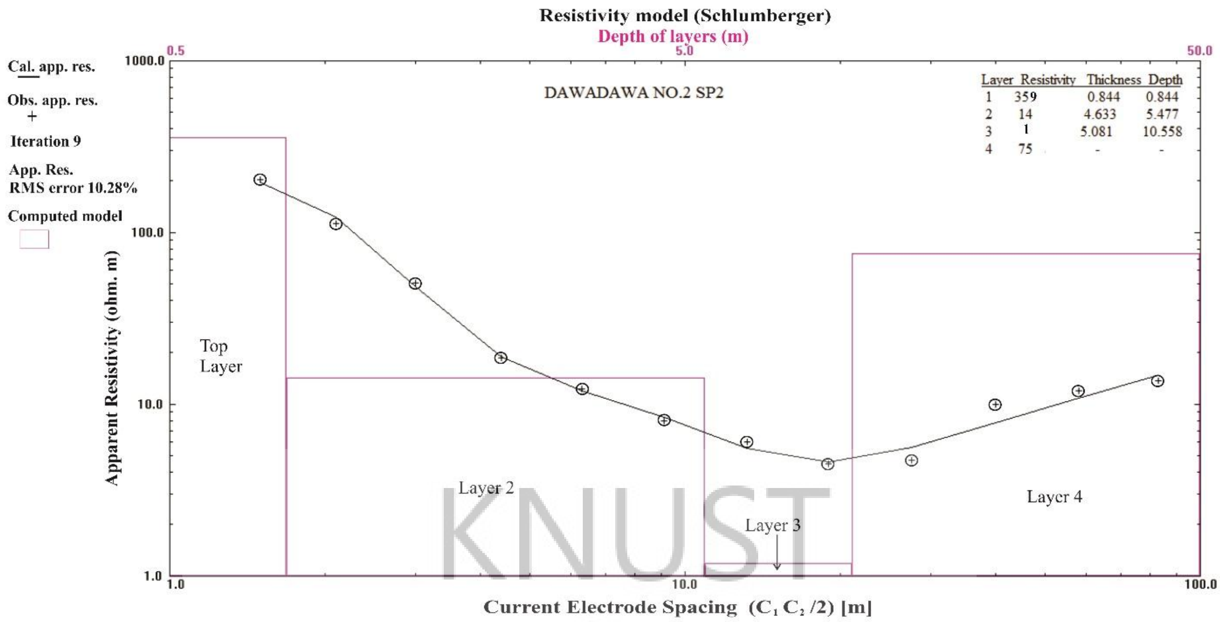

Fig 4.38 VES Model Curve at SP2, in the Dawadawa No. 2 community.

At spot sounding SP2 in the Dawadawa No.2 community, the subsurface consists of four layers as shown in figure 4.38 above. The top layers apparent resistivity is about 356 Ωm at a very shallow depth of about 0.8 m. The apparent resistivity of the second layer decreased from that of the first to about 14 Ωm. It further decreased to about 1 Ωm in the third layer. However, the fourth layers apparent resistivity rather increased to about 75 Ωm at a depth deeper than 12 m. The layer parameters of apparent resistivity, thickness and depth of the various layers showed that the overburden is not thick and the subsurface may be underlain by a fractured zone at a depth of about 12 m. Therefore, VES point SP2, is not recommended for drilling.

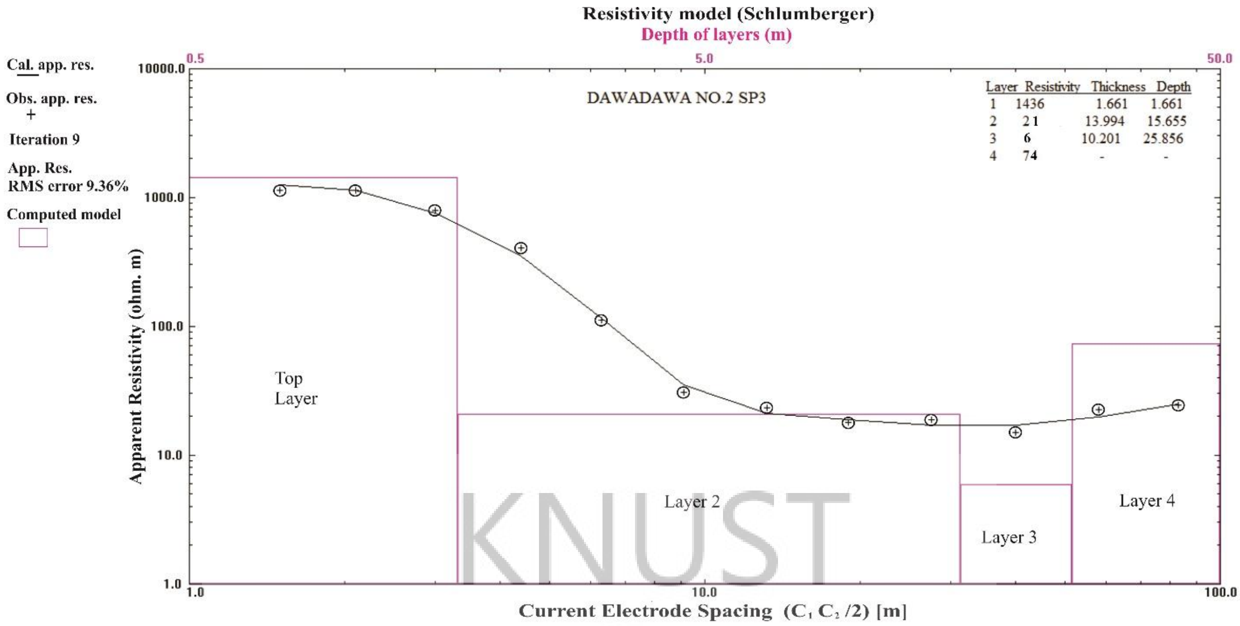

Fig 4.39 VES Model Curve at station SP3, in the Dawadawa No. 2 community.

Figure 4.39 above is the modelled curve of the spot sounding point SP3 in the Dawadawa No.2 community. The subsurface consists of four layers as shown in figure 4.39 above. The top layers apparent resistivity decreased drastically from 1436 Ωm to 21 Ωm in the second layer. The apparent resistivity of the third layer further decreased from that of the second layer to about 6 Ωm. It then increased to about 74 Ωm in the fourth layer. The layer parameters of apparent resistivity, thickness and depth of the various layers indicate that the overburden is quite thick and the subsurface may be underlain by a fractured zone at a depth of about 27.0 m. Therefore, the point SP3, is recommended for drilling to a maximum depth of about 30 m.

Table 4.6 Ranked VES points in Dawadawa No.2 community.

Community	VES Point	Layer	Resistivity (Ωm)	Thickness (m)	Depth (m)	Rank
Dawadawa No.2	A90	1	356	1.612	1.612	**3rd**
		2	1327	0.676	2.288	
		3	3	5.332	7.620	
		4	40	9.348	16.968	
		5	84	-	-	
	B60	1	661	1.467	1.467	**2nd**
		2	114	2.524	3.991	
		3	33	35.448	39.439	
		4	0.3	-	-	
	B130	1	460	0.728	0.728	**6th**
		2	26	2.091	2.819	
		3	2	2.493	5.312	
		4	14582	-	-	
	SP1	1	45	2.739	2.739	**4th**
		2	5	9.351	12.090	
		3	13	5.887	17.977	
		4	20	-	-	
	SP2	1	359	0.844	0.844	**5th**
		2	14	4.633	5.477	
		3	1	5.081	10.558	
		4	75	-	-	
	SP3	1	1436	1.661	1.661	**1st**
		2	21	13.994	15.655	
		3	6	10.201	25.856	
		4	74	-	-	

4.3.3.7 GU ALHAJI AKURA EM PROFILE AND MODELLED VES CURVES

EM profiling was carried out along 180 m traverse to select anomalous points for VES.

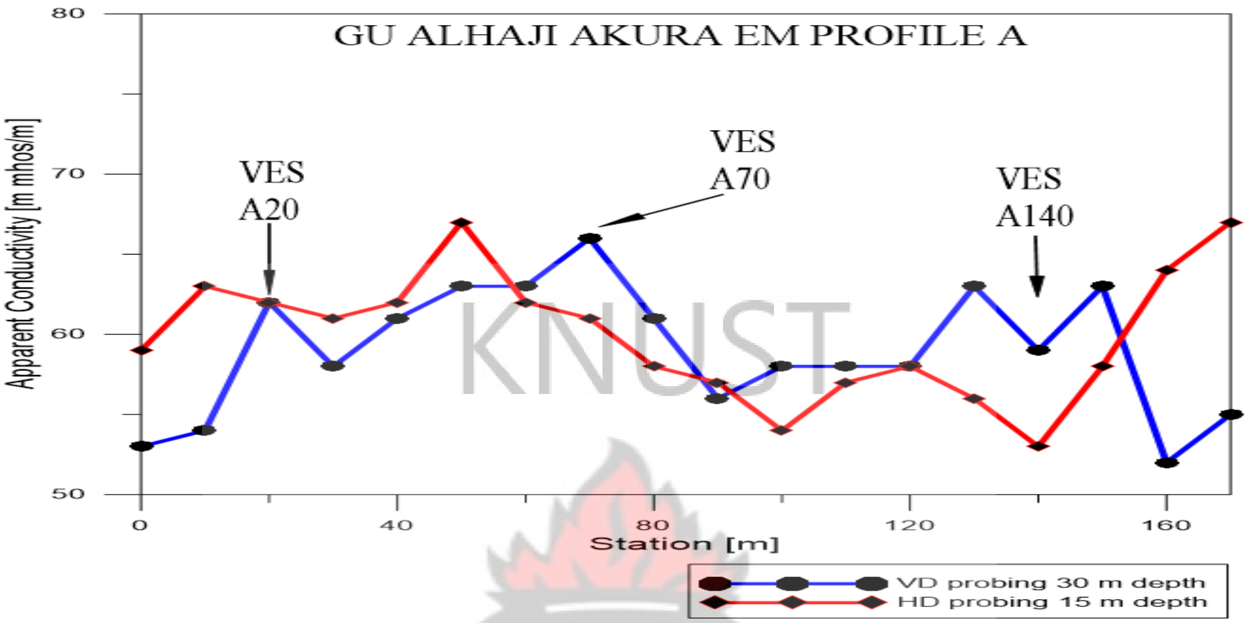

Fig 4.40 EM Profile along Traverse A, Gu Alhaji Akura community.

The EM profile Figure 4.40 depicts a varying apparent conductivity at the subsurface for both shallow (15 m) and deeper (30 m) dipole modes. The profile shows oscillating apparent conductivity values for both the VD mode and the HD mode at the subsurface throughout the entire profile length. This culminated in the formation of crossovers and neck. The crossovers occurred at station points A70 m, A100 m, A140 and the necks at A20 m and A120 m on the profile line as shown in the diagram above (Fig 4.40). These necks and crossovers indicates significant anomalies at the subsurface and may be fractured and weathered zones which could possible contain groundwater. Therefore, station points A20 m, A70 m and A140 m were choosing for further VES investigations.

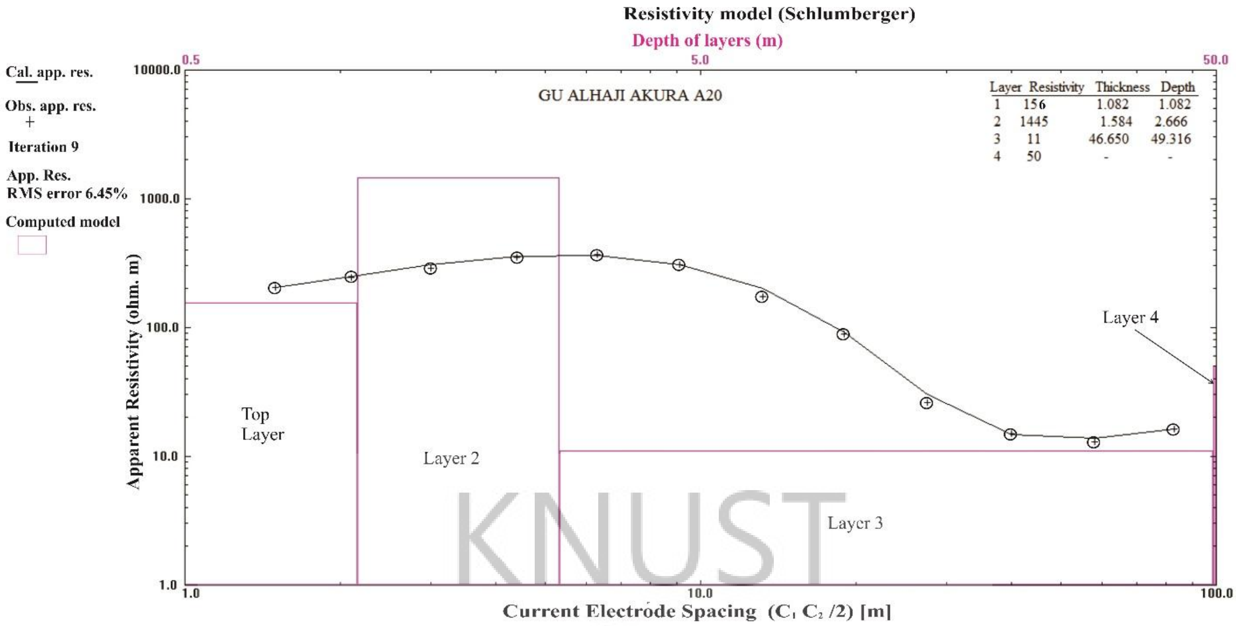

Fig 4.41 VES Model Curve at station A20 m, in the Gu Alhaji Akura community.

Quantitatively, the apparent resistivity model curve for station A20 m in the Gu Alhaji Akura community, Figure 4.41, shows a four layer subsurface structure. There is an increase in apparent resistivity from about 156 Ωm in the first layer (topsoil) to about 1446 Ωm in the second layer. However, there was a drastic drop in apparent resistivity of the second layer to about 11 Ωm in the third layer and then it increased to about 50 Ωm in the fourth layer. The layer parameters of apparent resistivity involving the thickness and depth of the various layers show that the overburden is thick and the subsurface may be underlain by deep fractured zone at a depth of about 50.0 m. Therefore, the VES point A20 m was recommended for drilling up to a depth of about 53.0 m.

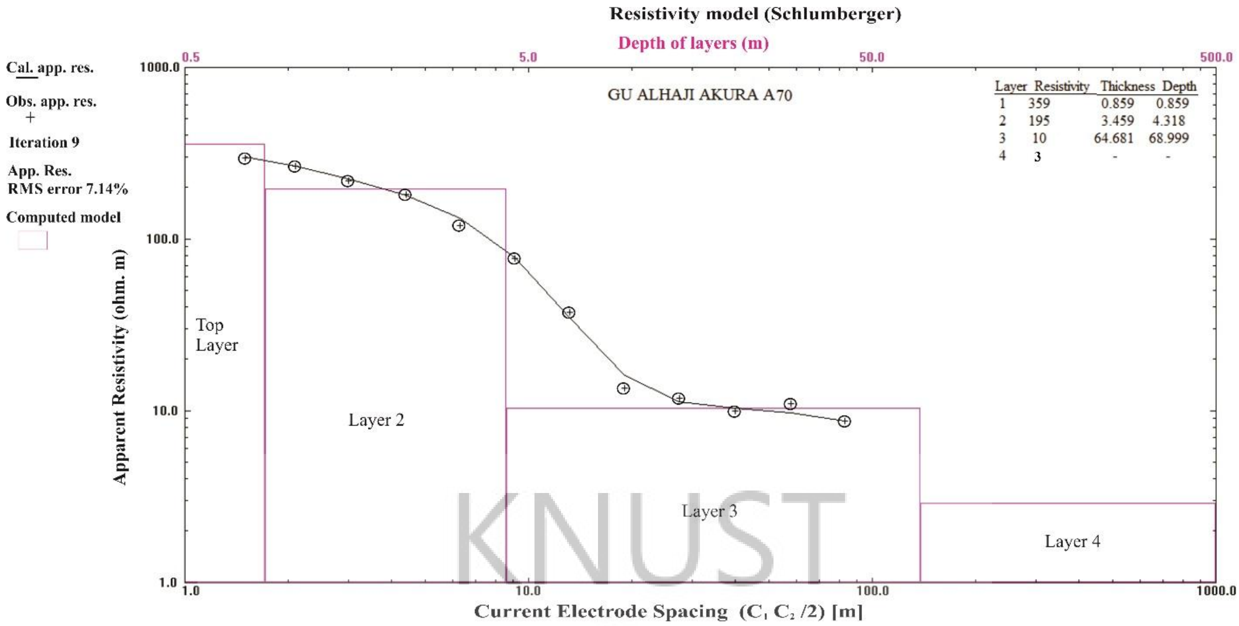

Fig 4.42 VES Model Curve at station A70 m, in the Gu Alhaji Akura community.

Figure 4.42 is the VES modelled curve for station A70 m in the Gu Alhaji Akura community. The subsurface consists of four subsurface layers as shown in Figure 4.42. The top layer's apparent resistivity of 359 Ωm decreased to about 195 Ωm in the second layer. The apparent resistivity of the third layer further decreased from the second layer to about 10 Ωm and decreased to about 3.0 Ωm in the fourth layer. The layer parameters of apparent resistivity, thickness and depth of the various layers indicates that the overburden is quite thick and the subsurface may be underlain by a fractured rock formation to a depth of about 69.0 m. Therefore, VES point A70 m in the Gu Alhaji Akura community, is recommended for drilling up to a maximum depth of about 70 m.

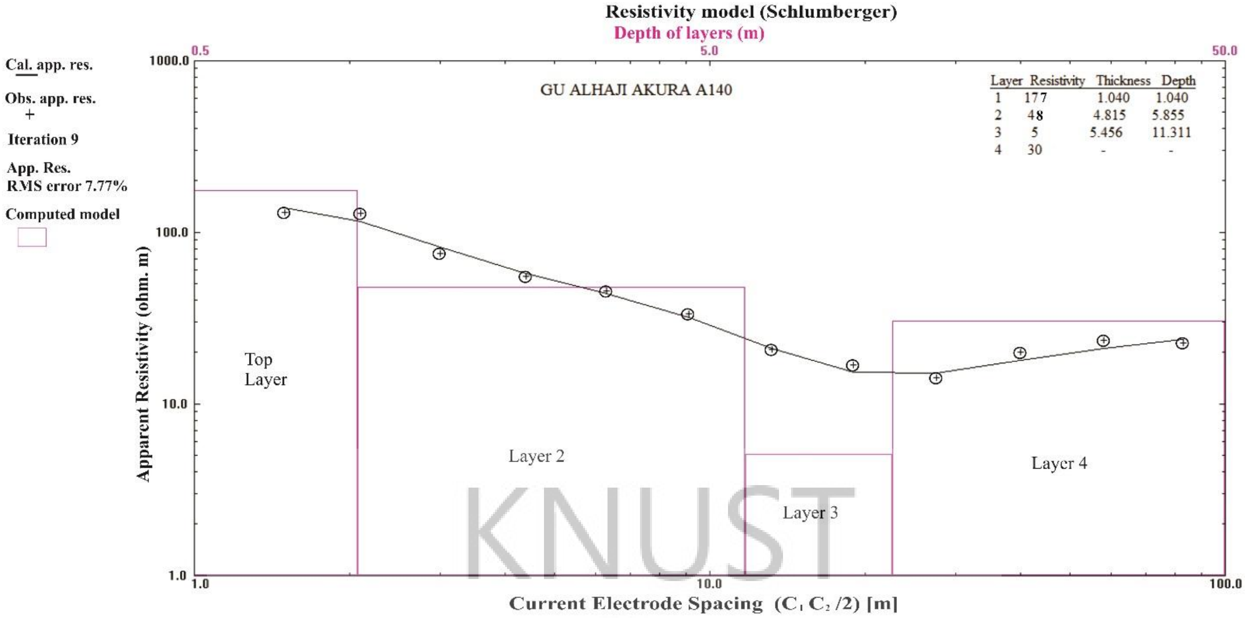

Fig 4.43 VES Model Curve at station A140 m, in the Gu Alhaji Akura community.

Figure 4.43 above shows the VES modelled curve at station A140 m in the Gu Alhaji Akura community. The subsurface depicts four layers as shown in Figure 4.43 above. The apparent resistivity of the top layer (top soil) decreased from 176 Ωm to about 48 Ωm in the second layer. The apparent resistivity of the third layer further decreased from that of the second layer to about 5 Ωm. However, there was an increase in apparent resistivity to about 30 Ωm in the fourth layer with respect to that of the third layer. The layer parameters of the apparent resistivity, thickness and depth of the various layers suggest that the overburden is shallow, and the subsurface is underlain by a fractured zone at a shallower depth of about 12.0 m. Consequently, the point A140 in the Gu Alhaji Akura community, is not recommended for drilling.

Table 4.7 Ranked VES points in Gu Alhaji Akura community.

Community	VES Point	Layer	Resistivity (Ωm)	Thickness (m)	Depth (m)	Rank
Gu Alhaji Akura	A20	1 2 3 4	156 1445 11 50	1.082 1.584 46.650 -	1.082 2.666 49.316 -	1st
	A70	1 2 3 4	359 195 10 3	0.859 3.459 64.681 -	0.859 4.318 68.999 -	2nd
	A140	1 2 3 4	177 48 5 30	1.040 4.815 5.456 -	1.040 5.855 11.311 -	3rd

4.3.3.8 GULUMPE KUKOMBA EM PROFILE AND MODELLED VES CURVES

Only one traverse-line, of 160 m long was profiled to obtain the apparent conductivity of the terrain using the EM method.

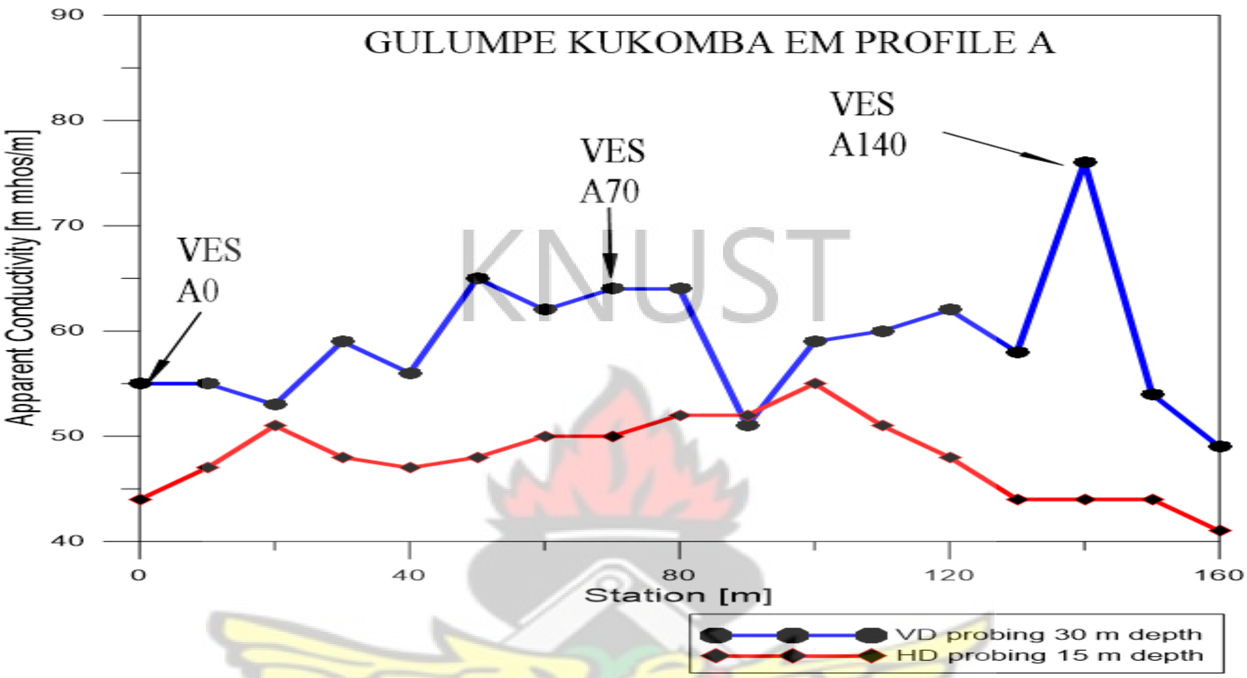

Fig 4.44 EM Profile along Traverse A, Gulumpe Kukomba community.

Figure 4.44 shows the variation of EM dipole response curves with depth along traverse A, a distance of about 160 m in the Gulumpe Kukomba community. The profile describes varying apparent conductivity at the subsurface for both the shallower (15 m) and deeper (30 m) depths. Almost all points on the profile show higher apparent conductivity values for VD mode than the HD mode of the subsurface except at station point A90 m, where a neck occurred. This neck could be a fractured and weathered zone. But the neck point is the lowest apparent conductivity point for the VD mode, which is expected to be at shallow depth (15 m). Hence, three peak points on the VD mode deeper depth (30 m) probing curve were selected for further VES investigation. These are A0 m, A70 m and A140 m points.

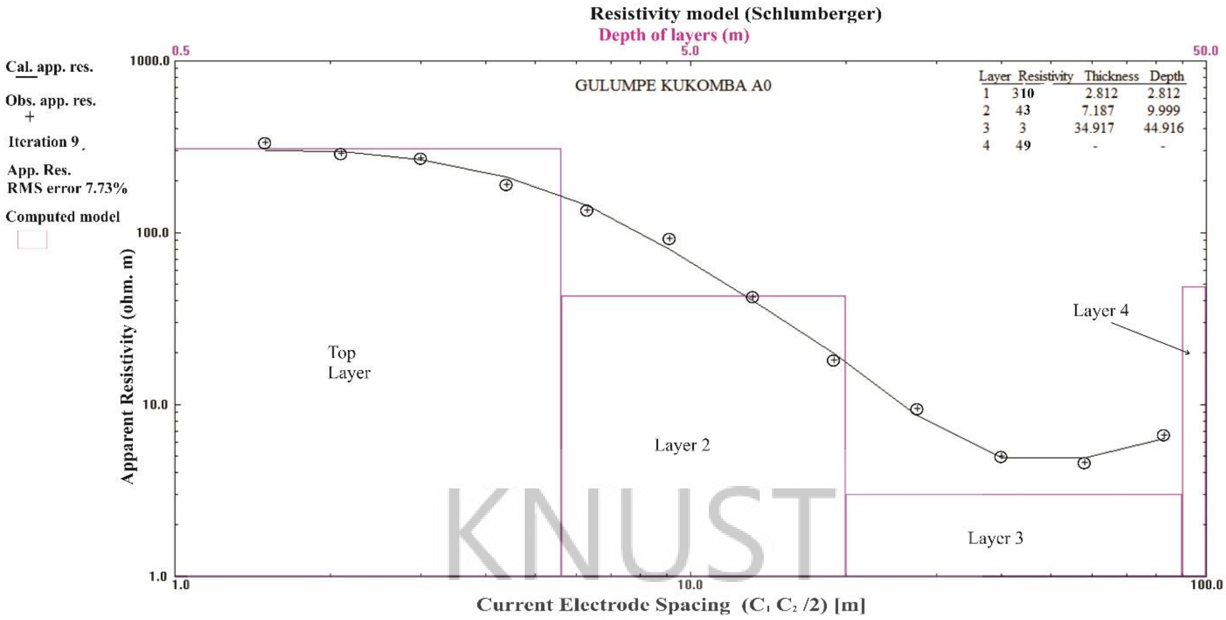

Fig 4.45 VES Model Curve at station A0 m, in the Gulumpe Kukomba community.

Figure 4.45 shows the apparent resistivity VES model curve at the station, A0 m on the traverse. The model depicts a moderately thin overburden of approximately 3.0 m. Quantitatively, it shows a four layered model with decreasing apparent resistivity from about 310 Ωm of the first layer (topsoil) to about 3 Ωm in the third layer at a depth of about 45.0 m. However, the apparent resistivity of the fourth layer rather increased to about 49 Ωm. The layer apparent resistivity values, thickness and depth of the various layers show that there may be a deep fractured zone ranging from the third to the fourth layer at depth beyond 45 m. Thus the VES point A0 m was chosen and recommended for drilling up to a depth of about 50 m.

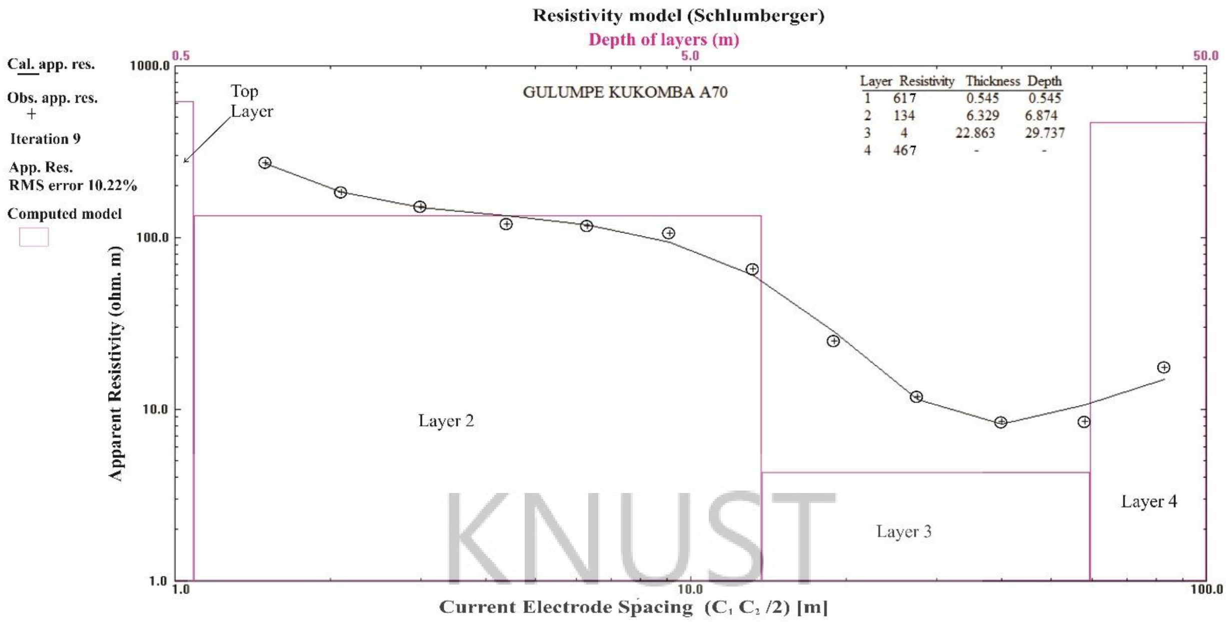

Fig 4.46 VES Model Curve at station A70 m, in the Gulumpe Kukomba community.

Figure 4.46 shows the VES modelled curve for station A70 m in the Gulumpe Kukomba community. The subsurface shows four layers as shown in Figure 4.46. The resistivity of the top layer (top soil) decreased from 617 Ωm to 134 Ωm in the second layer. The apparent resistivity of the third layer further decreased to about 4 Ωm. However, there was an increase in apparent resistivity to about 467 Ωm in the fourth layer compared to the third layer. The layer parameters comprising the apparent resistivity, thickness and depth of the various layers suggest that the overburden is very thin of about 0.5 m. The subsurface may be underlain by a fractured zone at a depth of about 30.0 m. Therefore, VES point A70 m in the Gulumpe Kukomba community, is recommended for drilling up to a depth of about 33.0 m.

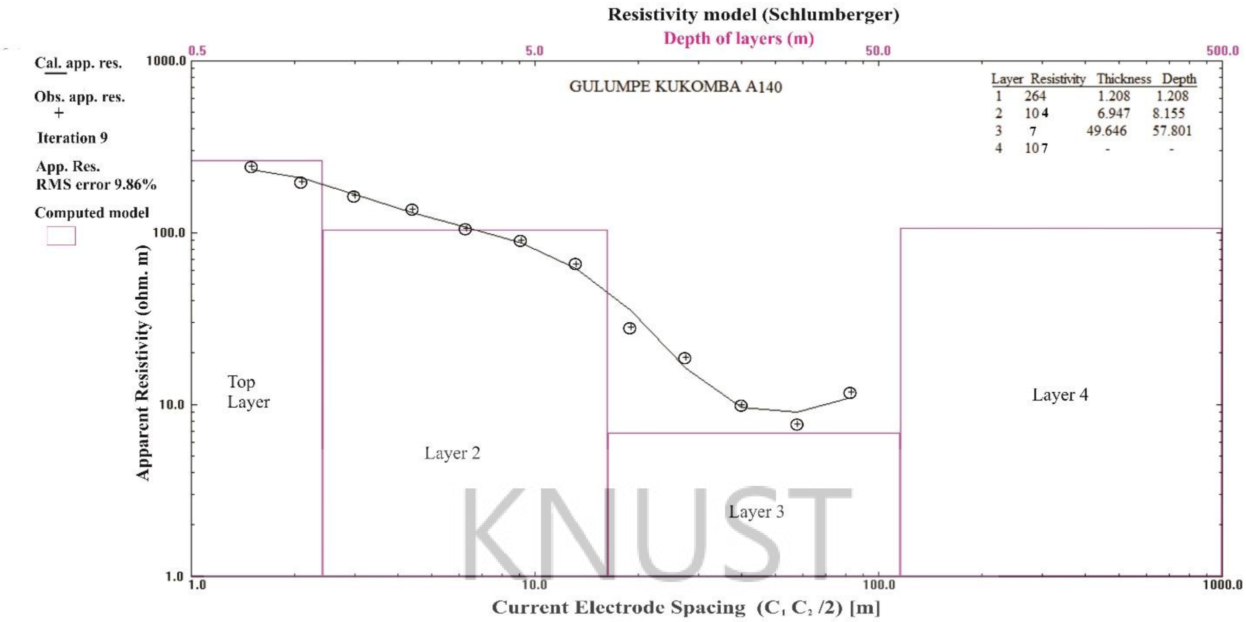

Fig 4.47 VES Model Curve at station A140 m, in the Gulumpe Kukomba community.

Figure 4.47 shows the apparent resistivity VES model curve at the station, A140 m on the EM traverse A, in Gulumpe Kukomba community. The model depicts a moderately thin overburden of approximately 1.2 m. It shows a four -layered model with decreasing apparent resistivity from about 264 Ωm of the first layer (topsoil) to about 7 Ωm in the third layer at a depth of about 57.0 m. However, the apparent resistivity of the fourth layer rather increased to about 106 Ωm. The parameters of apparent resistivity, thickness and depth of the various layers show that there may be a deep fracture zone between the third and the fourth layer at depth beyond 60.0 m. Thus the VES point A140 m was chosen and recommended for drilling up to an average depth of 60 m.

Table 4.8 Ranked VES points in Gulumpe Kukomba community.

Community	VES Point	Layer	Resistivity (Ωm)	Thickness (m)	Depth (m)	Rank
Gulumpe Kukomba	A0	1	310	2.812	2.812	1st
		2	43	7.187	9.999	
		3	3	34.917	44.916	
		4	49	-	-	
	A70	1	617	0.545	0.545	3rd
		2	134	6.329	6.874	
		3	4	22.863	29.737	
		4	467	-	-	
	A140	1	264	1.208	1.208	2nd
		2	104	6.947	8.155	
		3	7	49.646	57.801	
		4	107	-	-	

4.1.1.2 4.3.3.9 KAWAMPE EM PROFILES AND MODELLED VES CURVES

Two (2) EM profiles of length 340 m were investigated to determine subsurface anomalies in Kawampe community.

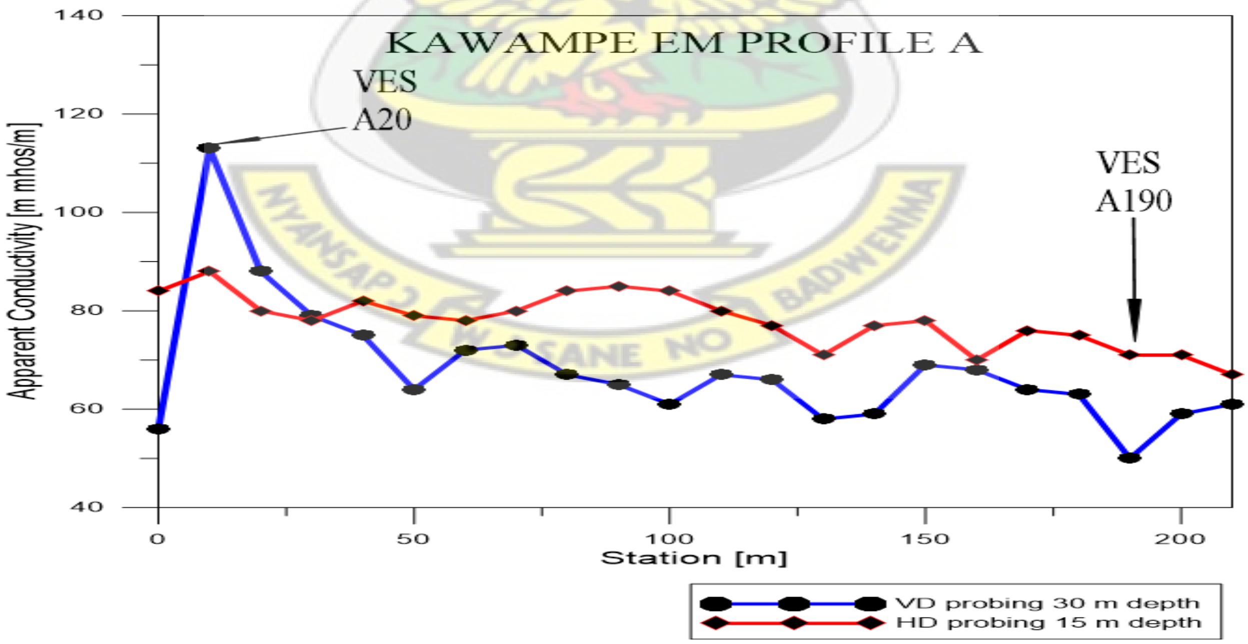

Fig 4.48 EM Profile along Traverse A, Kawampe community (Dagomba Mans' House).

Figure 4.48 above shows the variation of EM profile with depth along traverse A, a distance of about 220 m at the community, Kawampe. The profile describes varying apparent conductivity at the subsurface at both shallower (15 m) and deeper (30 m) depths. Almost all points on the profile shows higher apparent conductivity values for HD mode than the VD mode at the subsurface except at station point A20 m where a crossover occurred. This crossover is an indication of an anomally at the subsuface which could be a fractured and weathered zone. Additionally, spot A190 m which corresponds to the lowest apparent conductivity VD mode value, was intentionally chosen to ascertain the nature an anomaly using VES methodology.

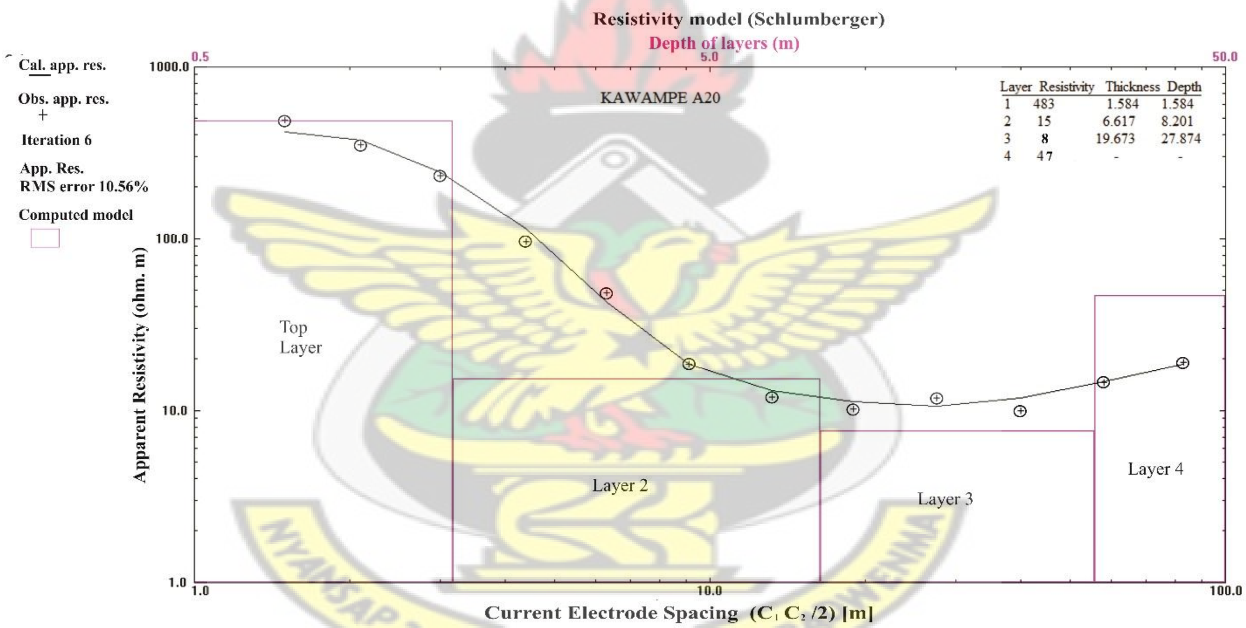

Figure 4.49 VES Model Curve at station A20 m, in the Kawampe community.

Quantitatively, the apparent resistivity VES model curve for station A20 m in the Kawampe community as shown in figure 4.49 above reveals a four layer subsurface structure. There is a drastic decrease in apparent resistivity from about 483 Ωm in the first layer (topsoil) to about 15.0 Ωm at the second; then another decrease to about 8 Ωm at the third layer at a depth of about 28.0 m. However, the apparent resistivity of the fourth layer rather increased to about 47 Ωm. The layer parameters of apparent resistivity, thickness and depth of the third and fourth layers show that the subsurface may be underlain by deep fractured zone at a depth higher than 28 m. Therefore, VES point A20 m in the Kawampe community was recommended for drilling up to a depth of about 32 m.

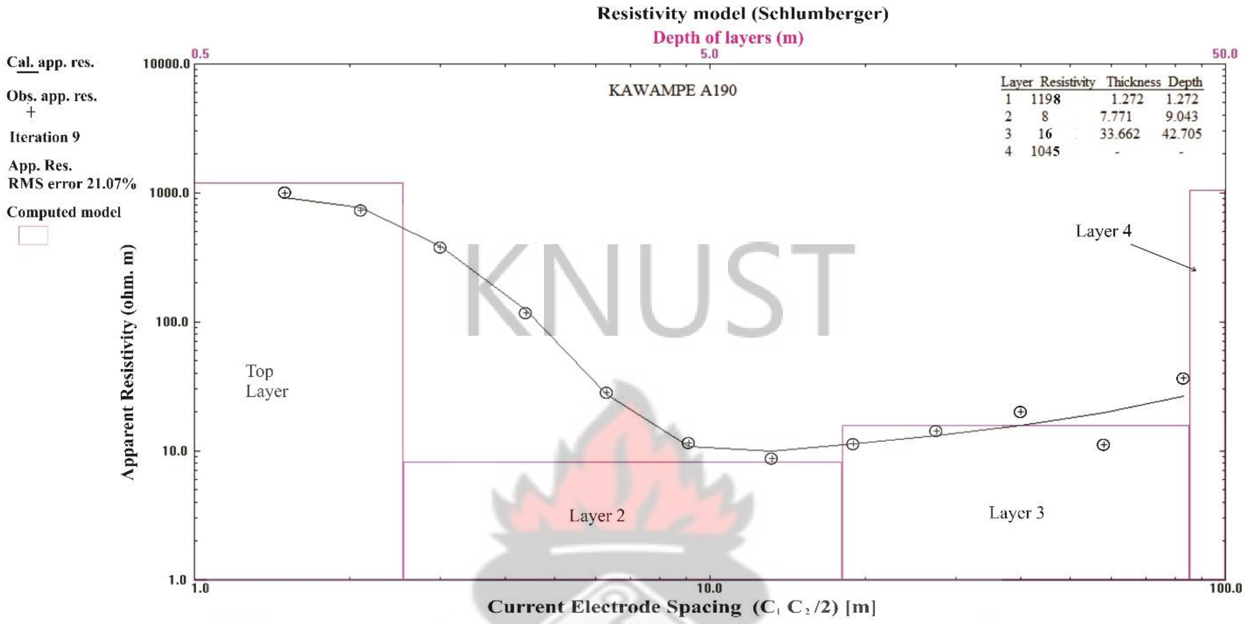

Fig 4.50 VES Model Curve at station A190 m, in the Kawampe community.

Figure 4.50 above shows the VES modelled curve at station A190 m in Kawampe community. The subsurface shows four layers as shown in Figure 4.50. The top layer's (top soil) apparent resistivity decreased from 1198 Ωm to about 8 Ωm in the second layer. The apparent resistivity of the third layer rather increased to 16 Ωm at a depth of about 43.0 m. However, there was an increase in apparent resistivity to about 1045 Ωm in the fourth layer. The layer parameters of apparent resistivity, thickness and depth of the various layers suggest that the overburden is paltry 1.2 m thick. The layer parameters also suggest a fractured zone at a depth of about 43.0 m. Therefore, VES point A190 m in the Kawampe community, was recommended for drilling up to a depth of about 45.0 m.

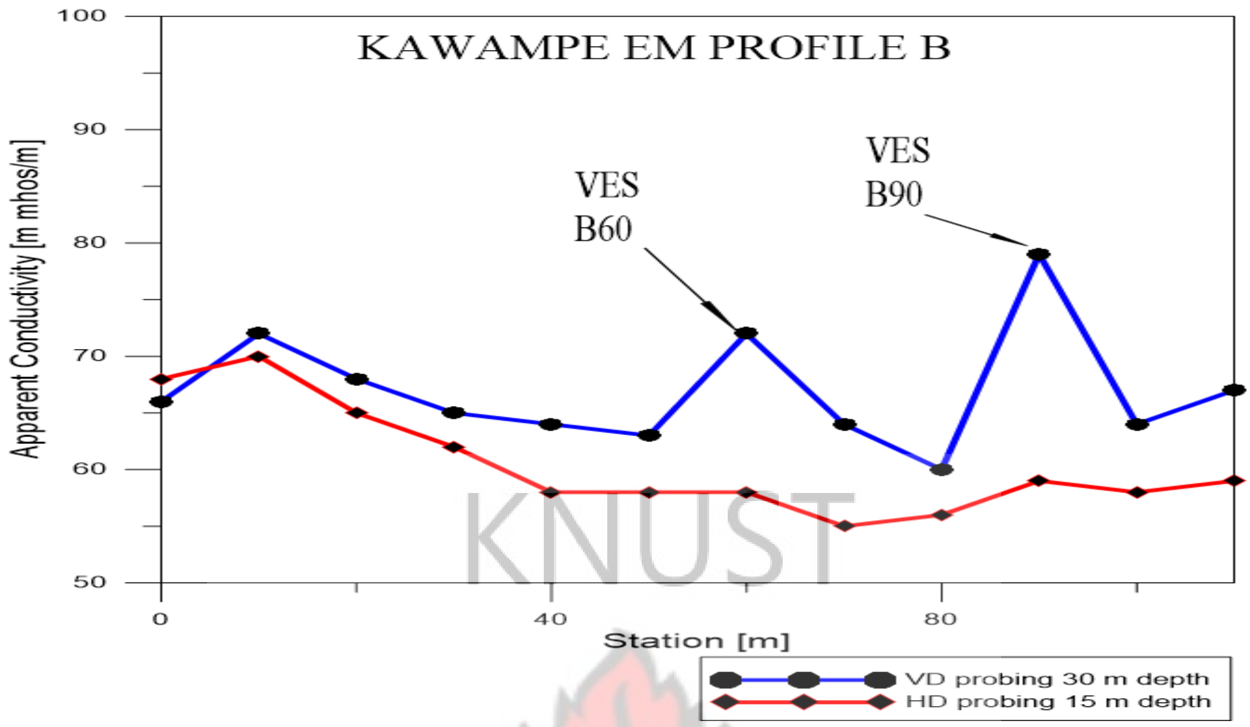

Fig 4.51 EM Profile along Traverse B, Kawampe community.

Figure 4.51 shows the EM profile of the subsurface conductivity along traverse B over a distance of about 120 m in Kawampe community. The profile depicts a varying apparent conductivity of the subsurface at both the shallower (15 m) and deeper (30 m) depths. Almost all parts of the profile shows higher apparent conductivity values for VD mode than the HD mode at the subsurface. However, for the station interval B0 m to B5 m the profile shows higher apparent conductivity values for HD mode than the VD mode. At B60 m and B90 m points on the traverse, the VD mode showed sharp peaks of higher apparent conductivity values. These sharp positive peaks may indicate a significant anomaly at the subsurface, which may be fractured zones. Thus, the two points were selected for further VES investigation.

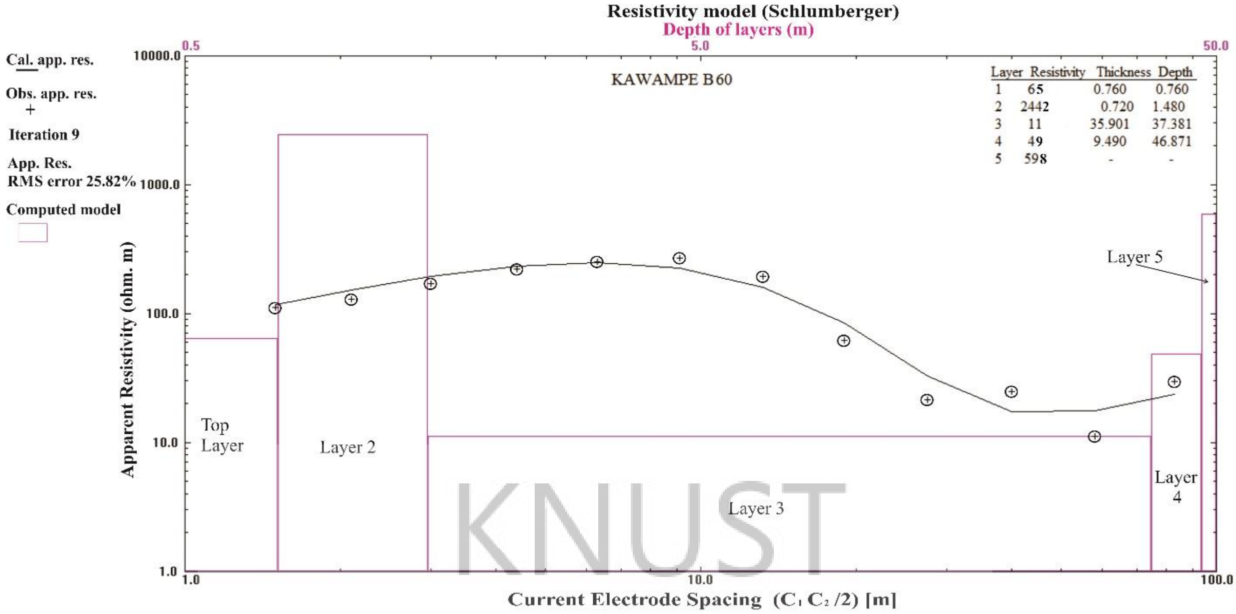

Fig 4.52 VES Model Curve at station B60 m, in the Kawampe community.

Figure 4.52 shows a five-layer subsurface structure at VES station B60 m in the Kawampe community. The apparent resistivity increased from about 65 Ωm in the top layer to about 2442 Ωm in the second layer. This was followed by a drastic resistivity drop to about 11 Ωm in the third layer. However, the apparent resistivity of the fourth layer rather increased to about 49 Ωm at a depth of about 47.0 m, and it further increased to about 598 Ωm in the fifth layer. The parameters (apparent resistivity, thickness and depth of the third and fourth layers) shows that there could likely be a fractured and weathered zone between 37 m and 47 m depth. Therefore, this VES point B60 m in the Kawampe community was recommended for drilling up to a depth of about 50 m.

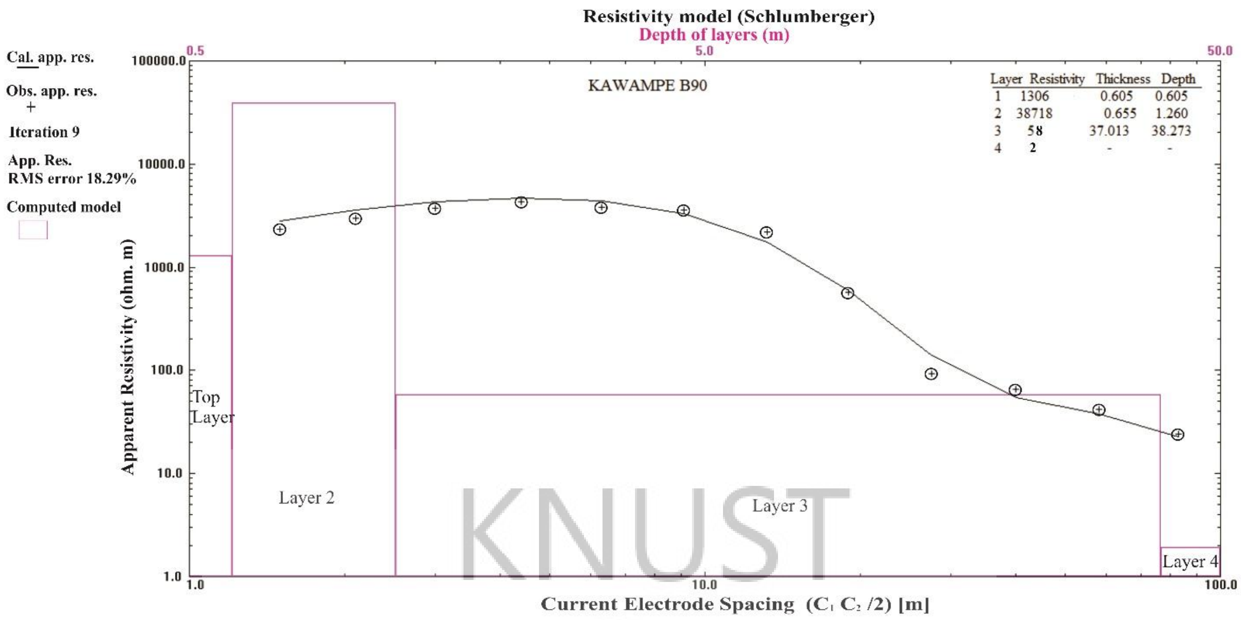

Fig 4.53 VES Model Curve at station B90 m, in the Kawampe community.

The apparent resistivity VES model curve for station B90 m in the Kawampe community, as shown in Figure 4.53 above reveals a four layer subsurface structure. There resistivity of the first layer is about 1306 Ωm. This increased to 38718 Ωm in the second layer and decreased sharply to about 58 Ωm at the third layer at a depth of about 38.0 m. The apparent resistivity of the fourth layer also decreased further down to about 2 Ωm. The layer parameters of apparent resistivity, thickness and depth of the third layer suggest that the subsurface may be underlain by deep fractured zone at a depth ranging from 38 m and below. Therefore, VES point B90 m in the Kawampe community is recommended for drilling up to a depth of about 40 m.

Table 4.9 Ranked VES points for drilling in Kawampe community.

Community	VES Point	Layer	Resistivity (Ωm)	Thickness (m)	Depth (m)	Rank
Kawampe	A20	1	483	1.584	1.584	**4th**
		2	15	6.617	8.201	
		3	8	19.673	27.874	
		4	47	-	-	
	A190	1	1198	1.272	1.272	**3rd**
		2	8	7.771	9.043	
		3	16	33.662	42.705	
		4	1045	-	-	
	B60	1	65	0.760	0.760	**2nd**
		2	2442	0.720	1.480	
		3	11	35.901	37.381	
		4	49	9.490	46.871	
		5	598	-	-	
	B90	1	1306	0.605	0.605	**1st**
		2	38718	0.655	1.260	
		3	58	37.013	38.273	
		4	2	-	-	

4.3.3.10 KINTAMPO MUNICIPAL HOSPITAL MODELLED VES CURVES

The Hospital set up coupled with locations of the septic tanks and overhead electrical cables restricted the team from conducting EM profiling. Consequently, three (3) Vertical Electrical soundings (VES) at suitable locations within the compound were carried out.

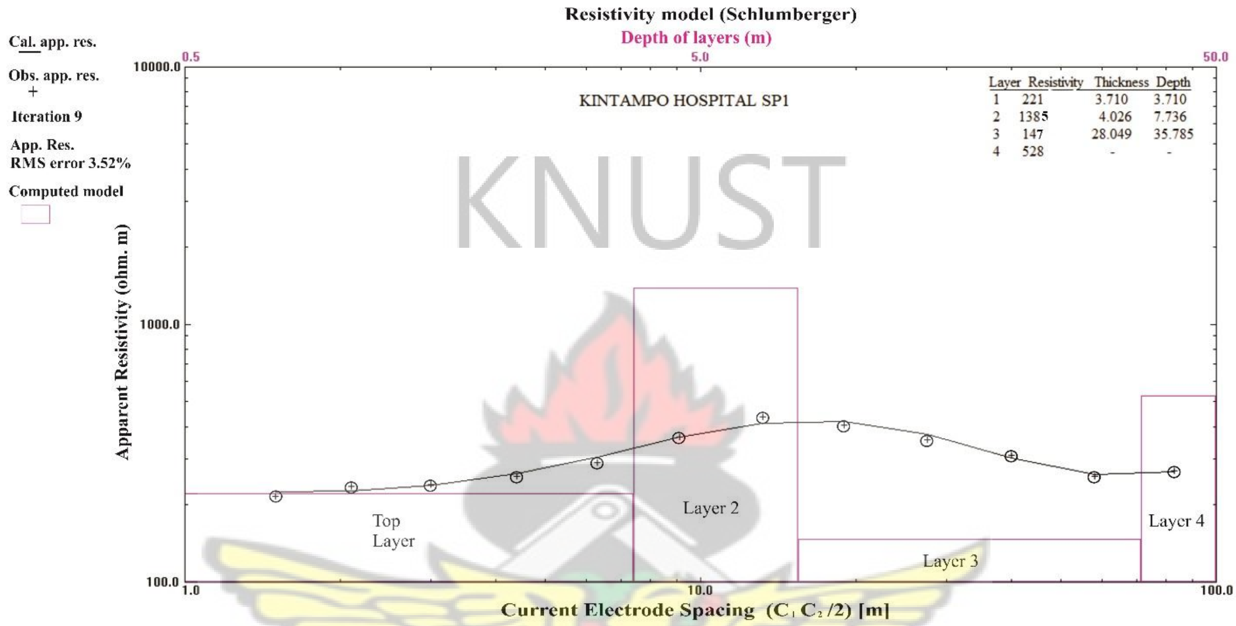

Fig 4.54 VES Curve at sounding point SP1, in the Kintampo Hospital.

Figure 4.54 is the VES modelled curve at the sounding station SP1 at Kintampo Hospital. The subsurface revealed four layers as shown in figure 4.54. The top layer's (top soil) apparent resistivity of 221 Ωm increased abruptly to about 1385 Ωm in the second layer. The apparent resistivity of the third layer rather decreased from that of the former to about 147 Ωm at a depth of about 36.0 m. However, there was another increase in apparent resistivity to about 528 Ωm in the fourth layer. The layer parameters of apparent resistivity, thickness and depth of the third layer suggest that there could be a fractured zone at a depth of about 36.0 m. Therefore, VES sounding point SP1 was recommended for drilling up to a depth of about 38.0 m in the Kintampo Hospital.

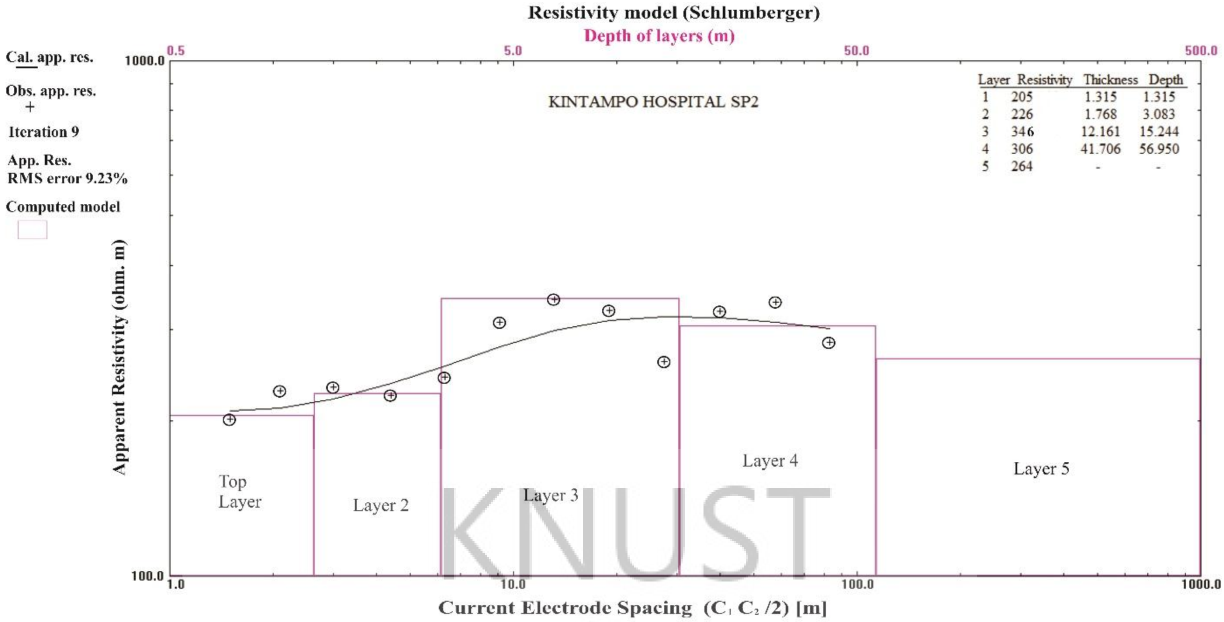

Fig 4.55 VES Model Curve at SP2, in Kintampo Hospital.

At spot sounding point SP2 at Kintampo Hospital, the subsurface consisted of five layers as shown in figure 4.55. The top layers apparent resistivity is about 205 Ωm at shallow depth of about 1.3 m. The apparent resistivity of the second layer increased slightly to about 226 Ωm. It further increased to about 346 Ωm in the third layer. However, the fourth layers apparent resistivity rather decreased to about 306 Ωm at a depth of about 57.0 m. Furthermore, the apparent resistivity of the fifth layer decreased to about 264 Ωm. The layer parameters of the apparent resistivity, thickness and depth of the various layers showed that the subsurface might not be fractured and weathered. Hence, VES SP2 was selected for drilling.

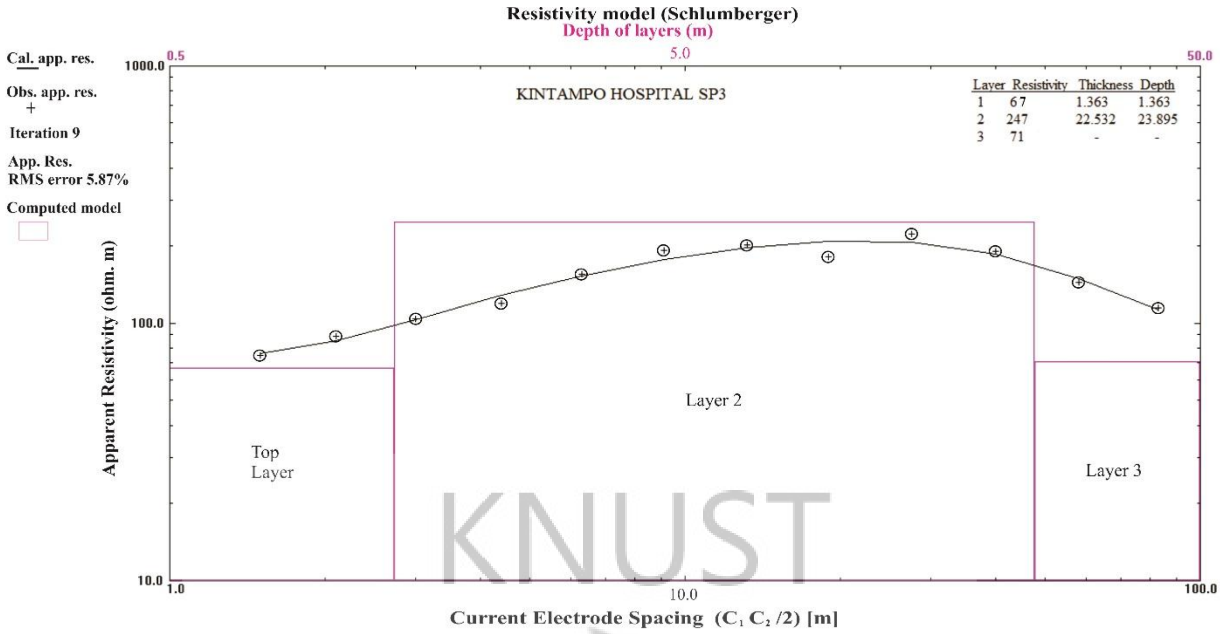

Fig 4.56 VES Curve at SP3, Kintampo Hospital.

Figure 4.56 is a VES modelled curve at SP3 in the Kintampo Hospital. It indicates a three layer subsurface with varying apparent resistivities at varying depths. The top soil has a resistivity of about 67 Ωm, which increased to about 247 Ωm in the second layer at a depth of about 24.0 m. The apparent resistivity however decreased to about 71 Ωm in the third layer at a depth deeper than 24.0 m. The layer parameters: (apparent resistivity, thickness and depth) indicates that the subsurface could be fractured and weathered at a depth deeper than 25 m. Therefore, this sounding point (SP3) was thus recommended for drilling up to a depth of about 30 m.

Table 4.10 Ranked VES points for drilling in Kintampo Municipal Hospital.

Community	VES Point	Layer	Resistivity (Ωm)	Thickness (m)	Depth (m)	Rank
Kintampo Municipal Hospital	SP1	1 2 3 4	221 1385 147 528	3.710 4.026 28.049 -	3.710 7.736 35.785 -	1st
	SP2	1 2 3 4 5	205 226 346 306 264	1.315 1.768 12.161 41.706 -	1.315 3.083 15.244 56.950 -	3rd
	SP3	1 2 3	67 247 71	1.363 22.532 -	1.363 23.895 -	2nd

4.3.3.11 NTRABAN EM PROFILES AND MODELLED VES CURVES

A total of 250 m long traverse was investigated for conductive anomaly in the school and within the Ntraban community.

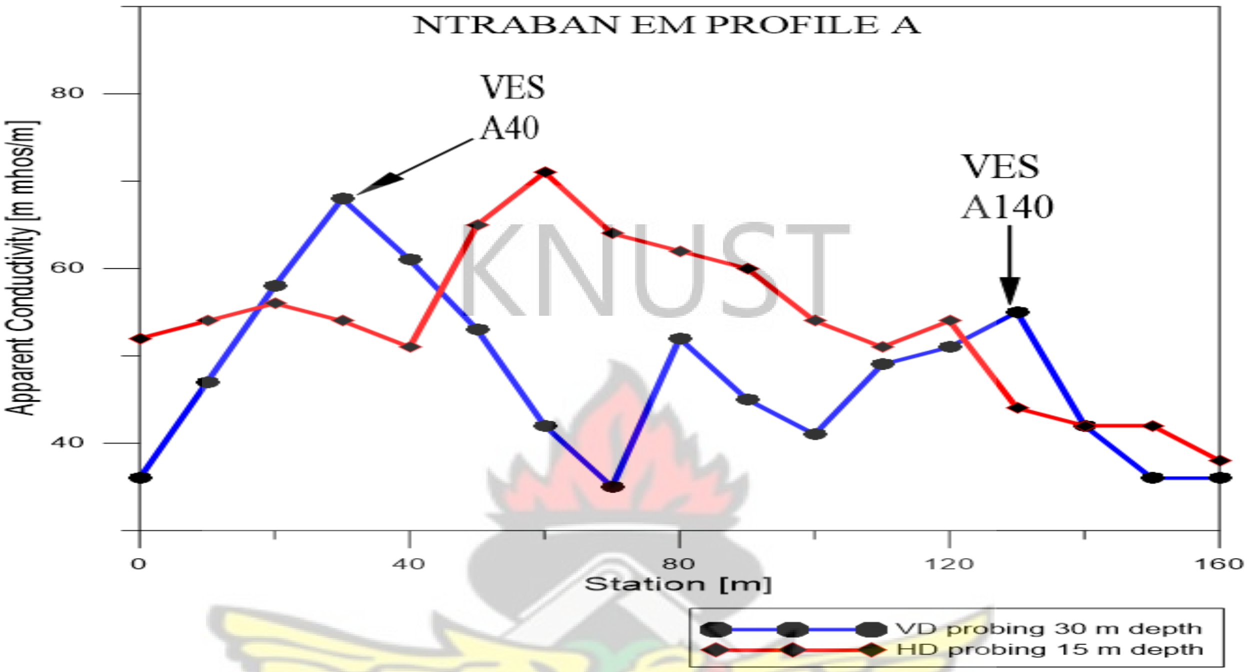

Fig 4.57 EM Profile along Traverse A, Ntraban community.

Figure 4.57 shows the EM profile of subsurface apparent conductivity along traverse A, a distance of about 160 m at the community, Ntraban. The profile depicts a varying apparent conductivity at the subsurface at both shallower, 15 m and deeper, 30 m depths. Most part of the profile shows higher apparent conductivity values for HD mode than the VD mode at the subsurface. But at station points A40 m and A140 m on the traverse, crossovers occurred, where the VD mode shows higher apparent conductivity values than the HD mode. These crossovers of sharp positive peaks, indicate significant anomaly at the subsurface. These crossover points may be deeply fractured zones. Thus, station A40 m and A140 m were selected for further VES investigation.

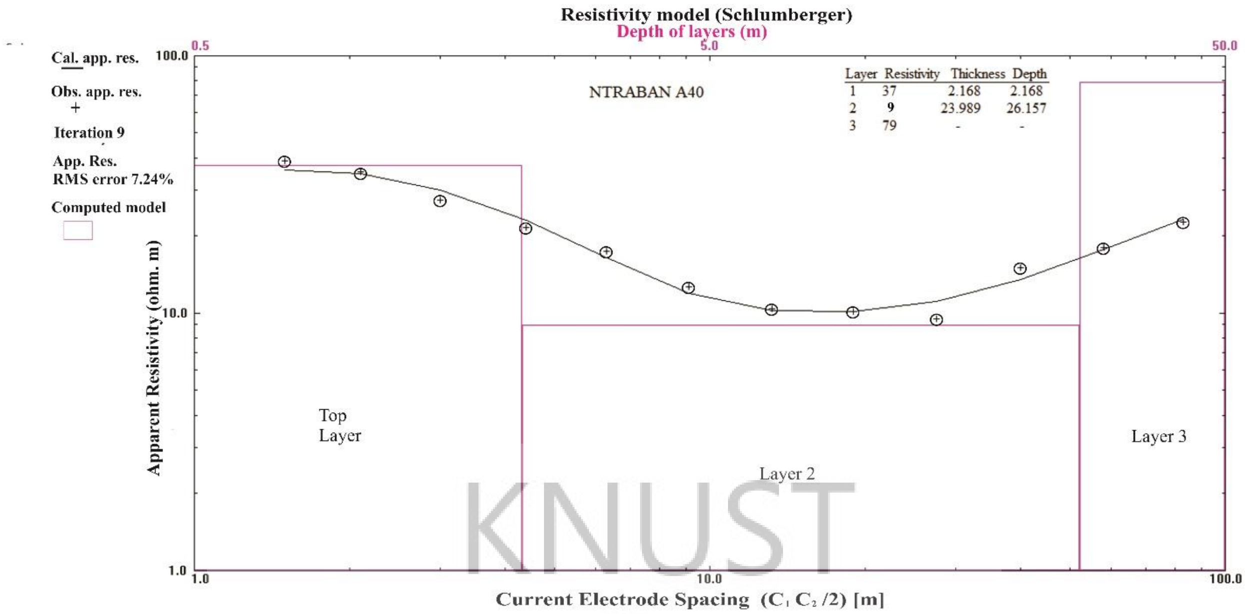

Fig 4.58 VES Curve at station A40 m, Ntraban community.

Figure 4.58 is the VES modelled curve for station A40 m in Ntraban community. It portrays a three layer subsurface structure with varying apparent resistivities. The top layer has a resistivity of about 37 Ωm, which drops to about 9 Ωm in the second layer at a depth of about 26 m. The apparent resistivity however increases to about 79 Ωm in the third layer at a depth deeper than 26 m. The third layer's resistivity of 79 Ωm could potentially be an indication of a fractured and weathered zone in the subsurface, which could contain ground water. For that matter, this point A40 m in the Ntraban community is thus recommended for drilling down to a depth of about 40 m.

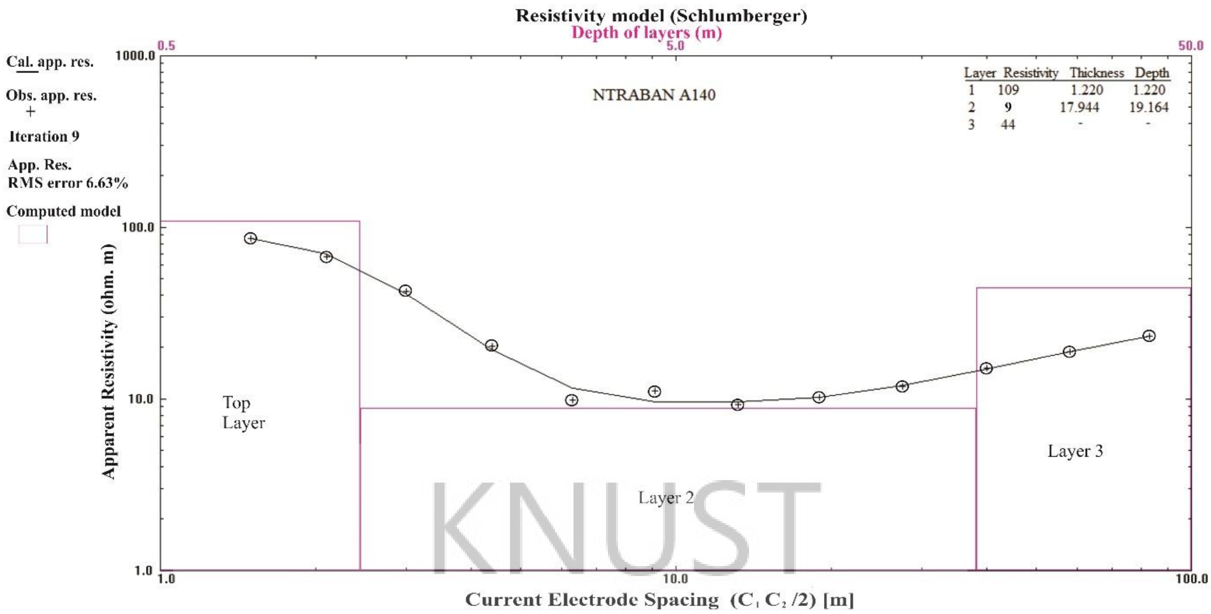

Fig 4.59 VES Curve at station A140 m, Ntraban community.

Figure 4.59 above shows the VES modelled curve at point A140 m at Ntraban community. It describes a three layer subsurface structure with varying apparent resistivities. The top layer has a resistivity of about 109 Ωm, which decreases to about 9 Ωm in the second layer at a depth of about 20 m. The apparent resistivity of the third layer however increases to about 44 Ωm at a depth greater than 20 m. The third layers resistivity of 44 Ωm could potentially be an indication of a fractured zone at the subsurface, which could contain ground water. Hence, point A140 m in the community is thus recommended for drilling down to a depth beyond 20 m.

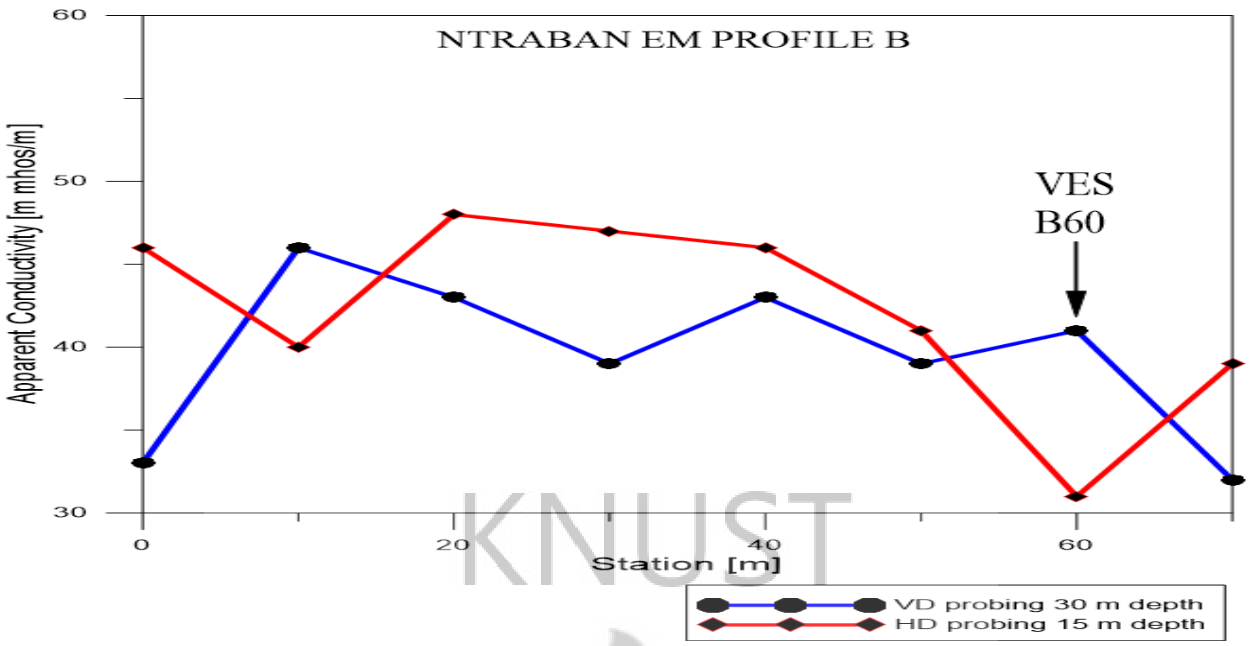

Fig 4.60 EM Profile along Traverse B, Ntraban community.

Figure 4.60 shows the EM profile of how the subsurface apparent conductivity varies with depth along traverse B, a distance of about 70 m in the community, Ntraban. The profile depicts a varying apparent conductivity at the subsurface for both the HD mode (shallow depth 15 m) and the VD mode (deeper depth, 30 m). A greater part of the profile show higher apparent conductivity values for the HD mode than the corresponding VD mode of the subsurface except at stations B10 m and B60 m where crossovers occurred on the traverse. These crossovers of sharp positive peaks may be an indication of significant anomaly at the subsurface. However, only station B60 m was selected for further VES investigation.

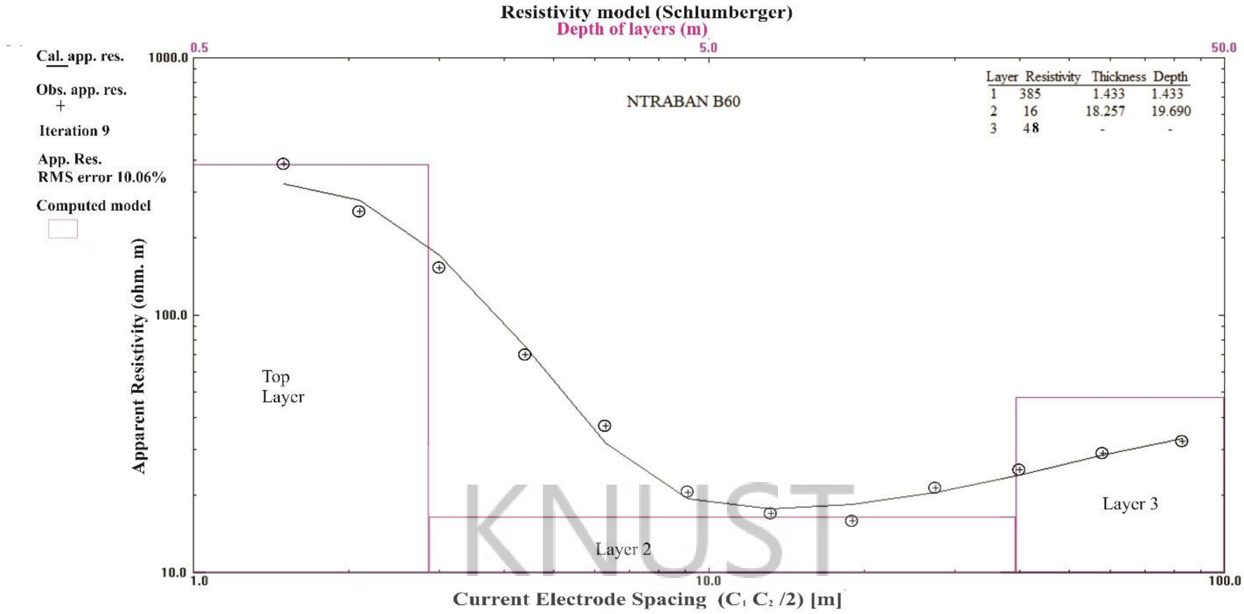

Fig 4.61 VES Curve at station B60 m, in Ntraban community.

Figure 4.61 above shows the VES modelled curve for station B60 m on the EM traverse B in Ntraban community. Quantitatively, the model showed three layers. The resistivity of the top layer's (topsoil) is about 385 Ωm and lies at a shallow depth of about 1.4 m. The apparent resistivity of the second layer decreased from 385 Ωm to about 16 Ωm at a depth of about 20 m. However, the apparent resistivity of the third layer rather increased to about 48 Ωm. The layer parameters comprising apparent resistivity, thickness and depth of the second and third layers showed that the subsurface may be underlain by fractured zone at a depth higher than 20 m. Therefore, VES point B60 m is recommended for drilling up to a depth of about 25 m.

Table 4.11 Ranked VES points for test drilling at Ntraban community.

Community	VES POINT	Layer	Resistivity (Ωm)	Thickness (m)	Depth (m)	Rank
Ntraban	A40	1 2 3	37 9 79	2.168 23.989 -	2.168 26.157 -	**2nd**
	A140	1 2 3	109 9 44	1.220 17.944 -	1.220 19.164	**3rd**
	B60	1 2 3	385 16 48	1.433 18.257 -	1.433 19.690 -	**1st**

4.3.3.12 WURUKWAN COMMUNITY MODELLED VES CURVES

The geophysical investigations in this community were limited to only vertical electrical sounding (VES). Three VES points were explored to determine their resistivity variation with depth.

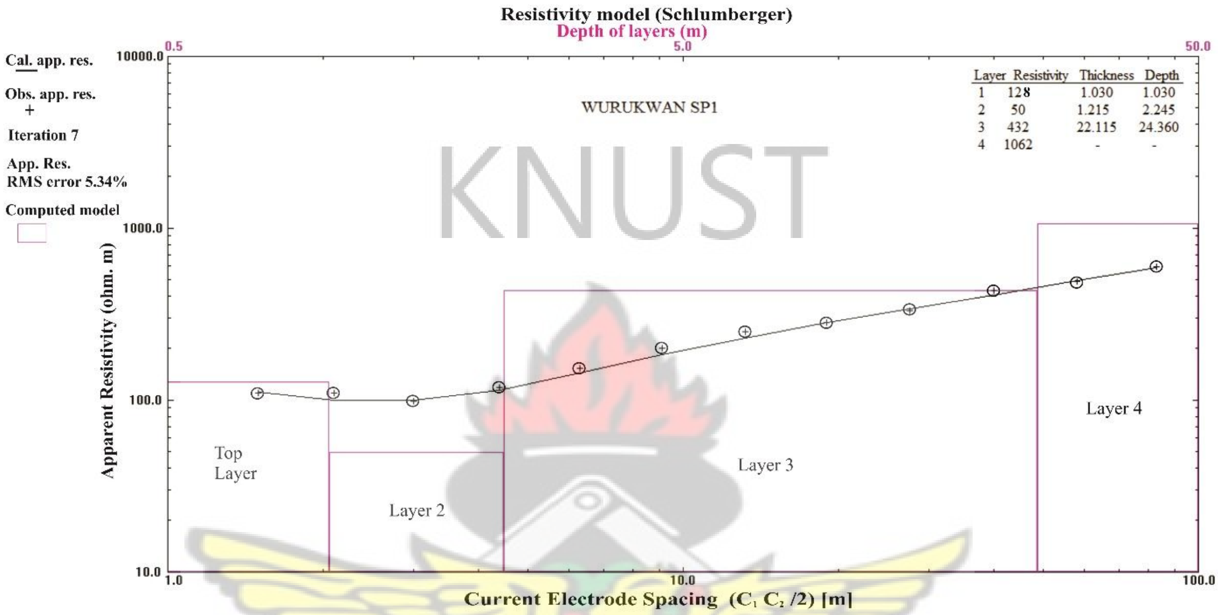

Fig 4.62 VES Curve at sounding spot SP1, Wurukwan community.

Figure 4.62 is the VES modelled curve at the sounding spot SP1 in Wurukwan community. It depicts a four layer subsurface structure with varying apparent resistivity values. The top soil has a resistivity of about 1280 Ωm, which drops to about 50 Ωm in the second layer. The apparent resistivity however increased to about 432 Ωm in the third layer at a depth of about 24 m. The fourth layers resistivity further increased to about 1062 Ωm. The layer parameters of the third and fourth layers suggest that, the subsurface might not be fractured since resistivity increases with depth. Hence may not contain groundwater. Consequently, sounding spot SP1 in Wurukwan community was thus not recommended for drilling.

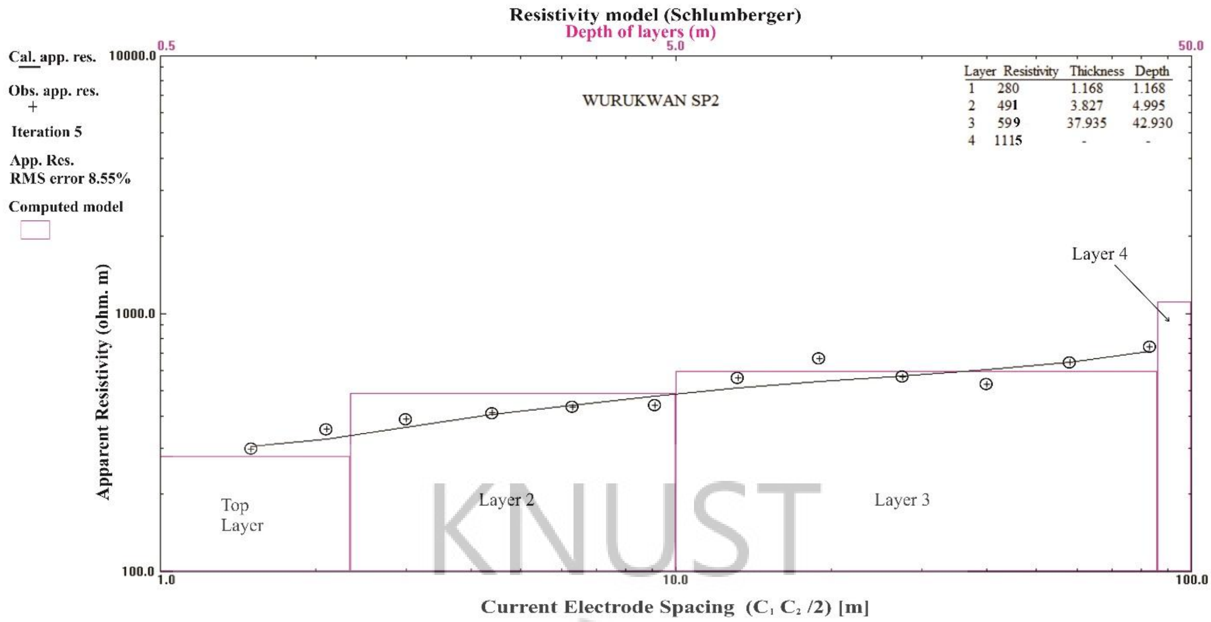

Fig 4.63 VES Curve at sounding spot SP2, Wurukwan community.

Figure 4.63 shows the VES modelled curve the sounding spot SP2 in Wurukwan community. It illustrates a four layer subsurface structure with increasing apparent resistivities. The top layer has a resistivity of about 280 Ωm, which increases in the other layers up to about 1115 Ωm in the fourth layer as displayed in figure 4.63 above. The layer parameters of the third and fourth layers, which are at deeper depths suggest that, the subsurface might not be fractured since their apparent resistivities increases with depth. Hence may not contain groundwater. Subsequently, sounding spot SP2 in the Wurukwan community was thus not recommended for drilling.

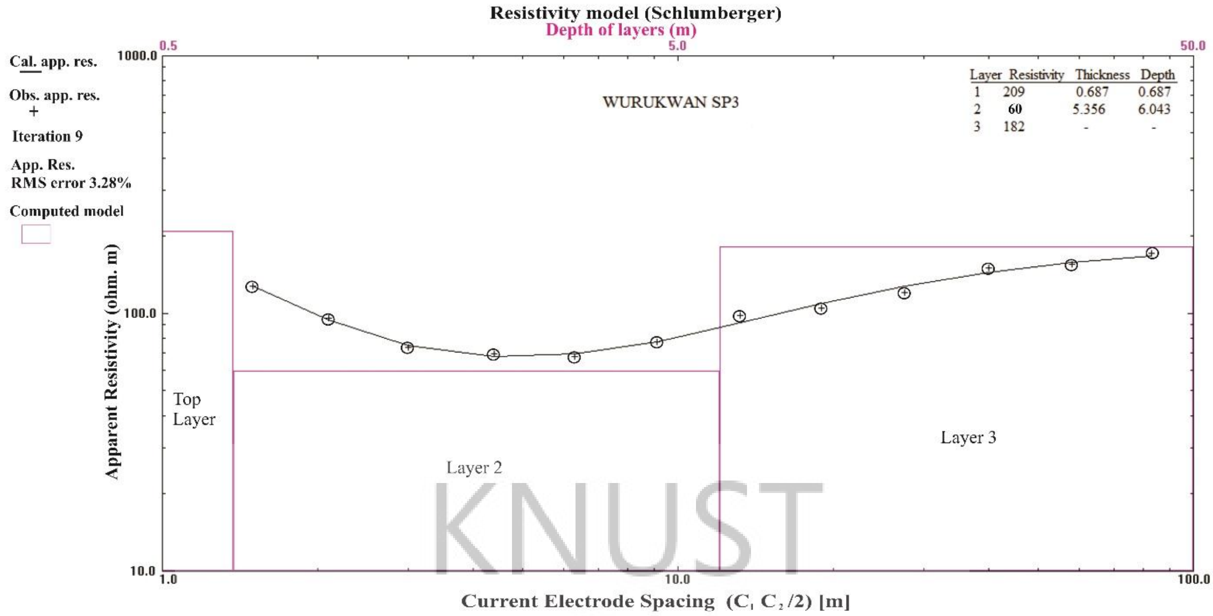

Fig 4.64 VES Curve at sounding spot SP3, Wurukwan community.

Figure 4.64 above shows the VES curve for the sounding spot SP3 in Wurukwan community. Quantitatively, the model showed three layers. The top layer's (topsoil) apparent resistivity is about 209 Ωm at a shallow depth of about 0.7 m. The apparent resistivity of the second layer decreased from 209 Ωm in the first layer to about 60 Ωm at a depth of about 6 m. The apparent resistivity of the third layer rather increased to about 182 Ωm. The layer parameters (apparent resistivity, thickness and depth) of the second and third layers showed that the subsurface may be underlain by fractured rock at a depth ranging from 7 m and more. Therefore, VES point SP3 in the Wurukwan community is recommended for drilling up to depth of about 40 m.

Table 4.12 Ranked VES points in the Wurukwan community.

Community	VES Point	Layer	Resistivity (Ωm)	Thickness (m)	Depth (m)	Rank
Wurukwan	SP1	1	128	1.030	1.030	**2nd**
		2	50	1.215	2.245	
		3	432	22.115	24.360	
		4	1062	-	-	
	SP2	1	280	1.168	1.168	**3rd** .
		2	491	3.827	4.995	
		3	599	37.935	42.930	
		4	1115	-	-	
	SP3	1	209	0.687	0.687	**1st**
		2	60	5.356	6.043	
		3	182	-	-	

4.3.3.13 YAARA EM PROFILES AND MODELLED VES CURVES

Four (4) EM traverses were run in Yaara community to investigate the anomalous behavior of the subsurface. Profiles A and B were ran within the community, Profile C, was run near the Catholic Church area whilst Profile D, was within the Local Authority School area.

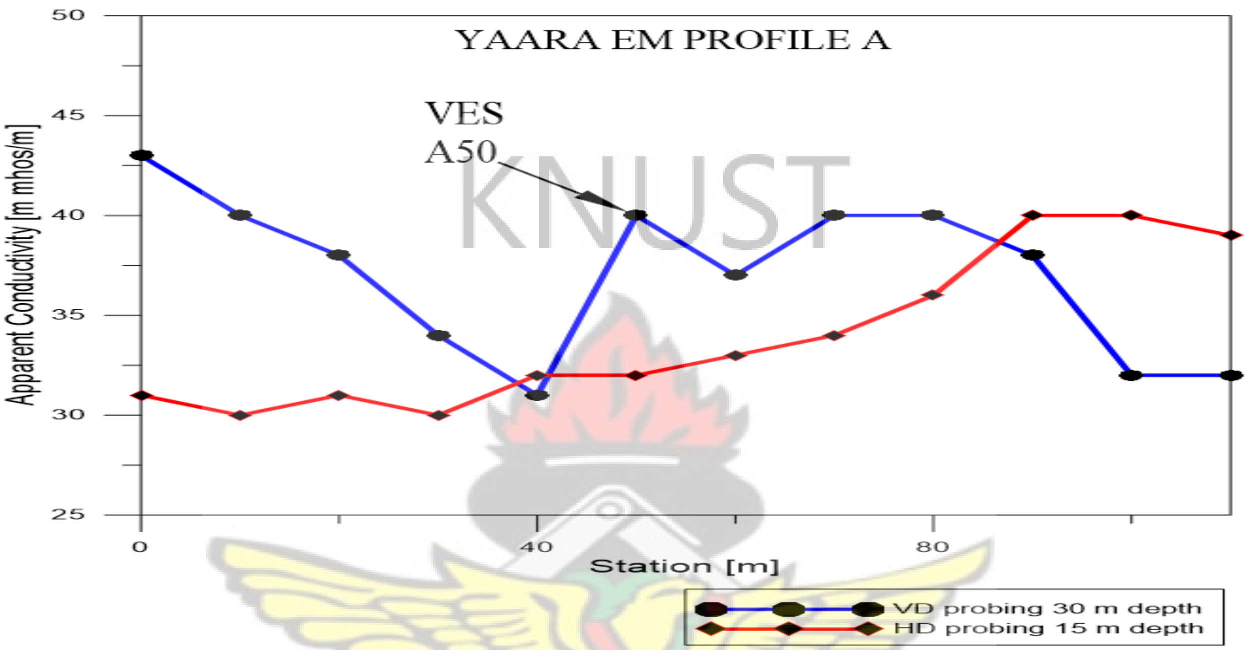

Fig 4.65 EM Profile along Traverse A, Yaara community.

Figure 4.65 above shows the EM profile of how the subsurface apparent conductivity varies with depth along traverse A, a distance of about 110 m in the community, Yaara. The profile depicts varying apparent conductivity at the subsurface at both the shallower (15 m) and deeper (30 m) depths. Most part of the profile show higher apparent conductivity values for the VD mode than the HD mode at the subsurface. But at station A40 m, the HD mode apparent conductivity value is slightly higher than the corresponding VD mode. Moreover, from station points A90 m up to 110 m, the HD mode continue to exhibit higher values than the VD mode. The sharp positive peak at station A50 m, indicated significant anomaly at the subsurface. Therefore, this point was selected for further VES investigation.

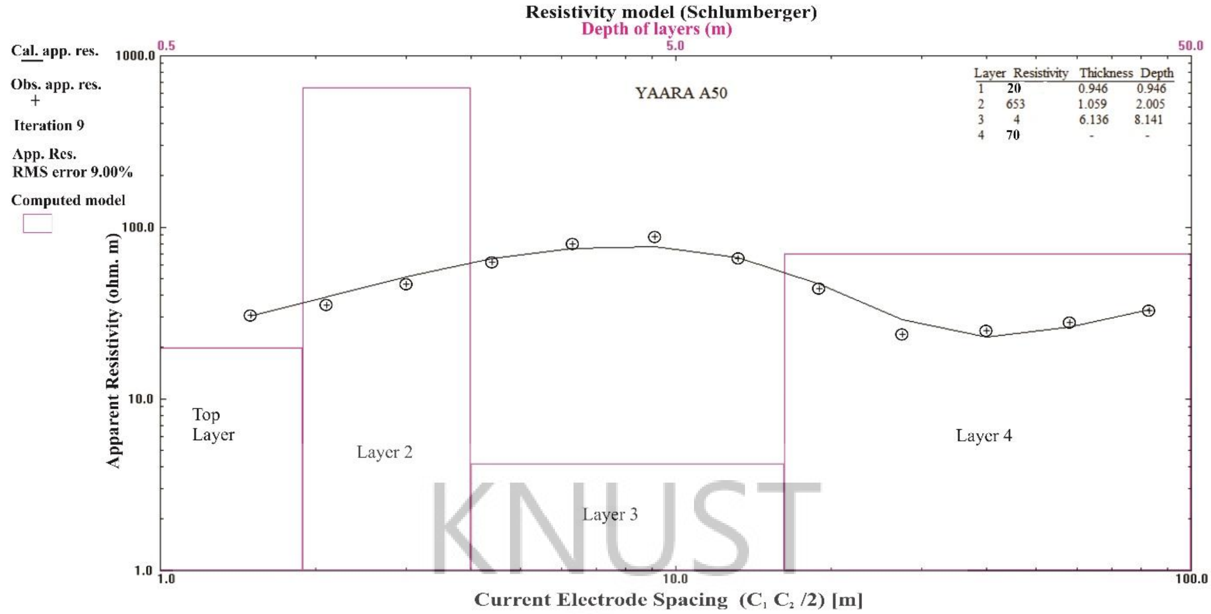

Fig 4.66 VES Curve at station A50 m, Yaara community.

Figure 4.66 above is the VES modelled curve for sounding station A50 m in Yaara community. It depicts a four layer subsurface structure with varying apparent resistivities. The top soil has a resistivity of about 20 Ωm, which increases significantly to about 653 Ωm in the second layer. The apparent resistivity of the third layer however decreased to about 4 Ωm at a depth of about 8.0 m. The fourth layer's resistivity rather increased to about 70 Ωm at a depth deeper than 10 .0 m. The layer parameters of the third and fourth layers suggest that, the subsurface might be fractured and weathered at shallow and at deeper depths. Consequently, sounding station A50 m in the community is thus recommended for drilling down to a depth greater than 50.0 m.

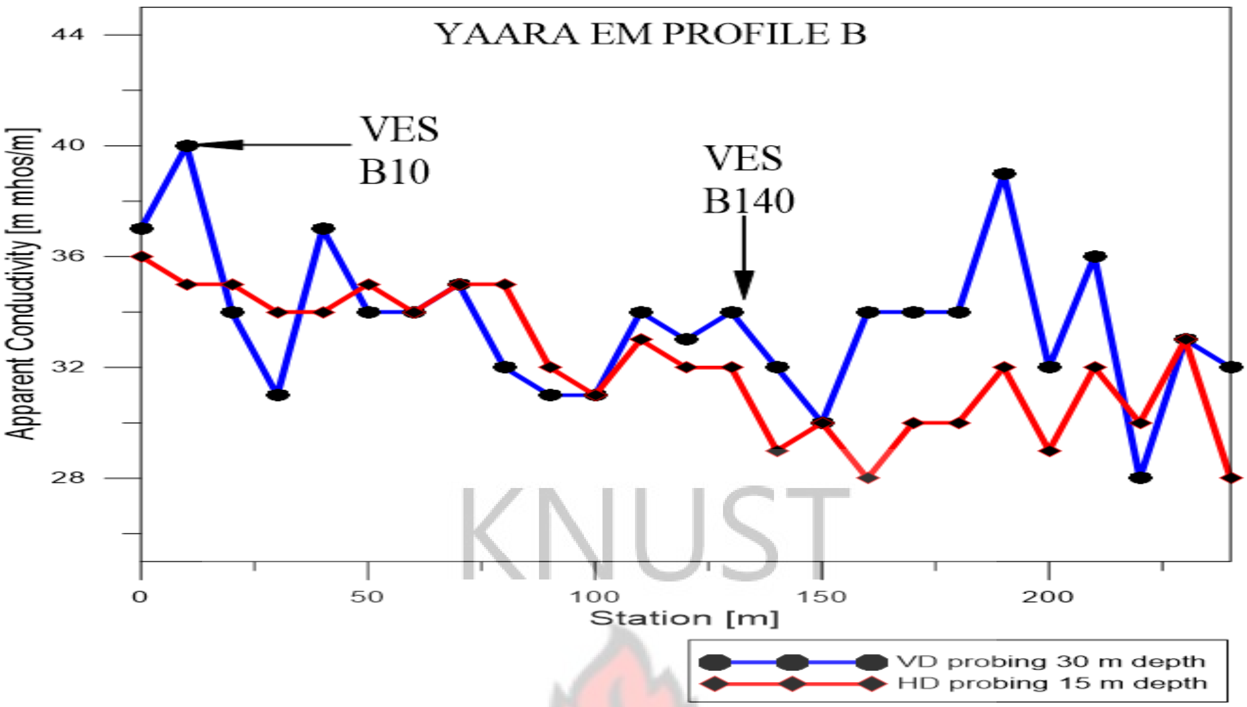

Fig 4.67 EM Profile along Traverse B, Yaara community.

Figure 4.67 above, depicts a varying apparent conductivity with depth for both the shallower 15 m HD mode and deeper 30 m VD modes. This profile shows erratic variation in apparent conductivity values for both the VD mode and the HD mode at the subsurface as shown in Figure 4.67. The profile displays series of necks and crossovers, suggesting a fractured subsurface at stations B10 m, B40 m, B60 m, B140 m, B150 m, and B180 m stations. However, only stations B10 m and B140 m were further investigated using VES methodology.

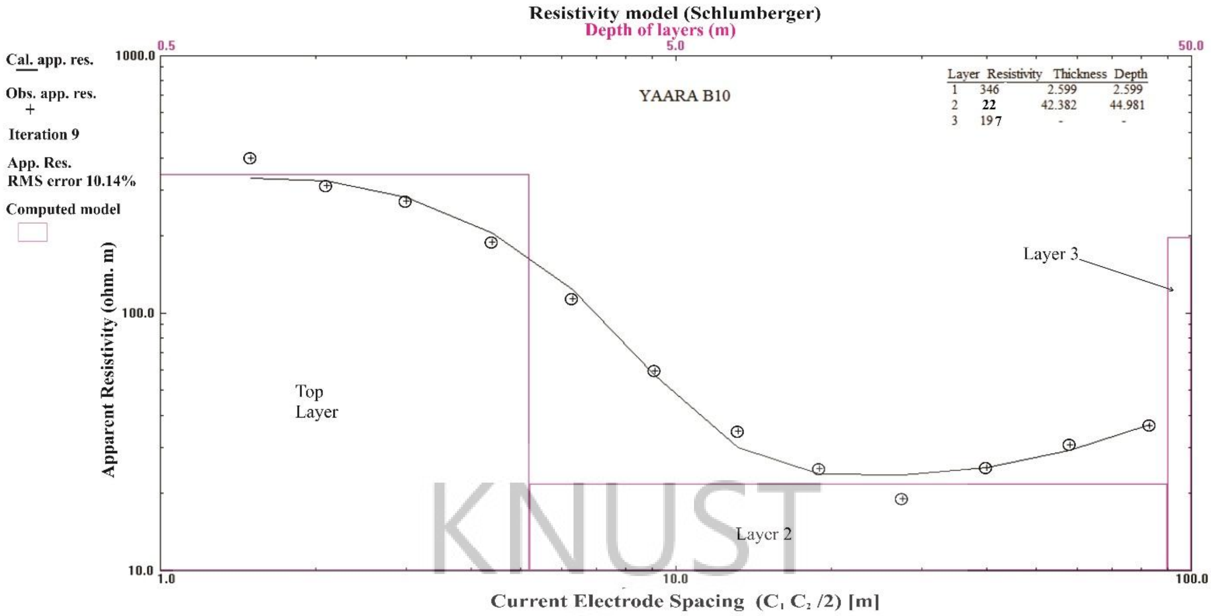

Fig 4.68 VES Curve at station B10 m, Yaara community.

Figure 4.68 above is a VES modelled curve for station B10 m in Yaara community. It depicts a three layer subsurface geological layers with varying apparent resistivities at varying depths. The top soil has a resistivity of about 346 Ωm, which decreased to about 22 Ωm in the second layer at a depth of about 45.0 m. The apparent resistivity however increased to about 197 Ωm in the third layer at an infinite depth. The layer parameters (apparent resistivity, thickness and depth) of second layer are inferred to be fractured and weather layer where ground water could be located. Therefore, this station B10 m in the Yaara community is thus recommended for drilling up to a depth of about 47.0 m.

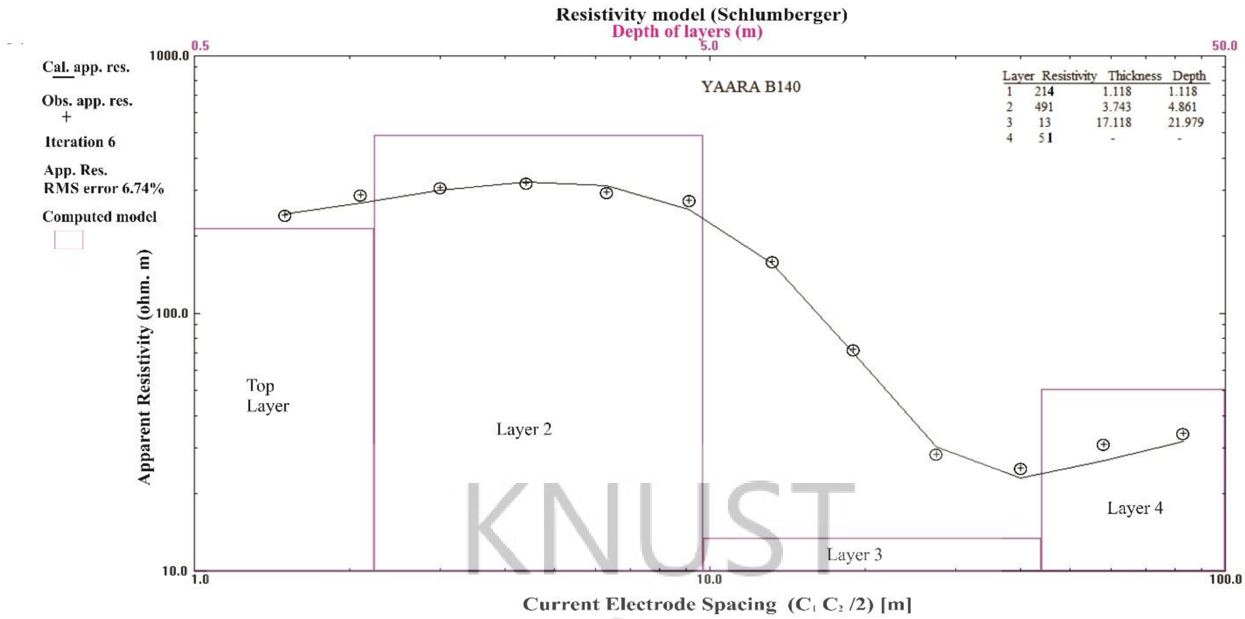

Fig 4.69 VES Curve at station B140 m,Yaara community.

Figure 4.69 is the VES modelled curve for station B140 m in Yaara community. The subsurface reveals four layers as shown in figure 4.69 above. The apparent resistivity increased from 214 Ωm in the first layer to about 491 Ωm in the second layer. The apparent resistivity of the third layer rather decreased from the former to about 13 Ωm at a depth of about 22.0 m. However, there was another increase in apparent resistivity to about 51 Ωm in the fourth layer with respect to that of the third. The layer parameters of apparent resistivity, thickness and depth of the third layer suggest that there could be a fractured zone at a depth of about 22.0 m. Therefore, VES point B140 m in the Yaara community is recommended for drilling up to a depth of about 25.0 m.

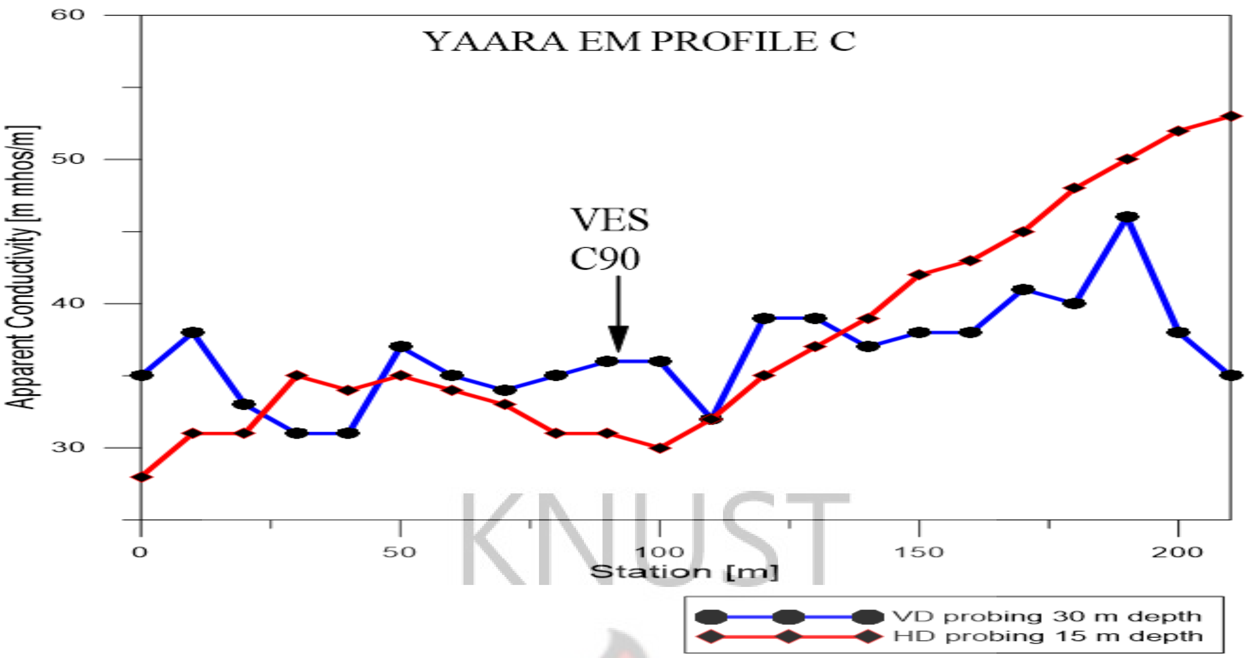

Fig 4.70 EM Profile along Traverse C, Yaara community.

Figure 4.70 shows the EM profile of the subsurface apparent conductivity along traverse C, a distance of about 210 m at the Catholic Church area in Yaara community. The profile depicts varying apparent conductivity at the subsurface for both the shallower (15 m), and deeper, (30 m) depths. Ranging from station C0.0 m to C20.0 m and also from C40.0 m to C130.0 m, the VD mode shows higher apparent conductivity values than their corresponding HD mode. But from station points C130 m up to C210 m, the HD mode shows higher apparent conductivity values than the VD mode. From figure 4.70 above, the average VD mode value corresponded to station C90 m, which was then considered for VES investigation.

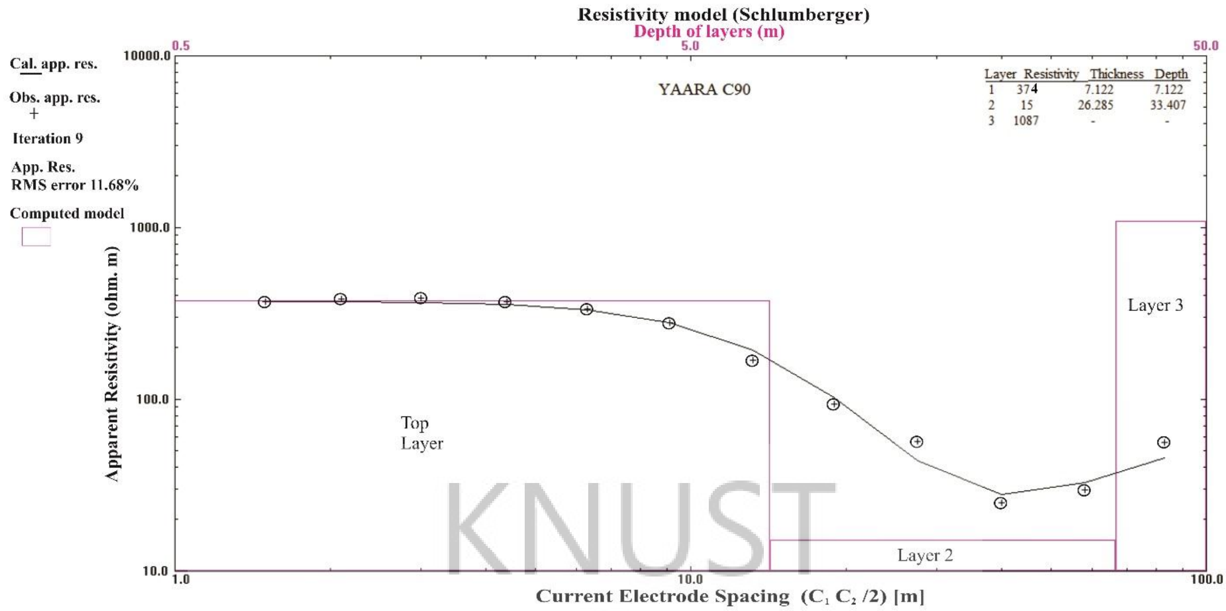

Fig 4.71 VES Curve at station C90 m, in Yaara Catholic Church area.

Figure 4.71 is a VES modelled curve for station C90 m in Yaara community Catholic Church area. It shows a three layer subsurface structure with varying apparent resistivities at varying depths. The top soil has a resistivity of about 374 Ωm, which decreased to about 15 Ωm in the second layer at a depth of about 33.0 m. The apparent resistivity however increased abruptly to about 1087 Ωm in the third layer at an infinite depth. The layer parameters (apparent resistivity, thickness and depth) of the second layer were inferred to be fractured and weather layer, where ground water could be located. Therefore, station C90 m in the Yaara Catholic Church area was recommended for drilling up to a depth of about 35.0 m.

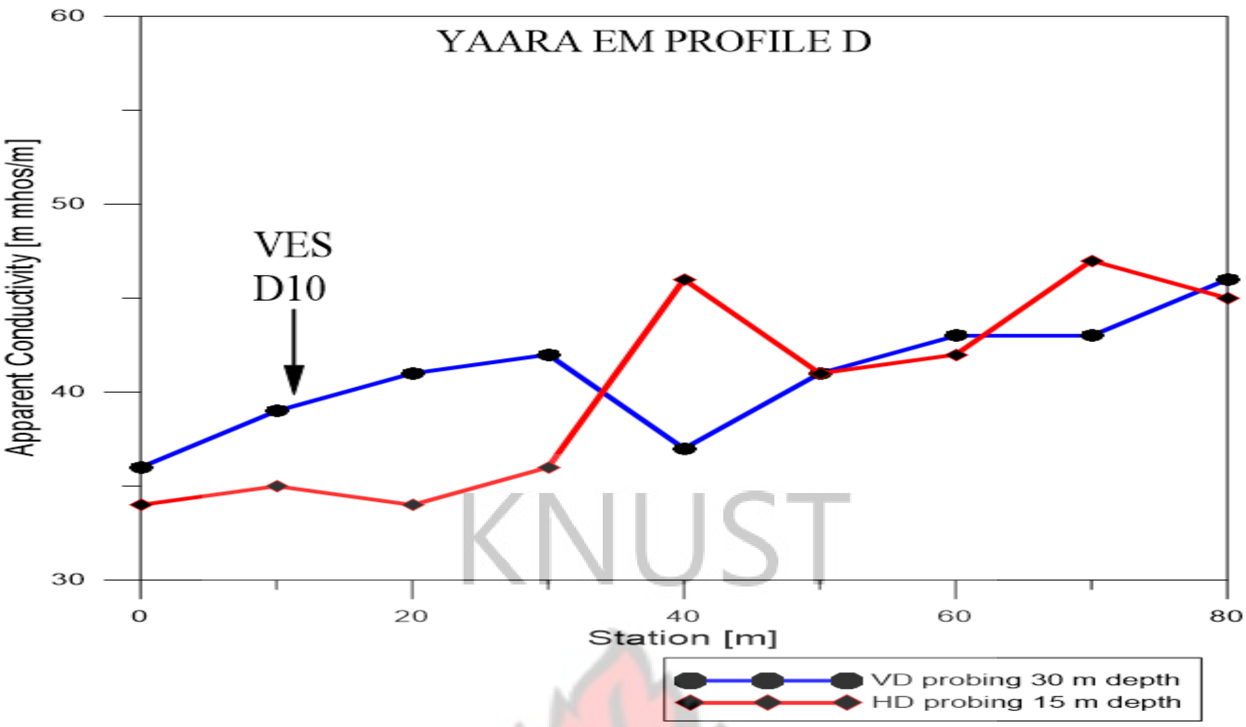

Fig 4.72 EM Profile along Traverse D at the LA School, Yaara community.

Figure 4.72 shows the EM profile of the subsurface apparent conductivity along traverse D over a distance of about 80 m in Yaara community. The profile exhibits a varying apparent conductivity at the subsurface for both the shallower (15 m) and deeper (30 m) depths. About half of the profile length shows higher apparent conductivity values for the VD mode than the HD mode at the subsurface up to station point 30 m. However, between stations 35 m up to 50 m and 60 m up to 85 m, the profile shows higher apparent conductivity values for the HD mode than the VD mode. At 10 m, and 60 m points on the traverse, there are crossovers indicating significant anomalies. These stations may be deep fractured zones, with relatively higher apparent conductivity VD mode values. However, only station D10 m was selected for further VES investigation.

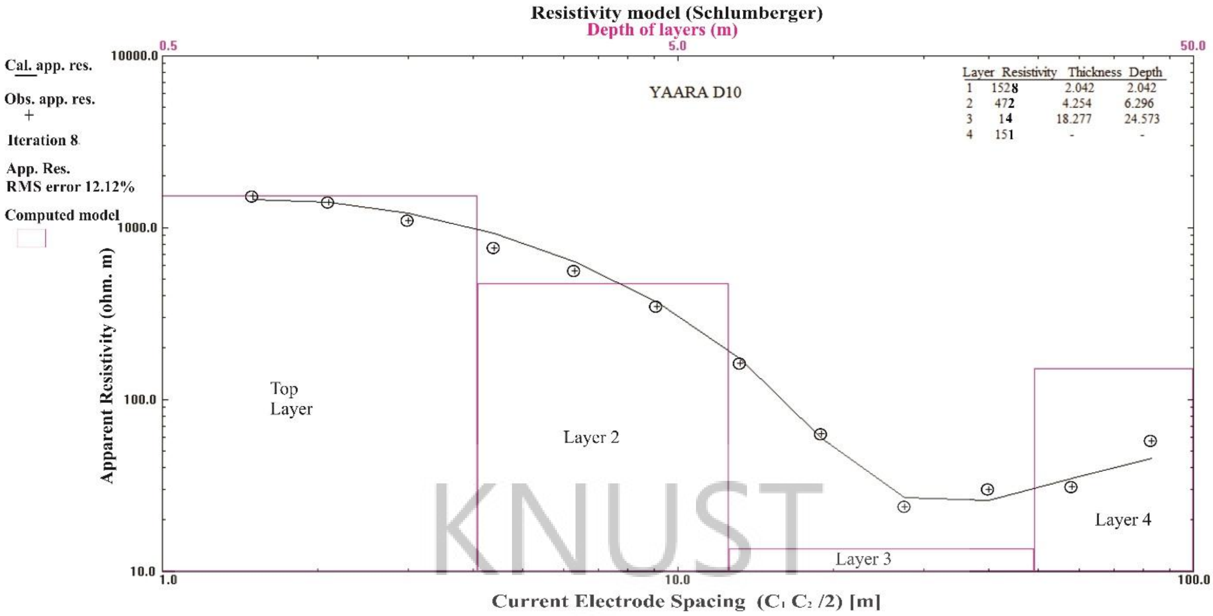

Fig 4.73 VES Curve at station D10 m, in Yaara LA School.

Quantitatively, the apparent resistivity VES curve for station D10 m in Yaara LA community School as shown in Figure 4.73. It depicts a four layer subsurface structure. There is a drastic decrease in apparent resistivity from about 1528 Ωm in the first layer (topsoil) to about 472 Ωm in the second; then another decrease to about 14 Ωm in the third layer at a depth of about 25.0 m. The apparent resistivity of the fourth layer however increased to 151 Ωm. The layer parameters of the apparent resistivity, thickness and depth of the various layers show that the overburden is expected to be thin and at a shallow depth of about 2.0 m. The subsurface at the third layer may be underlain by a fractured zone at a depth of about 28.0 m. Therefore, VES point D10 m was recommended for drilling up to a depth of about 30 m.

Table 4.13 Ranked VES points in Yaara Community

Community	VES Point	Layer	Resistivity (Ωm)	Thickness (m)	Depth (m)	Rank
Yaara Community	A50	1 2 3 4	20 653 4 70	0.946 1.059 6.136 -	0.946 2.005 8.141 -	**5th**
	B10	1 2 3	346 22 197	2.599 42.382 -	2.599 44.981 -	**1st**
	B140	1 2 3 4	214 491 13 51	1.118 3.743 17.118 -	1.118 4.861 21.979 -	**3rd**
	C90	1 2 3	374 15 1087	7.122 26.285 -	7.122 33.407 -	**2nd**
	D10	1 2 3 4	1528 472 14 151	2.042 4.254 18.277 -	2.042 6.296 24.573 -	**4th**

CHAPTER 5

RESULTS AND DISCUSSION

5.1.0 Results

After the qualitative interpretation of the EM graphs and quantitative analysis of the modelled VES curves, an average of two VES points in each community have been selected for drilling.

5.1.1 Recommended Drilling Points At Alhassan Akura

In the Alhassan Akura community, four VES points were selected for drilling. Two points within the community itself on profile A and two points at the primary/JHS School on profile B. At the community VES A40 m should be drilled first. Its coordinates are 08^o 43.034’ N, 001^o 29.183’ W at an altitude of 109 m above mean sea level (amsl). The second drilling point should be VES A110 m with coordinates 08^o 43.010’ N, 001^o 29.153’ W at an altitude of 112 m amsl.

At the primary/ JHS School, VES point B60 m should be drilled first. Its coordinates are 08^o 43.263’ N, 001^o 29.183’ W and its altitude is 111 m amsl. The second drilling point is VES B10 m, with coordinates 08^o 43.288’ N, 001^o 29.175’ W and at an altitude of 104 m amsl.

5.1.2 Recommended Borehole Drilling Points at Asukoko

At Asukoko, three VES points were recommended for drilling. VES A30 m should be drilled first. It has coordinates 08° 05.199’N, 001° 29.845’W and at an altitude of 238 m amsl. The second point to drill is VES A120 m with coordinates 08^o 05.244’N, 001^o 29.838’W. Its altitude is 222 m amsl. The third drilling point in this community should be at point A190 m with coordinates 08° 05.286'N, 001° 29.835'W. It has an altitude of 213 m amsl.

5.1.3 Recommended Drilling Points At Atta Akura

In Atta Akura community, four VES points were pegged for drilling. Two points inside the community on profile A and two points at the primary School on profile B. At the community, VES A50 m should be drilled first. Its coordinates are 08^o 16.854' N, 001^o 35.793' W and at an altitude of 128.8 m amsl. The second should be SP1 with coordinates 08^o 17.120' N, 001^o 35.926'W and at an altitude of 138 m amsl.

At the primary School, VES point B80 m should be drilled first. Its coordinates are 08^o 16.617' N

001^o 36.046' W and its altitude is 142.8 m amsl. The second drilling point is VES B140 m, with coordinates 08^o 16.589' N, 001^o 36.059'W and at an altitude of 143 m amsl.

5.1.4 Recommended Drilling Points At Benkrom Community

In Benkrom community, four VES points were sited for drilling. Two points on profile A and two other sounding points. VES point A10 m should be drilled first. Its coordinates are 08^o 45.410' N, 001^o 27.133' W and at an altitude of 98 m amsl. The second should be SP1 with coordinates 08^o 45.479' N, 001^o 27.108' W and at an altitude of 100 m amsl. The third drill VES point should be A60 m. Its coordinates are 08^o 45.387' N, 001^o 27.122' W and its altitude is 100 m amsl. The fourth drill point is SP2, with coordinates 08^o 45.509' N, 001^o 27.215' W and at an altitude of 94 m amsl.

5.1.5 Recommended Borehole Drilling Point At Dagarti Akura

The VES point A70 m is ranked as the first point for drilling. Its coordinates are 08^o 02.017' N, 001^o 53.387' W with altitude 203 m amsl. The second choice is A50/B30 m with coordinates 08^o 01.995' N, 001^o 53.377' W. It has an altitude of 212 m. Either of the two points could be drilled depending on the preference of the community.

5.1.6 Recommended Drilling Points at Dawadawa No.2 community.

In Dawadawa No.2 community, four VES points were also sited for drilling. Two points inside the community itself and two other points at the Dawadawa Basic School. VES point A90 m should be drilled first. Its coordinates are 08^o 21.628' N, 001^o 33.942' W and at an altitude of 128 m amsl. The second should be SP2 with coordinates 08^o 21.656'N, 001^o 34.112' W and at an altitude of 143 m amsl. At the school, VES point SP3 should be drilled first. It has coordinates 08^o 21.416' N, 001^o 34.141' W and its altitude is 134 m amsl. The second proposed drilling point at the school is B60 m, with coordinates 08^o 21.466'N, 001^o 34.116 W and at an altitude of 129 m amsl.

5.1.7 Recommended Drilling Points At Gu Alhaji Akura

The VES point A20 m is ranked as the first for drilling. Its coordinates are 08^o 31.574' N, 001^o 36.425' W with altitude 127 m amsl. The second option is A80 m with coordinates 08^o 31.543' N, 001^o 36.422' W. It has an altitude of 122 m.

5.1.8 Recommended Drilling Points At Gulumpe Kokomba

In Gulumpe Kukomba, two VES points were recommended for drilling. VES A0 m should be drilled first. It has coordinates 08 ^{o} 30.506' N, 001^{o} 34.223' W and at an altitude of 156 m amsl. The second drill point should be VES A160 m with coordinates 08° 30.443' N, 001^{o} 34.284' W. Its altitude is 151 m amsl.

5.1.9 Recommended Drilling Points At Kawampe

The recommended drilling points are four in this community. The first is A20 m, which is about 80 m away from an existing borehole. Its coordinates are 08^{o} 26.795' N, 001^{o} 33.942'W with an altitude of 128 m amsl. The second alternative being A190 m with coordinates 08^{o} 26.705' N, 001^{o} 33.937' W and altitude 131 m amsl. The third option should be B40 m with its coordinates as 08^{o} 26.798'N, 001^{o} 33.846'W. Its altitude is 135 m amsl. And the last alternative is B90 m. It has coordinates 08^{o} 26.806' N, 001^{o} 33.821' W and at an altitude of 137 m amsl.

5.1.10 Recommended Drilling Points At Kintampo Municipal Hospital

The recommended drilling points in Kintampo Municipal Hospital is SP3. It has coordinates 08^{o} 03.079' N, 001^{o} 43.913' W and at an altitude of 353 m amsl. The alternative point is SP2 with coordinates 08^{o} 43.288' N, 001^{o} 29.175' W. Its altitude is 351 m amsl.

5.1.11 Recommended Borehole Drilling Points At Ntraban

In Ntraban community, two drilling points were selected. The first drilling point should be B60 m with coordinates 08^{o} 13.199’ N, 001^{o} 48.248’ W. It has an altitude of 118.5 m amsl. The alternative is A40 m with coordinates 08^{o} 13.184’ N, 001^{o} 48.184’ W and at an altitude of 129.8 m amsl.

Recommended Borehole Drilling Point at Wurukwan

In Wurukwan community, SP3 of coordinates 08^{o} 08.993’ N, 001^{o} 33.738’ W should be drilled first. It has an altitude of 192 m amsl. The second drilling point should be SP1 of coordinates 08^{o} 08.963’ N, 001^{o} 33.667’ W and altitude 197 m amsl.

5.1.12 Recommended Borehole Drilling Point At Yaara

In Yaara community, four VES points were ranked for drilling, two within the community itself and two at the basic school. Within the community, VES B10 m should be drilled first. Its coordinates are 08^{o} 13.765’N, 001^{o} 50.542’W and its altitude is 97.6 m amsl. The second point is B140 m with coordinates 08^{o} 13.759’ N, 001^{o} 50.609’ W and at altitude 114 m amsl.

For the basic school, VES C90 m should be drilled first. Its coordinates are 08^{o} 13.734’N, 001^{o} 50.794’W and of altitude 89.9 m amsl.   The second point in the school should be C190 m. It has coordinates 08^{o} 13.746’ N, 001^{o} 50.837’ W and at an altitude of 85 m amsl.

5.2.0 Discussion

The interpretation of the EM profiles is qualitative and this involves visual inspection of the profile for points where the crossover anomaly or the neck anomaly occurs; such are usually suggestive of presence of conductive (weak) zones beneath the subsurface. Several of such points were identified on the profiles; which then became the prime locations for VES.

The interpreted results of VES data for each community are summarized as recommended drilling points with their coordinates and altitude provided to aid easy location of selected VES points. From the interpretation of the modelled VES curves, 3 to 5 subsurface layers were delineated in the study area. The resistivity values of the first layer ranged from 19 to 1.5×10^3 Ω.m with thickness ranging from 0.3 – 7.1 m, while the resistivity of the second layer ranged from 3 to 3.9×10^4 Ω.m with thickness ranging from 0.6 - 45 m and that of the third layer ranging from 1.2 to 1.1×10^3 Ω.m with thickness ranging from 1.5 to infinity in the 3 layer models. In the fourth layer, the resistivity values ranged between 0.3 and 1.5×10^4 Ω.m with thickness ranging from 9 m in the five layer cases to infinite thickness in the four layer cases. This layer represents an important aquifer in the study area. The bedrock, which occurs as either the third, fourth or fifth layer in different parts of the study area has resistivity values ranging from as low as 2 Ω.m and up to 1.5×10^4 Ω.m. The thickness of the fifth layer cannot be measured because it is infinite. The estimated depth to basement is in the range of 5 m to 66 m. Emphasis was put on locating boreholes in areas of thick overburden.

5.2.1 Problems with Data Presentation and Interpretation

The geology of the study district being sedimentary basin is underlain predominantly by sand- stone, shale, mudstone and limestone. The district also has large deposits of clay.

Because of the intersection of apparent resistivity values involving clay and fresh groundwater, it makes resistivity interpretations difficult and uncertain.

CHAPTER 6

CONCLUSIONS AND RECOMMENDATIONS

6.1.0 Conclusions.

Detailed geological, conductivity and electrical surveys were carried out to locate suitable sites for boreholes to be drilled to provide potable water to the study communities. The electromagnetic data confirm the presence of high conductivity zones/fractures and joints under and within the communities. These fractures and joints are believed to be filled with conductive fluid such as water. This was corroborated by running VES.

The Vertical electrical resistivity sounding method has proven to be successful and highly effective in the identification and delineation of subsurface structures that are associated with groundwater accumulation in a sedimentary formation. The VES method used in this project successfully delineated prime spots in the study communities revealing their subsurface geo-electrical layers.

In all, the number of layers delineated by the VES model curves varied from three to five. These layers are inferred to consist of surface layer (top soil), alluvium layer and saturated (bottom soil) layer. The underlying sandstone and shale bedrock is characterized by varying degree of fractures. It is possible to intercept some groundwater in all the sites but the yield would be low-to-moderate. From the results obtained in terms of depth, thickness, conductivity and resistivity, they suggest that any conductivity value within the range 30 – 90 $m\Omega m^{-1}$ is likely to be fractured and a weathered layer. The first layer resistivity values range from 19 - 1500 Ω.m with thickness ranging from 0.3 – 7.1 m. The second layer resistivity ranges from 3 - 39000 Ω.m with thickness ranging from 0.6 – 45.0 m. The third layer resistivity ranges from 1 – 1100 Ω.m with thickness ranging from 1.5 – 69.0 m in the 4 layer models. Fourth layer resistivity values range between 0.3 – 1500 Ω.m with thickness ranging from 9.0 – 95.7 m in the five layer cases.

The bedrock, which occurs as either the third, fourth or fifth layer in different parts of the study area has resistivity values ranging from 2 – 15000 Ω.m. The second, third and fourth layers are inferred to be the aquifer zones in the study area. The inferred depth to the aquiferous zone is expected to be in the range of about 30 - 60 m.

6.2.0 Recommendations

- Boreholes should be drilled at the recommended points to correlate the drill results with the geophysical findings.
- The minimum drilling depth should be in the range of 30 - 60 m; however, the drilling supervisor is mandated to determine the final drilling depth based on the ground conditions.
- Due to reasons beyond my control, the drill logs could not be obtained so as to correlate the geophysics findings with the drill logs. This is because, the drilling of the selected points was not done at the time of writing this research work. It is therefore recommended that future geophysical groundwater interpretations should include the drill logs.
- Further conductivity and resistivity modelling research should be done in the Voltaian to establish the conductivity and resistivity at depth for which groundwater can be obtained.

REFERENCES

Acheampong, S. Y., Owusu, D., Gyau-Boakye, P., and Ayibotele, N. B., 2005. "Groundwater utilization in the Afram Plains". International Report, Water Resources Research Institute, Council for Scientific and Industrial Research. Accra.

Acheampong, S.Y., and Hess, J.W ., 1998. "Hygrogeologic and Hydrochemical Framework of the Shallow Groundwater System in the Southern Voltaian Sedimentary basin, Ghana." *Journal of Hydrology* (Journal of Hydrology) 527-537.

Acheampong, S.Y., and Hess, J.M., 2000. "Origin of the shallow groundwater system in the southern Voltaian Basin of Ghana: an isotopic approach." *Journal of Hydrogeology* 233(1–4):37–53.

Ademilua, O. L., and Talabi, A. O., 2012. "The Use Of Combined Geophysical Survey Methods For Groundwater Prospecting: In A Typical Basement Complex Terrain; Case Study Of Ado – Ekiti, Southwest Nigeria." *Research Journal in Engineering and Applied Sciences* I: 362-376.

Affaton, P., Sougy, J., and Trompette, R., 1980. "The tectono-stratigraphic relationships between the Upper Precambrian and Lower Paleozoic Volta Basin and the Pan-African Dahomeyide orogenic belt (West Africa)." *American Journal of Science* (American Journal of Sciences) 224–248.

Agyekum, W.A, and Dapaah-Siakwan, S. 2007. Report of geo-logging and diver installation of HAP monitoring boreholes . Accra, Ghana: WRI Technical Report to Water Resources Commission.

Akudago, J. A; Chegbeleh, L. P; Nishigaki, M; Ananedo N; Ewusi, A; and Kankam-Yeboah, k. 2009. "Borehole Drying: A Review of the Situation in the Voltaian Hydrogeological System in Ghana." *Journal of Environmental Protection* 22.

Amuzu, A. T., 1978. The quality of groundwater in the Accra Plains of Ghana. Accra, Ghana: Water Resources Research Institute Technical Publication.

Anan-Yorke, R., and Cudjoe, J. E., 1971. Geology of the Voltaian Basin. Special Bulletin for Oil Exploration. Ghana Geological Survey. *Geological Survey Department* 29.

Apambire, W., 2000. "Geochemical modeling and geomedical implications of fluoriferous groundwaters in the Upper East Region of Ghana. University of Nevada, Reno: Unpublished Dissertation.

Appiah, F. F. and Momade, Z., 2012. "Analysis of quality of water at Kintampo." *International Journal of Water Resources and Environmental Engineering.* (ISSN

1991-637X ©2012 Academic Journals) 4 (10): 314-321. Accessed April 15, 2013. doi: 10.5897/IJWREE12.135 .

Ariyo S. O. and Adeyemi G. O., 2009. "Role of Electrical Resistivity Method for Groundwater Exploration in Hard Rock Areas: A Case Study from Fidiwo/Ajebo Areas of Southwestern Nigeria." *Pacific Journal of Science and Technology.* 1 (10). pp. 483-486.

Asare, E. B. and Boateng, M. S., 1992. A survey of excess iron problems and solutions as observed in some parts of Ghana. Accra, Ghana.: Unpublished technical report, Water Resources Research Institute.

Ayibotele, N. B., 1985. "Development and management of groundwater resources in Ghana — some current problems." *Lecture IV, 2nd International Advanced Course on Water Resources Management.* Perugia, : Centre for International Studies.

Beeson, S., and Jones, C. R. C., 1988. The combined EMT / VES Geophysical Method for sitting boreholes. Groundwater. Vol. 26, 54-63.

Berkeley Course in Applied Geophysics, 2002: DC Electric Methods. Course notes for DC Resistivity and IP techniques. Pp.24

Bernard, J. and Valla, P. 1991. "Groundwater exploration in fissured media with electrical and VLF methods. Geoexploration." 27, 87 – 91.

Bernard, J., 2003. "Short notes on the principles of geophysical methods for groundwater investigations."

Bozhko, N.A., 1969. "Stratigraphy and tectonics of the Voltaian Basin." 3–4.

Buckley, D. K., 1986. Report on advisory visit to water aid projects in Ghana. Wallingford: Unpublished Report, British Geological Survey, Hydrogeology Research Group.

Carrier, M. A.; Lefebvre, R.; Racicot, J. and Asare, E. B., 2008. "Access to Sanitation and Safe Water: Global Partnership and Local Actions. Northern Ghana hydrogeological assessment project." *33rd WEDC International Conference, Ghana.* Accra: refereed paper. 356.

Chegbeleh, L. P., Akudago, A. J., Nishigaki, M., and Edusei, S. N. K., 2009. "Electromagnetic geophysical survey for groundwater exploration in the Voltaian of Northern Ghana)." *Journal of environmental hydrology.*

Chilton, J. and Seiler, K. P., 2006. Groundwater occurrence and hydrogeological environments, in Protecting Groundwater for Health (eds O.Schmoll, G. Howard, J. Chilton and I. Chorus), IWA Publishing, London, pp. 21–47

Cobbing, A.J.E., and Davies, J., 2004. Understanding problems of low recharge and low yield in boreholes: an example from Ghana. In Water Resources of Arid Areas. Edited by Shemang & Chaoka. Stephenson.

Cooper, W.G.G., 1926. "Annual Report Gold Coast Geological Survey, April 1925 – March 1926,." 13–15.

CSIR-GWP Database, 2013. Existing water sources in the beneficiary communities in the Kintampo North Municipal.

Dapaah-Siakwan, S. and Gyau-Boakye, P., 2000. "Hydrogeologic framework and borehole yields in Ghana." *Hydrogeology Journal* 8: 405-416.

Darko, P.K., 2001. "Quantitative aspects of hard rock aquifers: Regional evaluation of groundwater resources in Ghana. Summary of PhD Dissertation." Charles University, Prague.

Darko, P.K., Krasny, J., 2007. "Regional transmissivity distribution and groundwater potential in hard rocks of Ghana. In: Krasny-Hrkal-Bruthans (ed) Groundwater in Fractured Rocks (2003)." Prague,Czech Republic.

Dobrin, M. B, and Savit, C. H., 1988. Introduction to geophysical prospecting Fourth Ed. New York: McGraw- Hill.

Driscoll, F.G., 1986. Groundwater and wells (2d ed.). St Paul, Minnesota.: Johnson Filtration Systems, Inc.

Emenike, E.A., 2001. "Geophysical Exploration for Groundwater in a Sedimentary Environment: A Case Study from Nanka over Nanka Formation in Anambra Basin, Southeastern Nigeria." *Global J. Pure Appl. Sci.*

Ewusi, A., 2006. "Groundwater Exploration and Management using Geophysics: Northern Region of Ghana." unpublished PhD THESIS.

Freeze, R.A., and Cherry, J.A., 1979. Groundwater: Englewood Cliffs. New Jersey: Prentice Hall.

Frempong, D.G., and Kortatsi, B.K., 1994. Some problems associated with the development of groundwater resources in Ghana. In: Suokko T, Soveri J (eds) Future groundwater resources at risk Publ 222. *Willingford: International Association of Hydrological Sciences.*

Ghana Geological Survey., 1965. Hydrogeological sub-provinces of the Voltaian System.

Ghana Population Census, 2010. Kintampo North Municipality report.

Gills, H.E., 1969. A groundwater reconnaissance of the Republic of Ghana, with a description of geohydrologic provinces. Washington: US Geological Survey, Water Supply Paper 1757-K.

GMBH, P. S., 1984. "The 30 well drilling project," Internal Report, Catholic Diocese of Accra." Accra.

Goldmann, M., and Neubauer, F.M., 2004. Groundwater exploration using integrated geophysical techniques. Surveys in Geophysics.

Gyau-Boakye, P., and Dapaah-Siakwan, S., 1999. "Groundwater: Solution to Ghana's Rural Water Supply Industry? The Ghana Engineer." Accra, Ghana.

Hazel, J., Cratchley, C.R., and Preston, A.M., 1988. "“The Location of Aquifer in Crystalline Rocks and Alluvium in Northern Nigeria using Combined Electromagnetic and Resistivity Techniques”." *Quarterly Jour. Enh. Geol* 159-175.

Heather, R., Beth, S., and Jeffrey, W., 1999. Electrical Imaging: A method for identifying potential collapse and other karst features near roadways. Middletown Pennsylvania.: Science Applications international cooperation.

Junner, N.R. and Hirst, T., 1946. "The geology and hydrogeology of the Volta Basin." *Gold Coast Geological Survey* 50.

Kearey, P., and Brooks, M., 1987. An Introduction Geophysical Exploration. Blackwell Scientific Publication.

Kearey, P., Brooks, M., and Ian, H., 2002. An Introduction to Geophysical Exploration. Vol. 9. Blackwell Scientific Publication, Bristol. pp 183-192, 208, 209, 216.

Keller,G.V. and Frischknecht, F.C., 1966. Electrical Methods in Geophysical Prospecting. Oxford: Pergamon Press.

Kesse, G.O., 1985. "The mineral and rock resources of Ghana." Rotterdam: A.A Balkema. pp. 11, 12, 44-49.

Kortatsi, B.K., 1994. "Groundwater utilization in Ghana." *Future Groundwater Resources at Risk (Proceedings of the Helsinki Conference).* IAHS Publ. no. 222. 149.

Kwei, C.A., 1997. Evaluation of groundwater Potential in the Northern Region of Ghana. Accra, Ghana: Canadian international Development Agency (CIDA). pp. 1-2, 39-41, 67.

Liu, S. and Yeh T.J., 2004. "An Integrative Approach for Monitoring Water Movement in the Vadose Zone." *Vadose Zone J.* (Vadose Zone J.) 681–92.

Loke, M. H., 2001. "Constraint time-lapse resistivity imaging inversion. Procs." Symposium on the Application of Geophysics to Engineering and Environmental Problems, *SAGEEP*. Denver, Colorado, March 4-7.

Loke, M. H., 1999. "Electrical imaging surveys for environmental and engineering studies. A practical guide to 2-D and 3-D surveys." 1-4.

Lutz, A., Thomas, J. M., Pohll, G., and McKay, W. A., 2007. "“Groundwater resource sustainability in the Nabogo Basin of Ghana"." *J African Earth Sci.* 61–70.

MacDonald, A.M., Calow, R.C., Andrews, A.J., Appiah, S., 1997. Groundwater management in drought prone area of Africa Northern Ghana. Nottingham: Keyworth. British Geological Survey.

Martin, N., & Van de Giesen N., 2005. Spatial distribution of groundwater use and groundwater potential in the Volta River basin of Ghana and Burkina Faso. IWRA Water Intern.

Mato, R. R. A. M., 2002. "Groundwater Pollution in Urban Dar es Salaam, Tanzania. Assessing vulnerability and priorities." Unpublished PhD Thesis Technische Universiteit Eindhoven.

McNeil, J. D., 1980. Electrical Conductivity of Soils and Rocks. London: Cambridge University Press.

McNeil, J. D., and Snelgrove, F. B., 1995. Electromagnetic Geophysical Methods Applied to Groundwater Exploration and Evaluation. Geonics Limited. .

McNeil, J. D., 1990. "Use of Electromagnetic Methods for Groundwater Studies. In: Ward, S. H. (Ed.). Geotechnical and Environmental Geophysics.vol 1: Review and Tutorial, Society of Exploration Geophysicists Investigations No.5." 107-112.

McNeil, J. B., & Snelgrove, F.B., 1986. Electromagnetic Geophysical Method Applied to Ground Water. Exploration and Evaluation. Developing World Water.

Menyeh, A., Noye, R. M., and Danour, S. K., 2005. "Prospecting for groundwater using the electromagnetic method in the Voltaian Sedimentary basin in the Northern Region of Ghana- A case study of the Gushigu- Karaga District." *Journal of Science and Technology* 54.

Morris, D. A., Johnson, A. I. 1967. "Summary of hydrologic and physical properties of rock and soil materials, as analyzed by the hydrologic laboratory of the U.S. Geological Survey." *USGS Numbered Series.*

Mussett, A.E. & Khan, M.A. 2000. Looking into the earth, An introduction to geological geophysics. Cambridge, UK.: Cambridge University Press.

Mygatt, E., 2006. Eco-Economy Indicators-Water Resources. http://www.earth-policy.org/index.php?/indicators/C57/.

Obuobie, E. and Boubacar, B. 2010. Groundwater in sub-Saharan Africa: Implications for food security and livelihoods. Ghana Country Status on Groundwater. Final Report. http://gw-africa.iwmi.org/Data/Sites/24/media/pdf/Country_Report-Ghana.pdf

Okrah, C., Danuor, S. K., and Dapaah - Siakwan, S., 2012. "Geophysical investigations for groundwater in the middle Precambrian province of upper Denkyira District using electromagnetic and electrical resistivity methods." *Journal of Ghana science association* 14 (1): 106.

Olayinka, A.I, Amidu, S.A., and Oladunjoye, M.A. 2004. "Use of Electromagnetic Profiling and Resistivity Sounding for Groundwater Exploration in the Crystalline Basement Area of Igbeti, Southwestern Nigeria." *Global Journal of Geological Sci.* 2 (2): 243-253.

Palacky G. J. 1987. "Resistivity characteristics of geologic targets. Electromagnetic Methods in Applied Geophysics." 1, 53-129.

Palacky, G.J., Ritsema, I.L., and De Jong, S.J. 1981. "Electromagnetic Prospecting for Groundwater in Precambrian Terrains in the Republic of Upper Volter". Geophy. Prospect.

Parasnis, D.S. 1986. Principles of Applied Geophysics Fourth edition.

Patton, M. Q., 1990. Qualitative evaluation and research methods. Newsbury Park: Sage Publication.

Pelig-Ba, K. 1989. "Hydrochemical study of groundwater in some aquifers in the upper regions of Ghana." *13th Biennial Conference, West African Science Association,* . Accra, Ghana: University of Ghana, Legon.

Reynolds, J. M. 1997. An introduction to applied and environmental geophysics.

Rhoades, J.D., Halvorson, A.D., 1977. Electrical conductivity methods for detecting and delineating saline seeps and measuring salinity in Northern Great Plains soils, ARS W-42. USDA-ARS Western Region, Berkeley, CA, USA, pp. 1–45

Robinson, E.S. and Coruh, C. 1988. Basic Exploration Geophysics. New York: Wiley.

Roman, I. 1951. "Resistivity reconnaissance in American Society of Testing and Materials." *Symposium on surface and subsurface reconnaissance: American Society of Testing Materials Special technical publication122.* 171-220.

Santosh, K. G. 1996. Water Supply Engineering. Delhi: Khanna Publishers.

Sharma, P. V., 1997. Environmental and Engineering Geophysics. Cambridge: Cambridge University Press. pp. 28, 231, 265-269, 280-296.

Sharma, P. V., 1999. Applied and Environmental Geophysics. Cambridge University Printing Press.

Sharma, P. V., 1986. Geophysical methods in Geology. Elsevier Science Pub I. Co. Inc. 2nd Ed 301.

Sheriff, R. E. 1991. " Encyclopedic dictionary of exploration geophysics, 3rd ed. Society of Exploration Geophysicists."

Singh, C.L. 1985. "Role of Surface Geophysical Methods for Groundwater Exploration in Hard Rock Areas". Proceedings of International Workshop on Rural Hydrology and Hydraulics in Fissured Basement Zones." 59-68.

Singhal, B.B.S, & Gupta, R.P. 1999. Applied Hydrogeology of Fractured Rocks.

Tebutt, T.H .Y. 1992. "Principles of water Quality control." Pergamon press Oxford.

Telford, W. M., Gerdart L. P., and Sheriff, R. E. 1990. Applied Geophysics. *2nd Ed.* London: Cambridge University Press. pp. 283-287, 289, 306-309, 522-525, 535-544.

Telford, W. M., Gildart, L. P., and Sheriff, R. E. 1994. Applied Geophysics. Cambridge: Cambridge University Press. pp. 306, 309, 343.

The Voltaian Basin, Ghana Workshop and Excursion, March 10-17, 2008. http://www.geus.dk/DK/int_devel_projects/Documents/voltaian_workshop_report.pdf

Unihydro Limited, 2002. "Water quality monitoring report." Accra, 1-28.

Unihydro Limited. 2000. IDA funded drilling program. Unpublished Technical report.

Vanderberghe, J. 1982. Geoelectrical investigation of a fault system in Quaternary deposits. Vol. 30. Geophysical prospecting. vol.30,pp.879-897

Vogelsang, D. 1994. Environmental Geophysics, A practical guide, springer-Verlag.

Water Aid Ghana, 2002. http//www.wateraid.org/ghana/. Access on May 10th, 2012.

WHO, 2006. Guidelines for drinking-water quality: Incorporating first addendum. 3rd ed. WHO. Geneva: http//www.who.int/water_sanitation_health/dwq/gdwq0506.pdf. Accessed April 15th, 2013

Water Resources Research Institute (WRRI)., 1992. Preliminary report on the inventory and assessment of potential for handdug wells in the Volta region. Main report. Rural Drinking Water Supply and Sanitation Project in the Volta Region Vol. 1. Accra: Report prepared for the Royal Danish Embassy (DANIDA).

INTERNET SOURCES

http://en.openei.org/wiki/Direct-Current_Resistivity_Survey. Accessed on 5th May, 2012.

http://www.*wateraid.org/ghana*. Accessed on 10th June 2012.

http://www.*kintamponorth.ghanadistricts.gov.gh*. Accessed on the 15th June, 2013.

http://www. *iris-instruments.com*. Accessed on 12th Nov, 2012.

http://*www.tulane.edu/~sanelson/geol111/groundwater.htm.* Accessed on the 1st September, 2013.

http://www.*tshaonline.org/handbook/online/articles/gru01*. Accessed on the 15th June, 2013.

http://www.hwe.org.ps/Education/Birzeit/GroundwaterEngineering/. Accessed on 10th Mar, 2012.

APPENDIX A: SAMPLE EM PROFILE DATA

Appendix A 1: Sample EM profile data at Alhassan Akura

Community:	Alhassan Akura	**District:**	Kintampo North
Bearing:	258^{o}	**Profile Length:**	210 m
Profile No.	A	**Date:**	21-Mar-13

STATION	**20-m Separation**		Remarks
	HD mode	**VD mode**	
0	54	59	
10	57	58	
20	58	60	
30	60	66	
40	61	66	VES
50	57	65	
60	60	64	
70	63	70	
80	68	70	
90	64	72	
100	65	74	
110	70	80	
120	74	69	VES
130	73	65	
140	70	62	
150	68	63	
160	63	60	
170	59	55	
180	61	57	
190	65	60	
200	60	56	

APPENDIX B : SAMPLE VES DATA

Appendix B 1: Sample VES station data at Asukoko

Location:	**Asukoko**		Date:	**14-Mar-13**
District:	**Kintampo North**		Elevation:	**238 m** *amsl*
Station:	**A30**		Coordinate:	**08° 05.199'N, 001° 29.845W (***accuracy=9 m***)**

C1C2/2 (m)	P1P1/2 (m)	Resistance (Ohms)	Multiplying Factor	Apparent Resistivity (Ohm-m)
1.5	0.5	100.6	6.3	634
2.1	0.5	34.6	13.1	453.26
3.0	0.5	10.57	27.5	290.7
4.4	0.5	3.29	60.0	197.4
6.3	0.5	1.03	124.0	127.7
9.1	0.5	0.33	259.0	90.7
13.2	0.5	0.14	547.0	76.6
19.0	0.5	0.058	1133.0	65.71
27.5	0.5	0.031	2375.0	73.63
40.0	0.5	0.015	5026.0	75.39
40.0	5.0	0.14	495.0	69.3
58.0	5.0	0.073	1049.0	76.58
83.0	5.0	0.043	2156	92.71